January 2020

Electron Beam Irradiation As A Potential Lipid Decontamination Technique For Life Detection Instruments

Denise Kathleen Buckner

ELECTRON BEAM IRRADIATION AS A POTENTIAL LIPID DECONTAMINATION TECHNIQUE FOR LIFE DETECTION INSTRUMENTS

by

Denise Kathleen Buckner
Bachelor of Science, Saint Louis University, 2015

A Thesis
Submitted to the Graduate Faculty

of the

University of North Dakota

In partial fulfillment of the requirements

for the degree of

Master of Science

Grand Forks, North Dakota

August
2020

This thesis, submitted by Denise Kathleen Buckner in partial fulfillment of the requirements for the Degree of Master of Science from the University of North Dakota, has been ready by the Faculty Advisory Committee under whom the work has been done and is hereby approved.

_____
Dr. Mike Gaffey

_____
Michael Dodge

_____
Dr. Brian Darby

_____
Dr. Mary Beth Wilhelm

This thesis is being submitted by the appointed advisory committee as having met all of the requirements of the School of Graduate Studies at the University of North Dakota and is hereby approved.

_____
Dr. Chris Nelson
Dean of the School of Graduate Studies

_____
Date

PERMISSION

Title Electron Beam Irradiation as a Potential Lipid Decontamination Technique for Life Detection Instruments

Department Space Studies

Degree Master of Science

In presenting this thesis in partial fulfillment of the requirements for a graduate degree from the University of North Dakota, I agree that the library of this University shall make it freely available for inspection. I further agree that permission for extensive copying for scholarly purposes may be granted by the professor who supervised my thesis work or, in his absence, by the Chairperson of the department or the dean of the School of Graduate Studies. It is understood that any copying or publication or other use of this thesis or part thereof for financial gain shall not be allowed without my written permission. It is also understood that due recognition shall be given to me and to the University of North Dakota in any scholarly use which may be made of any material in my thesis.

Denise Buckner

07/30/20

TABLE OF CONTENTS

LIST OF FIGURES

LIST OF TABLES

ACKNOWLEDGMENTS

I would like to thank the University of North Dakota Department of Space Studies for allowing me to earn my M.S. and for supporting me in all my educational and professional endeavors. I would especially like to thank Dr. James Casler for all his advice, Dr. Mike Gaffey and Professor Michael Dodge for their guidance in my research and for serving on my thesis committee, and all of the professors who taught me along the way. I would also like to thank the Department of Biology for allowing me to enhance my space education with a minor in Biology, especially Dr. Brian Darby for guiding my research and serving on my thesis committee.

I would also like to thank NASA Ames Research Center for hosting me, supporting my work, and for enabling me to search for life in the universe. In particular, I would like to thank Dr. Mary Beth Wilhelm for her support, mentorship, and friendship, and for serving on my thesis committee; Linda Jahnke for allowing me to conduct my experiments in her laboratory and for providing me with profound guidance on lipid biomarkers; Dr. Jessica Koehne for allowing me to work in her laboratory; and Dr. Tony Ricco for advising me. Special thanks to NASA Ames Research Center for supporting this thesis research financially with an Ames Center Innovation Funds grant.

Thanks to the North Dakota Space Grant Consortium, especially Caitlin Nolby and Marissa Saad, for supporting me, providing me with funding opportunities, going above and beyond to set up the internship at Ames that led to this thesis work, and for all the advice and encouragement. Additional thanks to Space Grant for supporting this work financially with research fellowship funding!

A very special thanks to Bev Fetter for being amazing and always helping me with any question I had during my time at the University of North Dakota- none of this would be possible without her!

Finally, thanks to all of my classmates for taking this educational journey with me, and to my family and friends for always being there for me.

To Steve and Kathy,

The best parents around!

ABSTRACT

In the search for extraterrestrial life, identification of molecular biosignatures is a key technique. Lipids are important molecular biosignatures: they are ubiquitous to terrestrial life, survive for billions of years in the geologic record, can form biotically and abiotically (bearing molecular features indicating biogenicity), and are detected throughout the Solar System. Lipid-based life detection instruments require stringent contamination control to prevent false positives, but traditional decontamination techniques are unlikely to sufficiently remove lipid contamination without compromising instrument materials. This thesis investigates Electron Beam Irradiation (EBI) as a potential decontamination technique; five representative lipid standards, including palmitic acid, oleic acid, heneicosane, 5α-cholestan-3β-ol, and 5-α-cholestane, were subjected to EBI at 0, 50, and 100 kilogray doses, then analyzed with gas chromatography mass spectrometry to determine removal efficiency. No significant degradation of lipids was observed at doses tested, suggesting EBI should not be utilized as a lipid decontamination technique for life detection instruments.

CHAPTER I: INTRODUCTION AND BACKGROUND

The search for life beyond Earth is a driving force of space exploration, identified by NASA as a high-priority focus for current and future missions to Mars, Icy Moons, and beyond.[1,2] This goal makes up the burgeoning field of Astrobiology, or "the study of the origin, evolution, and distribution of life in the universe."[3] Finding evidence of extraterrestrial life and studying how that life operates would help determine how life originated on Earth and would revolutionize our understanding of our place in the universe.[1,4,5] Identifying and analyzing organic molecules- the building blocks that make up life- is an important technique leveraged in this search. Lipids are organic molecules of special interest for life detection applications, as they can indicate the presence of extant or ancient life, as they are potentially preserved for billions of years after that life has ceased.[6] Astrobiology missions searching for lipids require highly sensitive instruments capable of extracting, purifying, and analyzing these molecules from geologic samples *in situ* (i.e., on the surface of another planetary body).[7] To prevent false positives and validate results, stringent contamination control (CC) techniques are needed to properly remove terrestrial lipid contaminants from instrument hardware prior to flight, but traditional and laboratory-based decontamination procedures are either unable to sufficiently remove lipids or are incompatible with the sensitive materials used to construct these instruments.[8–10] To bridge this gap in the knowledge, there is a need to identify and test a CC technique that can effectively remove lipids from life detection instruments below analytical instrument limit of detection (LoD) without harming the materials those instruments are made of.

1.1 Background

1.1.1 Introduction to Life Detection

Although humanity has long wondered if life exists on other planets, the 1976 Viking mission to Mars is the only mission to date that has explicitly searched for life *in situ*; this mission sought molecular signs of metabolism in surface soils and organic compounds indicative of life, but failed on both accounts.[11] However, these results are disputed for a number of reasons, including that a lack of any organic signal could have been caused by reactions between native organics and perchlorates in the regolith during the heating phase of sample analysis.[12–15] The recent discoveries that liquid water was abundant on Mars during its earlier epochs and that warm subsurface oceans are currently active on Saturn's moon Enceladus and Jupiter's moon Europa have extended the range of potentially habitable bodies to encompass other Solar System planets beyond Earth.[16–19] Did life ever exist on Mars? Does life now exist on Icy Moons? To bridge this gap in knowledge, answer the questions first asked by Viking's investigations, and determine if we are alone in the universe, NASA is presently developing technologies to enable *in situ* life detection surveys within the next decade.

1.1.2 NASA Motivation for Life Detection

"Searching for Life Elsewhere" is one of the three core contexts of NASA's first Strategic Goal for Planetary Science (Strategic Objective 1.1: Understand The Sun, Earth, And Universe) in the 2018 Strategic Plan.[20] According to NASA's Visions and Voyages for Planetary Science in the Decade 2013-2022, "The prime focus of the first high-priority goal for the exploration of Mars in the coming decade is to determine if life is or was present on Mars."[21] The Mars Exploration Program Analysis Group (MEPAG), designated by NASA HQ, has placed "Determine if Mars

ever supported, or still supports, life" as Goal I for 2020 in MEPAG Science Goals, Objectives, Investigations, and Priorities: 2020.[22] Finally, NASA asks "what were the primordial sources of organic matter, and where does organic synthesis continue today?" and "beyond Earth, are there contemporary habitats elsewhere in the solar system with necessary conditions, organic matter, water, energy, and nutrients to sustain life, and do organisms live there now?" as two of the three Priority Questions for exploration of Planetary habitats in the decade 2013-2022.[21]

1.1.3 Biomarkers: Signs of Life

To accomplish these goals and objectives, multiple astrobiology mission concepts to Mars and Icy Moons are presently being developed. Like Viking, many of these missions will search for molecular biosignatures as biomarkers.[7,22,23] According to Peters and Moldowan, "Biological markers or biomarkers are molecular fossils, meaning that these compounds are derived from formerly living organisms. Biomarkers are complex organic compounds composed of carbon, hydrogen, and other elements. They are found in rocks and sediments and show little or no change in structure from their parent organic molecules in living organisms."[24] In other words, biomarkers are compounds required by, produced by, and indicative of life, and must have the potential for long-term preservation in the rock record.

Biomarkers are synthesized by biotic (i.e., biological) chemical reactions, but their molecular precursors can form through abiotic (i.e., non-biological/geological) chemical reactions. Amino acids, nucleic acids, and fatty acids are a few examples of key molecular precursors for life that can form through biotic or abiotic processes. These subunits make up the bulk of larger biomarkers like proteins, DNA, and membrane phospholipids. Both biomarkers and molecular precursors are targeted for astrobiological significance.[1] Identifying these compounds on another

planet can indicate that life as we know it did emerge or could potentially emerge, so further search and analysis is needed to characterize the compound, elucidate its origin, and determine the presence (or absence) of biotic processes.[25]

1.1.4 Lipid Biomarkers

Lipids are ideal biomarkers for identifying ancient life, identified as high priority targets for astrobiological exploration.[1,26] Lipids represent a wide, diverse class of molecules that are essential for all life as we know it, primarily for building cell-encompassing membranes that protect and segregate biological materials from the outside environment.[27,28] They also serve as an energy source for organisms and facilitate transportation of other biomolecules into and out of the cell. Lipids are defined as compounds that are soluble in organic solvents[29]. Some important biological lipids, including membrane phospholipids and the fatty acids they are made up of, are amphiphilic, meaning that one end is soluble in organic solvents but insoluble in water, while the other end contains a polar functional group (i.e., -OH/hydroxyl group) that is soluble in water, which provides important biological functionality.[29] Additionally, strong carbon-carbon bonds that build lipid molecules render them hardy and recalcitrant, allowing them to become molecular fossils that can provide information about ancient life, eons after all other traces of the organism have been petrologically erased.[6,28,30,31]

Fatty acids (i.e., carboxylic acids) are a lipid with special utility. They contain a hydrophilic (water-soluble) head group and a hydrophobic (water-resistant) hydrocarbon tail, which enables them to self-assimilate and form mono- and bi-layer sheets that make up cell membranes, with the hydrophilic heads facing out towards the aqueous environment and the hydrophilic tails facing inward, repelled by the aqueous environment, illustrated in Figure 1. Fatty acids attached to

phosphate or glycerol head groups make up phospholipids and glycolipids that make up the lipid bilayer of many cells.[28]

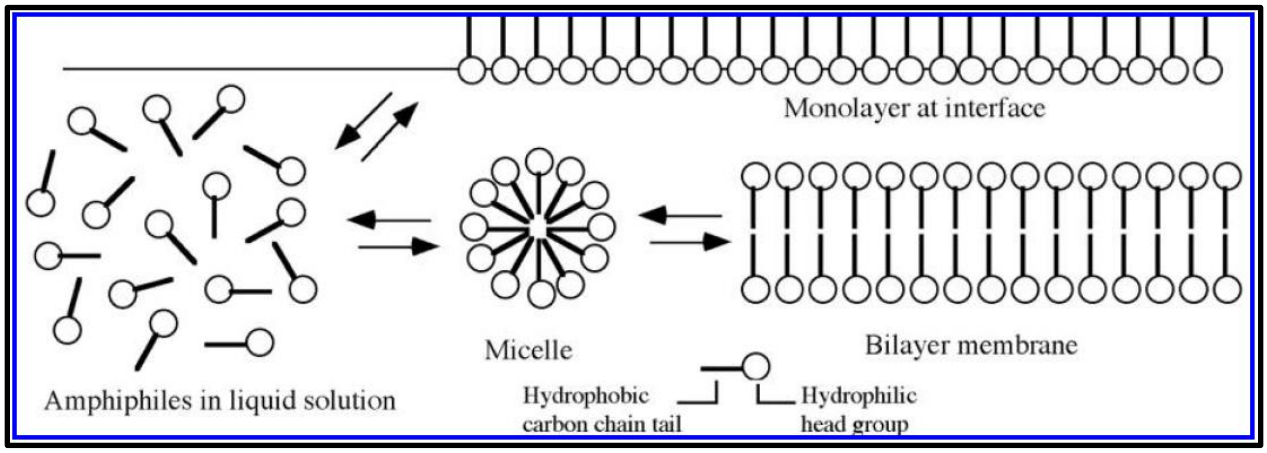

Figure 1. Lipid bilayer comprising dual sheets of fatty acids (i.e., amphiphiles), with hydrophilic head groups facing out towards the aqueous environment, and hydrophobic tails facing inward and repelled by the aqueous environment[27]

It has been postulated that life on Earth first formed when abiotically-formed fatty acids were introduced to watery settings, then self-assembled into vesicles that emerged as the first primitive cells; this chemical property (vesicle-forming capability) makes lipids likely required for any form of cell-based life, either on Earth or beyond.[27,32–35] While extraterrestrial life could reasonably utilize different biomolecules than terrestrial life does (i.e., set of amino acids, information-containing biopolymers other than DNA), putative cellular life in an aqueous environment cannot exist without membranes.[27,36] Encapsulation provides a protected environment for segregating biological material and allowing biochemical reactions to proceed and evolve. Lipids are the only known class of organics able to provide this functionality in water.[28]

Other important lipids for life detection include aliphatic alkanes (i.e., straight-chain hydrocarbons) and cyclic compounds. Alkanes make up the tails of fatty acids and the waxes that plants, animals, and insects use for coatings that protect against desiccation and low temperatures.

Cyclic compounds (e.g., pentacyclic triterpenoids, steroids, sterols) are incorporated into cellular membranes to regulate fluidity.[6,24,28,37]

1.1.5 Origin-Diagnostic Molecular Features

Biomarkers contain origin-diagnostic molecular features and patterns in features that can help indicate whether they came from biotic or abiotic processes.[24,25,38–40] While most lipids on Earth are formed biotically, they can also form abiotically (i.e., through Fischer-Tropsch type synthesis) and display origin-diagnostic molecular features that indicate synthesis pathways. For example, biotic synthesis of fatty acids elongates the hydrocarbon backbone by adding two-carbon acyl groups at a time, resulting in a propensity of even-chain-length fatty acids; even-over-odd preference indicates biogenicity.[28,37] Alternatively, abiotic synthesis of fatty acids can proceed with Fischer-Tropsch-type synthesis, whereby the hydrocarbon backbone is elongated with the addition of single CO groups, resulting in a Poisson distribution of chain lengths with no preference for even versus odd carbon number.[41,42] Various lipid structures also impart mechanical and chemical functionality to cells, so identification of those life-enabling structures can also indicate biogenicity. For example, cyclic moieties are important for increasing membrane fluidity in a cell, so the presence of cyclic compounds can indicate that the lipids found in a geologic sample came from an organism.[37] Origin-diagnostic patterns and distributions in lipids extracted from biotic (i.e., terrestrial) and abiotic (i.e., meteoritic, laboratory synthesized) specimens are well-established in the literature, shown in Figure 2. For lipids, some of these features and patterns include molecular weight/chain length, position of unsaturations and branch points, presence of cyclic moieties and functional groups, and conformation/isomerization.[6,27,28,30,43–46]

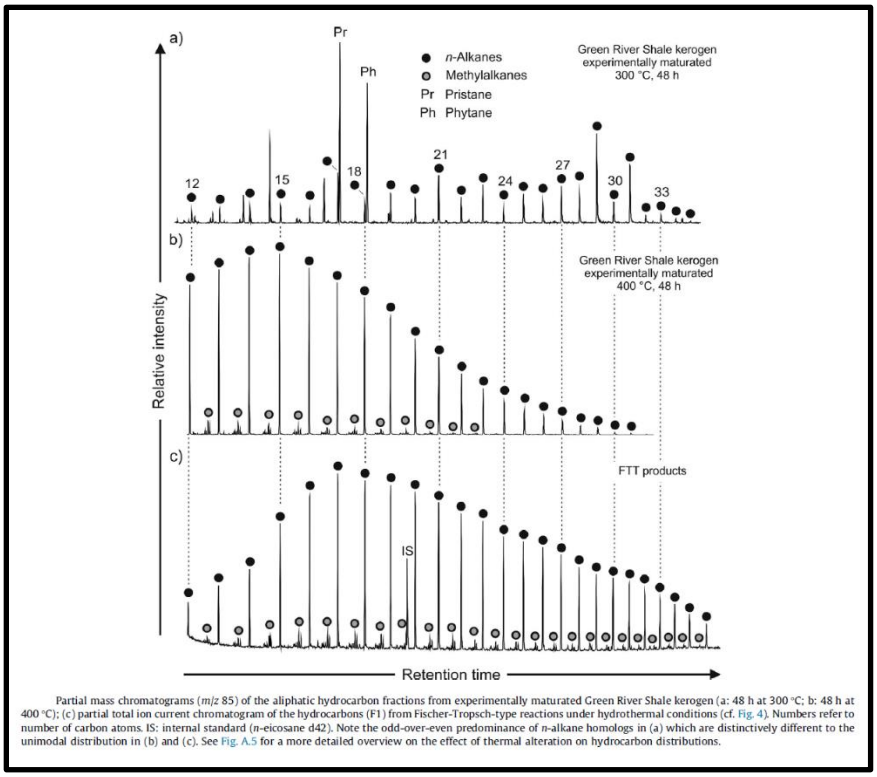

Figure 2. Origin-diagnostic patterns in fatty acid chain lengths: (a) is a natural/biotic sample, (b) is a thermally/geologically reprocessed natural/biotic sample, (c) is a synthetic/abiotic sample generated with Fischer-Tropsch-type reaction in the laboratory[41]

1.1.6 Lipids in the Solar System

Hardy lipid molecules can last for billions of years in the geologic record, orders of magnitude longer than any other biomarker (i.e., proteins, DNA, amino acids). While lipids do undergo some molecular changes during diagenesis, like loss of unsaturations due to oxidation and cyclization of aliphatic molecules due to heat/pressure, they largely retain origin-diagnostic information, allowing scientists to elucidate their source and synthesis and reconstruct the biological, chemical, and geological history of the environment in which they are preserved.[6,25,39,47–49] Preserved lipids are found in a wide range of environments on Earth and are detected throughout the Solar System. The Sample Analysis at Mars (SAM) instrument on the Curiosity rover identified small, aliphatic hydrocarbon fragments on Mars.[50,51] Carboxylic acids,

hydrocarbons, and polycyclic aromatic hydrocarbons (PAHs) have been extracted from carbonaceous meteorites (distributions in Figure 3).[43–45,52,53] Hydrocarbons and PAHs have been found in interplanetary dust particles (IDPs)[54] and cometary samples returned from Comet 81p/Wild 2 by the Stardust mission.[55]

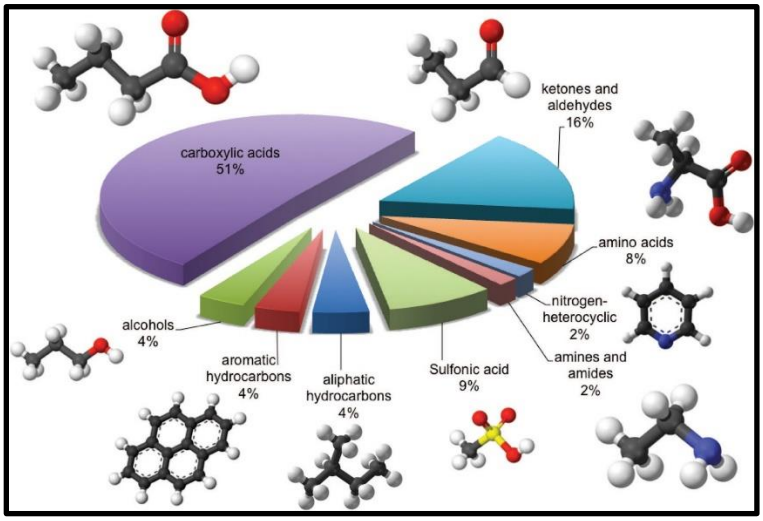

Figure 3. Relative abundances of soluble organic matter in the Murchison meteorite extracted by Remusat et al.; fatty acids make up over 50%[56]

Lipid biomolecules are synthesized by organisms, but smaller lipids that these biomolecules comprise can be synthesized abiotically, and include those found in primitive bodies (i.e., asteroids, IDPs, and comets). It has been posited that infalling organic matter from these primitive bodies could have provided the seed material for the emergence of life on early Earth ~3.5 Gyr (i.e., billion years), particularly during the Late Heavy Bombardment (LHB) ~3.8-4.5 Gya, when meteorite flux peaked on the interior planets.[32,34,45,57] In addition, lipids are also synthesized abiotically in hydrothermal vents. This *in situ* synthesis could have been an alternate source of the first lipids used by terrestrial life, and hydrothermally-synthesized lipids could potentially be generated today in the subsurface oceans of Icy Moons, or in the past on ancient

Mars during the warm/wet Noachian ~3.7-4.1 Gyr, when lakes and oceans dominated the planetary surface.[58–60]

There are many ways known to preserve lipids over geological timescales and protect them from degradative processes (e.g radiation). For example, entombment in a mineral matrix, burial beneath regolith, or sequestration under an icy crust could protect these molecules from radiolytic or oxidative breakdown over geologic timescales, meaning that if life- ancient or extant- ever existed on another planet, lipids containing origin-diagnostic information should remain preserved in the surface or subsurface.[39,54,61–65] Desiccating environments provide particularly amenable conditions for preserving lipids long-term. The most arid locations on Earth are still one to three orders of magnitude wetter than present-day Mars, and although these environments are too dry to host metabolically active microbial life as we know it today, ancient lipids remain in the soil, unaltered for billions of years.[47–49] If Mars hosted life during its early, warm, wet epochs, lipids from these organisms could remain as evidence long past, making lipids the best biomolecular target for ascertaining the presence of life in either case (past or extant). Alternately, if Mars did not ever host life, lipids sourced from the same infalling matter and potential *in situ* generation should still be present, bearing abiotic origin-diagnostic features and distributions.

1.1.7 Life Detection Instrumentation

To perform detailed analyses of molecular biomarkers and elucidate origin-diagnostic features, instruments are needed that can autonomously process regolith samples *in situ*, isolate biomarkers, and characterize molecular structures. Recent technological advancements have enabled development of instruments with this capacity.[7,66] Lipids are abundant on Earth but expected to be in low concentration in an exobiological sample. Only approximately ppm

concentrations of total organic carbon on Mars are expected for a purely abiotic case, where ancient life did not exist, and the only lipids present were delivered by infalling matter and/or synthesized *in situ*). Highly sensitive analytical instruments with low limits of detection (LoD) are necessary to definitively identify lipids in a low-biomass or abiotic sample.[1,54,66] Additionally, the amphiphilic properties of lipids make them sticky and often difficult to remove from instruments with traditional cleaning techniques,[8] and recent studies on microbial contamination in the cleanrooms where life detection instruments are fabricated show that biological matter (e.g., live microbes, dead microbes, fungi, viruses, and human skin cells) is more prevalent than previously estimated.[67–73] Since lipids make up the cell membranes of all life on Earth, machine oils (i.e. alkanes/long chain hydrocarbons) are common contaminants on metal and machined components, and future instruments will concentrate lipid extracts to increase signal from presumed organic-lean regolith samples, stringent decontamination protocols are essential to ensure successful life detection measurements without false positives.

1.1.8 Planetary Protection

Planetary Protection (PP) is an important aspect of any space mission, mandated by NASA and COSPAR (Committee on Space Research) and agreed upon by spacefaring nations as part of the United Nations Treaties and Principles on Outer Space (The Outer Space Treaty [OST].[74,75] According to the NASA Office of Safety and Mission Assurance (OSMA), "Planetary Protection is the practice of protecting solar system bodies from contamination by Earth life and protecting Earth from possible life forms that may be returned from other solar system bodies. NASA's Office of Planetary Protection promotes the responsible exploration of the Solar System by implementing and developing efforts that protect the science, explored environments and Earth."[76] PP is focused

on (1) preventing forward contamination from Earth to other bodies, i.e., preventing viable/living terrestrial organisms from being transported to another planet where they could potentially live and/or multiply, thus harming any potential extraterrestrial lifeforms and (2) preventing back contamination from other bodies to Earth, i.e., preventing viable extraterrestrial organisms from being transported from another body back to Earth where they could potentially live and/or multiply, thus harming life here.[77–79] To mitigate this risk, strict regulations are placed on spacecraft to limit the number of viable microbial contaminants prior to launch; limits are dictated by the potential habitability of the target body and the chances that life did, does, or could exist there. For life detection missions, <30 viable microbes are allowed per spacecraft.[80]

1.1.9 Contamination Control

Beyond space mission PP, life detection instruments require strict contamination control (CC). While PP is focused on sterilization, i.e., killing viable microbes, CC is focused on removing or chemically degrading bacterial, biological, and molecular contamination to prevent false positives. PP-approved decontamination methods include dry heat microbial reduction (DHMR) and application of vapor phase hydrogen peroxide (VHP); these techniques are tuned to kill microbes and are compatible with many materials used in instruments and spacecraft hardware, but they do not remove or destroy molecular lipid contamination.[81,82] Cleanrooms are highly-controlled environments designed to limit contamination during instrument fabrication and spacecraft integration and employ CC techniques like high efficiency particulate air (HEPA) filters, use of bunny suits/protective gear, surface decontamination with water/detergent/alcohol wipes, and verification of cleanliness with frequent sampling and microbial assays.[83] These techniques are tuned to kill microbes and remove particulate matter and are compatible with many

materials used in space hardware, but they do not kill all microbes and do not sufficiently remove or destroy molecular lipid contamination below instrument LoDs. CC techniques used in organic chemistry laboratories include ashing/combusting at >450°C and washing or flushing with organic solvents and acids.[8,84] These techniques are highly effective at destroying microbial and molecular lipid contamination through combustion and chemical degradation, but are harsh and incompatible with most instrument materials and spacecraft hardware.

1.1.10 Electron Beam Irradiation

To combat the challenge of removing lipid contamination from life detection instruments below instrument LoD (~ppb) without destroying the instrument materials, better CC techniques are needed. Electron beam irradiation (EBI) is a decontamination method widely utilized in food, medical, and wastewater treatment industries[85–88] and has been proposed for PP and spacecraft CC applications, but effects on organic contaminants have not previously been elucidated.

EBI works by applying a beam of concentrated electrons to surfaces, imparting high amounts of ionizing energy that can potentially destroy contaminant compounds by breaking molecular bonds. These electrons are machine-generated, so no radioactive materials are required, making EBI a relatively safe process. Dose rates are highly tunable, and the beam can penetrate several centimeters into materials (depending on dose and material density), with potential to destroy any encapsulated contamination embedded in the substrate.[86,89] Although EBI can degrade biological and organic matter, it is compatible with many of the inorganic materials used in life detection instruments and spacecraft hardware.[90]

Previous EBI-lipid research shows that a range of breakdown products, some of them unique or novel compounds, are created following irradiation, but these food industry studies

analyzed low dose levels applied to complex plant and animal matter, not hardware that is already relatively clean.[91–94] Studies proposing EBI for PP and spaceflight CC applications focus on sterilization and materials compatibility, but not the effects on molecular contamination.[89,90]

To bridge this gap in knowledge, this thesis will test the effects of EBI on lipid molecules from representative classes identified as targets for astrobiology missions, using doses tolerable by the major materials used to construct life detection instruments. Following irradiation, samples will be analyzed to determine whether the lipids have been degraded or destroyed, and recommendations will be made for/against use of EBI as a decontamination method for astrobiological applications.

This potential decontamination technique would nominally apply in sequence with other techniques as a final, whole-instrument cleaning step to remove lingering lipid contamination not removed with traditional techniques. It could potentially be applied as the primary cleaning technique for certain components (i.e., sensitive porous materials that are incompatible with other lipid decontamination techniques and have high potential for encapsulated contamination), but the main proposed application is as a last step applied to the entire instrument.

1.2 Problem Statement

Life detection instruments searching for lipid biomarkers *in situ* as signs of extraterrestrial life require highly effective contamination control techniques to reduce terrestrial lipid contamination below analytical instrument limits of detection (LoD), prevent false positives, and validate results. Traditional and laboratory-based decontamination techniques are either unlikely to sufficiently remove lipid contaminants or are incompatible with sensitive instrument materials, particularly after instrument fabrication. To bridge this gap in the knowledge, the experiments

performed as a part of this thesis will test electron beam irradiation (EBI) as a potential decontamination technique for radiolytically degrading these organics without damaging or seriously degrading the underlying instrument material.

CHAPTER II: LITERATURE REVIEW

Terrestrial contamination is a serious concern for astrobiological surveys. PP regulations place strict limits on number of allowable microbial contaminants, but recent studies on microbial contamination in instrument fabrication and spacecraft assembly cleanrooms have shown that these environments contain far more biological contamination than previously estimated, including viable microbes, fungi, viruses, and dead cells. Additionally, assaying methods are unlikely to detect the full range of materials, like lipids, present in cleanrooms and on instrument hardware, and traditional decontamination methods are unable to sufficiently remove the lipids found in these biological contaminants. EBI is one potential solution proposed for spaceflight application and potential integration into PP regulations but has not yet been tested for effects on reducing molecular lipid contaminants.

2.1 Planetary Protection

Spacefaring nations are held to the regulations laid out in the 1967 Outer Space Treaty, which states in Article IX that: “States Parties to the Treaty shall pursue studies of outer space, including the Moon and other celestial bodies, and conduct exploration of them so as to avoid their harmful contamination and also adverse changes in the environment of the Earth resulting from the introduction of extraterrestrial matter and, where necessary, shall adopt appropriate measures for this purpose.”[74] PP focuses on limiting the spread of viable microorganisms between potentially habitable planetary bodies.

2.1.1 Legal Framework

Signatories to the OST, including the United States, must abide by Article IX's requirement to protect organisms, both terrestrial and potential extraterrestrial, from contamination that could threaten life. In 1958, the Committee on Space Research was established; this body oversees PP for spacefaring nations, and state space agencies (e.g., NASA) are responsible for adhering to COSPAR regulations.[75] PP focuses on limiting total bioburden, defined as viable aerobic spore-formers. Viable means the microbe is alive and capable of persisting and potentially reproducing, aerobic means the microbe can live and grow in an oxygenated environment, and spores are dormant phases that some types of microbes can enter whereby they are protected for long periods of time in harsh conditions, surrounded by peptidoglycan and keratin-like layers outside of the cell membrane (Figure 4). Spores can return to a vegetative state when conditions are amenable to metabolism and growth, so preventing their dispersal across potentially habitable bodies is essential.[95]

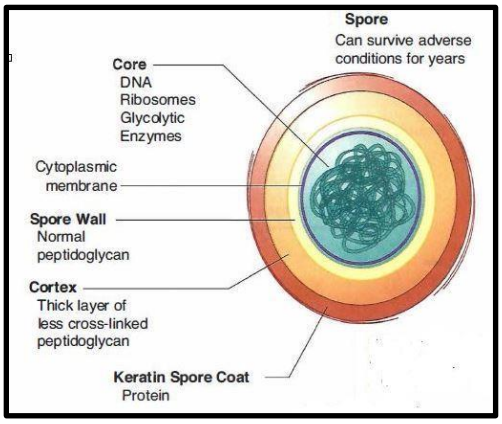

Figure 4. Bacterial endospore with the microbe surrounded by a spore wall, cortex, and keratin spore coat[95]

2.1.2 Target Body Categories

COSPAR designates five major categories for space missions; categories are based upon the target body's potential for habitability and/or hosting extant life. Category I carries the least risk and Category V carries the highest; i.e., a flyby of an asteroid is considered lowest risk (Category I), an orbiter around Mars is medium risk (Category III), and a sample return mission from Mars is considered highest risk (Category V), detailed in Figure 5.[75,96]

Planetary protection categories and planetary targets. Active bioburden reduction is required only on missions to targets having the potential to host Earth life.

Planetary target	Mission type[a]	Mission category[b]
Undifferentiated, metamorphosed asteroids; Io; others TBD	Flyby, orbiter, Lander	I
Venus; Earth's Moon; Comets; non-Category I Asteroids; Jupiter; Jovian Satellites (except Io and Europa); Saturn; Saturnian Satellites (except Titan and Enceladus); Uranus; Uranian Satellites; Neptune; Neptunian Satellites (except Triton); Kuiper-Belt Objects (<1/2 the size of Pluto); others TBD	Flyby, orbiter, Lander	II
Ganymede (Jupiter); Titan (Saturn); Triton, Pluto and Charon (Neptune); others TBD	Flyby, orbiter, Lander	II*
Mars; Europa; Enceladus; others TBD. • IVa is for lander systems not investigating extant martian life or special regions • IVb is for lander systems investigating extant martian life • IVc is for missions investigating martian special regions	Flyby, orbiter Lander, probe	III IV(a–c)
Restricted Earth-Return: • Mars; Europa; Enceladus; others TBDUnrestricted Earth-Return: • Venus, Moon; others TBD	Earth-return (restricted or unrestricted)	V

[a] If gravity assist is utilized during a flyby, constraints for the planet with the highest degree of protection may be required.
[b] For missions that target or encounter multiple planets, more than one planetary protection category may be assigned.

Figure 5. Planetary protection categories for target body, mission type, and mission category[96]

Astrobiology missions performing *in situ* analysis typically fall under Category IV and include lander missions to Mars, Enceladus, Europa, and other bodies TBD. Category IV missions encompass those seeking life- ancient or extant- and/or those going to a region where life did, does, or could exist. Mitigating biological contamination is important, both for protecting the fidelity of that mission's investigations and for preserving the environment to protect the fidelity of any future investigations to the same region.

2.1.3 Bioburden Limits

Mission categories drive bioburden limits that set restrictions on the total number of viable aerobic spore-formers allowed on spacecraft and hardware surfaces (internal and external), encapsulated in porous materials, and trapped between mated parts. For PP purposes, viability is determined by cultivability, i.e., ability for the microbes to be cultured or grown in the laboratory on a pre-set nutrient medium.[97] However, not all microbes are spore-formers, and a mere 1% -10% of viable microbes are cultivable, so *acceptable* levels of viable microbes are, logically, reasonably higher than the legal language may suggest.[72,98]

Category IV missions to Mars are further subdivided into IVa, IVb, and IVc, with different bioburden limits for each. IVa missions are not searching for extant life (but could be searching for past life) and are limited to $\leq 3*10^5$ total spores (or $\leq$300 spores per square meter). IVb missions are searching for extant life and are limited to 30 total spores or to levels of bioburden reduction driven by the nature and sensitivity of the particular life-detection experiments. IVc missions may or may not be searching for life but are traveling to Special Regions and are limited to 30 total spores. "A Special Region is defined as a region within which terrestrial organisms are likely to replicate. Any region which is interpreted to have a high potential for the existence of extant martian life forms is also defined as a Special Region."[99,100]

To meet bioburden limits, mission plans must implement risk mitigation strategies that are based upon both category and potential for causing contamination to any region throughout the mission lifetime. Category IV missions conducting life detection surveys must include protocols for preventing, cataloging, and reducing microbial contamination throughout instrument fabrication, spacecraft integration, and mission operations as listed in Figure 6.[99]

Table 1. Categories for Solar System Bodies and Types of Missions
(DeVincenzi et al. 1983, 1994; COSPAR 1984, 1994; Rummel et al. 2002)

	Category I	Category II	Category III	Category IV	Category V
Type of Mission	Any but Earth Return	Any but Earth Return	No direct contact (flyby, some orbiters)	Direct contact (lander, probe, some orbiters)	Earth return
Target Body	See Appendix	See Appendix	See Appendix	See Appendix	See Appendix
Degree of Concern	None	Record of planned impact probability and contamination control measures	Limit on impact probability Passive bioburden control	Limit on probability of non-nominal impact Limit on bioburden (active control)	If restricted Earth return: • No impact on Earth or Moon; • Returned hardware sterile; • Containment of any sample.
Representative Range of Requirements	None	Documentation only (all brief): • PP plan • Pre-launch report • Post-launch report • Post-encounter report • End-of-mission report	Documentation (Category II plus) • Contamination control • Organics inventory (as necessary) Implementing procedures such as: • Trajectory biasing • Cleanroom • Bioburden reduction (as necessary)	Documentation (Category II plus) • P_c analysis plan • Microbial reduction plan • Microbial assay plan • Organics inventory Implementing procedures such as: • Trajectory biasing • Cleanroom • Bioburden reduction • Partial sterilization of contacting hardware (as necessary) • Bioshield Monitoring of bioburden via bioassay	*Outbound* Same category as target body/ outbound mission *Inbound* If restricted Earth return: • Documentation (Category II plus) • P_c analysis plan • Microbial reduction plan • Microbial assay plan • Trajectory biasing • Sterile or contained returned hardware • Continual monitoring of project activities • Project advanced studies/research. If unrestricted Earth return: • None

Figure 6. Categories for Solar System bodies and types of missions, including contamination risk and requirements. Life detection missions to Mars, highlighted in red, fall under Category IV[99]

Organics inventory, i.e., cataloging non-living organics present, is an important caveat of these missions and hearkens back to the IVb requirement to "limit spores to levels of bioburden reduction driven by the nature and sensitivity of the particular life-detection experiments." Although reduction of viable/cultivable aerobic spore-formers is the baseline metric for PP, life

detection analyses (including lipid analyses) are often sensitive to other biological contaminants, including viable but non-cultivable spores, anaerobic microbes, dead cells, and extracellular organic biomarkers. These materials and compounds must be reduced to fulfill the spirit of COSPAR PP requirements.[78,99,100]

2.1.4 Planetary Protection Contamination Control

Space mission PP plans must include COSPAR-approved methods for sterilization applied to both individual components and the entire spacecraft to ensure bioburden limits are met. Standard techniques include dry heat microbial reduction and vapor phase hydrogen peroxide; other sterilization techniques may be approved on a case-by-case basis if the method is proven effective and justification is made for its application (for example, sensitive electronics that cannot withstand DHMR or VHP).[80,81,100] To assess if bioburden is sufficiently reduced, microbial assays check for viable spores on spacecraft and instrument surfaces (interior and exterior), typically through cultivation-based methods where any microbes present are collected from surfaces with swabs, then cultured on a nutrient medium. These checks must be performed throughout the hardware fabrication process, then again after the components are integrated.[78,99]

In addition to DHMR and VHP sterilization, additional CC techniques are typically included in mission PP planning, aimed at preventing contamination introduction during hardware assembly, and include processes for removing contamination and verifying cleanliness. Assembly typically occurs in a cleanroom- sometimes with robots or in an oxygen-free anaerobic glovebox- where numerous techniques are employed to maintain sterility and cleanliness (i.e., protective clothing worn by human operators, high efficiency particulate air [HEPA] filtration, detergent/alcohol/water washes, etc.).[83] Once instruments are assembled and integrated, protective

covers known as biobarriers are used to seal off individual instruments and cover the whole spacecraft so there is no recontamination during launch, cruise, and landing.[101]

2.2 Contamination in Spacecraft Assembly Cleanrooms

To develop a successful decontamination strategy, first it is important to understand the organic and biological contamination expected on hardware during and after assembly. Although spacecraft assembly cleanroom (SAC) decontamination methods are largely effective at reducing viable microbes and airborne particulate matter to levels required for compliance with planetary protection sterilization requirements (≤300 spores/m^2 for Category IVa and ≤30 total spores for Category IVb and IVc missions), biological matter is more pervasive. The NASA standard spore assay and cloning techniques are traditionally used as metrics for assessing contamination,[79] but viable contamination is often much higher than these methods suggest. Further, sterilization-based decontamination methods are not sufficient for reducing non-living cellular and molecular contamination below the analytical life detection instrument LoDs.[9,10,97,102]

2.2.1 Extremophiles, Rare, and Novel Microbes

SACs host diverse, varied microbiomes that include bacteria, viruses, fungi, novel organisms, and extremophiles.[68,73,103,104] Microbiomes (i.e., small, local populations of microorganisms) vary drastically between cleanrooms, and populations can shift in as little as 4 weeks, which makes it difficult to characterize the environment.[73,105] Many microbes are extremely hardy and able to survive PP-approved sterilization treatments, spaceflight, and potentially other planetary environments.

PP requires mitigation of aerobes, but anaerobes may dominate the cleanroom environment. Anaerobic microbes can survive and metabolize in the absence of oxygen, and these types of organisms are more likely to survive both the cleaning techniques employed in cleanrooms and conditions encountered during spaceflight.[103,106] Further, anaerobic capabilities are likely to co-occur with other extremotolerant capabilities, including the ability to survive extreme temperatures, pH ranges, radiation, desiccation, etc,[107,108] but the prevalence of these extremotolerant bacteria in SACs has only recently been discovered.

During assembly of the Mars Odyssey spacecraft, microbial characterization was performed and found numerous extremotolerant and hardy organisms, including those able to survive UV radiation, H_2O_2-rich peroxidizing conditions, and desiccation.[68] Analysis of the literature finds novel species in nearly every SAC studied in recent years, with as many as 17 novel extremophile species discovered in the SACs during assembly and integration of the Phoenix spacecraft.[73,105,106,109] Since cleanrooms are engineered to be unforgiving environments, they can provide ideal habitats for extremotolerant organisms to thrive.

Horneck et al. conducted project EXPOSE-E, which tested two species of common *Bacillus* spores previously isolated from SACs for ability to survive "trip to Mars" and "stay on Mars" (i.e., Mars surface-like) conditions for 1.5 years. Samples were either exposed to laboratory-simulated spaceflight conditions or were flown outside of the international space station (ISS) where they were exposed to the actual space environment. For "spaceflight-like" conditions, the study found that microbes exposed to the sun during spaceflight were largely destroyed by radiation, but microbes not exposed to the sun (i.e., on shielded/dark portions of the spacecraft, trapped in enclaves, etc.) and exposed to all other spaceflight-like environmental conditions had a

15%- 50% survival rate over the course of the study. For “stay on Mars” simulated Martian conditions, 70%- 75% of the *Bacillus* spores survived for the 1.5 year study duration.[103]

While PP regulations limit the number of cultivable, spore-forming aerobic microbes, some non-sporulating microbes can also survive spaceflight. For example, in 1969, the crew of Apollo 12 collected a camera from the lunar surface deployed by the unmanned Surveyor III spacecraft two years prior. Once returned to Earth and tested for microbial presence, viable *Streptococcus mitis* was retrieved from the camera and cultured.[110]

2.2.2 Efficacy of Microbial Sampling Techniques

Recent surveys on the efficacy of microbial sampling techniques have suggested that true bioburden is underestimated because mechanical swabbing only picks up a percentage of microbes and is generally unsuccessful at isolating low-abundance species in the population.[10,72] If microbes are not effectively collected during sampling, contamination cannot be accurately assessed.

A study conducted by Kwan et al. assessed the recovery efficiency of various cleanroom sampling swabs. They used cotton swabs, nylon-flocked swabs, Biological Sampling Kit (BiSKit, a commonly used foam-based medium for collecting microbes) swabs, and polyester wipes to recover microbes from a model microbial community (MMC, i.e., a known collection of different species of viable microbes cultivated in the laboratory and used for testing) comprising 11 species of bacteria, archaea, fungi, aerobes, anaerobes, spores, and non-spore-forming vegetative cells previously found in SACs. They seeded the MMC onto substrates of commonly used spacecraft metals, swabbed the surfaces with the four types of swabs, washed the swabs to collect microbes that were picked up, and performed DNA sequencing. Recovery percentages varied between individual species and swab types, but overall recovery was below 50%.[111]

A study by Bargoma et al. followed a similar protocol on a wider range of metals commonly used in spacecraft, and found similar results, but overall recovery was below 40% (Figure 7).

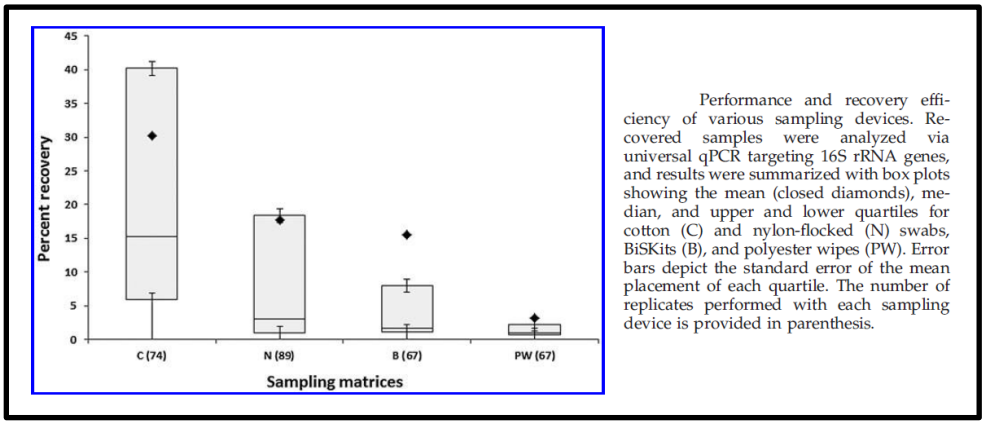

Figure 7. Recovery efficiency of four types of wipes used to swab and sample surfaces for microbes, as reported by Bargoma et al.[112]

Recovery efficiency varied by both substrate material and by species, which suggests that some microbes or spores exhibit stronger adhesive properties than others, making them more difficult to recover from surfaces. However, this has no bearing on the viability of those microbes. In fact, spores most strongly adhering to surfaces may have higher survival rates than those easily removed with mechanical swabbing.[112]

Aluminum and titanium are widely used in spacecraft, and a study by Venkateswaran et al. tested the efficiency of various cleaning and recovery methods to remove *Bacillus subtilis* spores seeded on hardware, finding that aluminum is particularly susceptible to the adhesive characteristics displayed by spores. When the two metals inoculated with *B. subtilis* spores (a common organism frequently found in cleanrooms) and subjected to five different cleaning methods were swabbed, far fewer spores were recovered from the aluminum coupons than from titanium ones, especially when the aluminum was unpolished. They hypothesize that small enclaves in the metal could enable aggregation of the spores. Interestingly, scanning electron

microscopy of the surfaces showed numerous “dome-like” structures on the aluminum but absent the titanium, with *B. subtilis* spores found underneath. These dome structures are a possible survival mechanism, appearing to enhance adherence to the substrate, thus protecting the underlying spore. Surface cleaning did not remove them, swabbing did not pick them up, and recovery was only possible following application of nitric acid or sonication, which appeared to lyse open the domes and release the spores underneath (Figure 8).

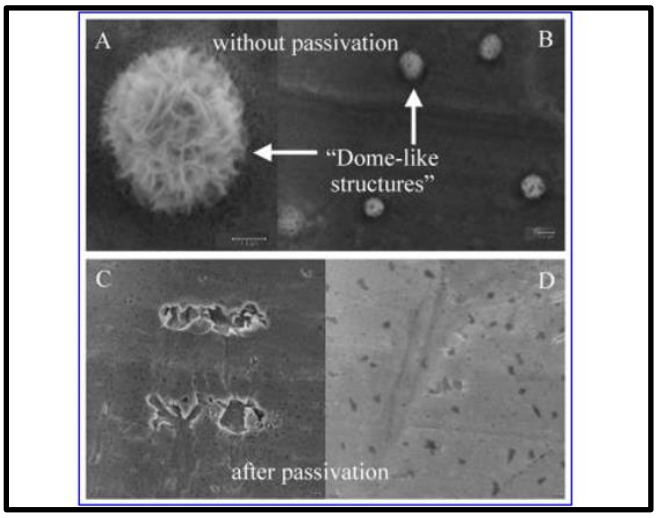

Figure 8. Venkateswaran et al. found (A and B) Bacillus spores adhered to aluminum metal coupons under protective "dome-like" structures, (C) Domes removed following nitric acid passivation, (D) Etched aluminum resulting from nitric acid passivation[97]

Nitric acid is a harsh treatment that damaged the metal and should not be applied to space hardware, and sonication-like conditions are experienced during launch, atmospheric entry, and landing. Therefore, dome-protected spores cannot be readily removed with normal cleaning techniques but could be released from their protective shells during launch and landing, potentially re-contaminating the spacecraft, instruments, and planet below.[97]

2.2.3 Efficacy of Microbial Identification Techniques

Identifying individual microbes and elucidating overall population structure on space hardware is difficult with the NASA standard spore assay.[67,72] For this technique, surfaces are swabbed or wiped, spores are removed by suspension in sterile water or buffer, heat shocked at 80°C for 15 minutes to destroy non-sporulating microbes, surviving spores plated on nutrient (i.e., tryptic soy agar), incubated at 32°C for 72 hours, and colonies that form are then counted.[80] However, only 1%- 10% of viable microbes are cultivable, so microbiome diversity is often concealed.[113] This is especially true of low-biomass surfaces like spacecraft hardware that are already kept quite clean. Further, not all microbes are spore-formers, and many non-sporulating microbes are heat-shock resistant, making them more likely to survive spaceflight.[95]

Polymerase chain reaction (PCR)- based techniques are also approved by NASA for detecting and identifying microbes. PCR isolates rRNA, amplifies the sample by cloning these strands with purified DNA segments, reads the amplified strands, and identifies them by comparison to a library of known genetic sequences. While PCR-based techniques are more effective than the standard spore assay, downfalls are that they are cultivation-based, the limit of detection for PCR-based techniques is high and requires ~10^2-10^3 initial copies of the target, sequencing can be expensive, and clone libraries are unable to detect low-abundance organisms.[67,107]

Numerous new methods of detecting low-biomass samples have recently been tested in SACs to measure the efficiency of traditional methods; one highly effective device is called PhyloChip. This small photolithography chip analyzes rRNA strands found in ultra-low biomass samples and delivers an accurate and rapid readout of the genetic sequences present to identify the population members present, even when individual organisms are low abundance in a sample. The

limit of detection for this chip is 10^{-4} abundance of the total sample, as opposed to 10^{2}-10^{3} for PCR methods.[114]

Ghosh et al. used cultivation and PCR-based methods to characterize microbes found in SACs during assembly of the Mars Phoenix lander and found that for 28 sampling events, viable microbes ranged between $3.2x10^{3}/m^{2}$- $3.4x10^{5}/m^{2}$, but 0%- 26.7% of those viable organisms are cultivable, and spore-formers made up less than 1% of total viable microbes, with 11 of the 28 samples yielding zero spore-formers.[73] This shows that even PCR-based methods identify significant numbers of microbes in SAC environments.

Cooper et al. conducted a study of flight hardware in spacecraft assembly cleanrooms, comparing NASA standard spore assay results to PhyloChip results, and found that there is little correlation between numbers of spore-formers and total number of viable organisms. While many of the 107 surfaces samples yielded low spore abundances (most with less than 20 spores and no surface having greater than 160 spores), total extrapolated cell density on those same surfaces ranged from $1x10^{6}$- $1x10^{10}$, as seen in Figure 9.

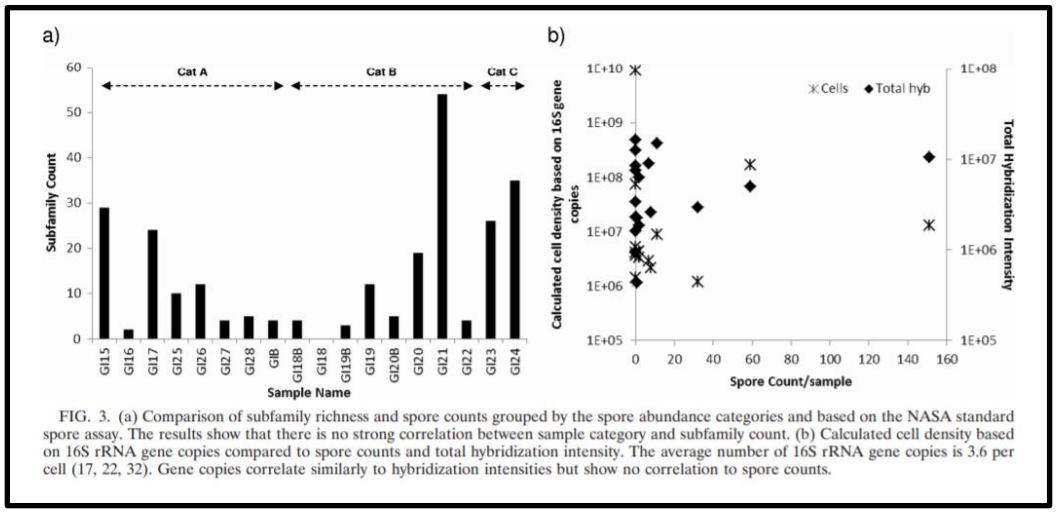

FIG. 3. (a) Comparison of subfamily richness and spore counts grouped by the spore abundance categories and based on the NASA standard spore assay. The results show that there is no strong correlation between sample category and subfamily count. (b) Calculated cell density based on 16S rRNA gene copies compared to spore counts and total hybridization intensity. The average number of 16S rRNA gene copies is 3.6 per cell (17, 22, 32). Gene copies correlate similarly to hybridization intensities but show no correlation to spore counts.

Figure 9. Comparison of (a) spores identified by the NASA standard spore assay and (b) extrapolated cell counts based on 16S rRNA assay from SAC samples, as reported by Cooper et al.[115]

Many individual surfaces yielded 0 spores but hosted an excess of 100 operational taxonomic units (OTUs, i.e., genetically distinct microbial types, typically resolved at the genus level), but at the same time, surfaces with higher spore counts did not yield proportionally higher numbers of OTUs.[116] Overall, flight hardware sampled met PP limits for spores with an average of ~5.8 spores/m^2, but there were about ~$1.8x10^5$ cells/m^2 on the same surfaces. These microbes were genetically diverse, with a propensity of non-spore-forming heat-shock-resistant microbes.[115]

La Duc et al. used PhyloChip and PCR to study contaminant populations at Kennedy Space Center, Jet Propulsion Laboratory, and Lockheed Martin Aeronautics Multiple Testing Facilities during assembly of the Phoenix and Mars Science Laboratory spacecraft and successfully identified 9-70 fold more species than with PCR-based methods. A total of 173 families were detected, with PhyloChip responsible for identifying 169 of these families (30 of which come from unclassified bacterial groups). A mere 3 families were detected with both methods, and only 4 families were detected with PCR cloning methods alone. Of the 140 known bacterial families, nearly 100 were never before observed in clone libraries (Figure 10).[67]

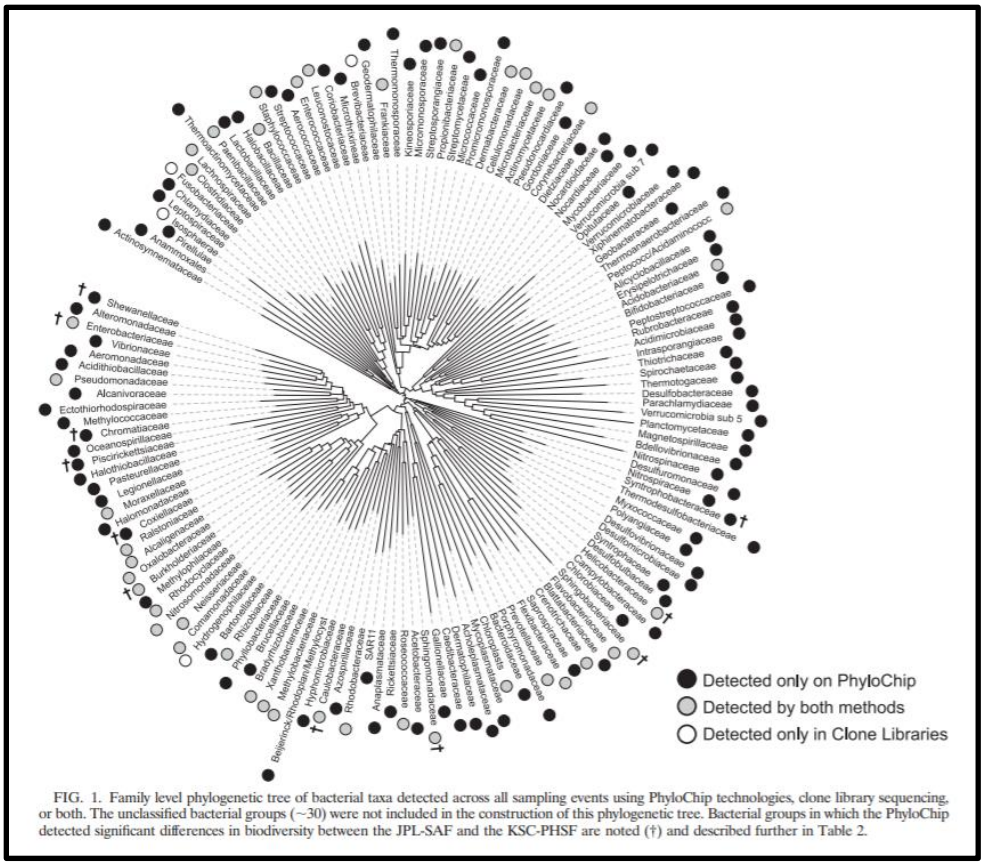

FIG. 1. Family level phylogenetic tree of bacterial taxa detected across all sampling events using PhyloChip technologies, clone library sequencing, or both. The unclassified bacterial groups (~30) were not included in the construction of this phylogenetic tree. Bacterial groups in which the PhyloChip detected significant differences in biodiversity between the JPL-SAF and the KSC-PHSF are noted (†) and described further in Table 2.

Figure 10. Family level phylogenic tree of microbes in a SAC detected by Phylochip only (black), clone libraries only (white), and both methods (grey), as reported by La Duc et al.[67]

Probst et al. also compared PCR cloning methods to PhyloChip sampling in three cleanrooms where the Mars Science Laboratory rover was assembled and found that PhyloChip detected a ~10-fold increase in individual species detected over PCR methods.[107] In another study, Vaishampayan et al. utilized PCR and PhyloChip on various locations from cleanrooms where the Mars Phoenix Lander was assembled and found that PCR-based cloning methods identified a total of 258 OTUs in the three locations while PhyloChip identified 1922.[71]

It is important to note that although contamination levels are higher than previously expected, microbe counts did not exceed the total limit set by PP regulations for any of the

spacecraft sampled in these studies.[67,71,107,115] However, these numbers do show that microbe counts in SACs are too high for sensitive life detection instruments that have ~ppb LoDs.[117]

2.2.4 Non-Viable Microbial, Cellular, and Molecular Contamination

Living microbes are a concern for PP, but dead microbes and intracellular material are arguably more concerning to astrobiology missions, since PP spore limits do not apply to dead microbes (although "organics inventory" does), traditional sampling techniques rely on living or viable cells, and intracellular molecular material and free lipids are much more difficult to remove than larger cells due to the sticky nature of lipids and because lipids are orders of magnitude smaller than the particles removed with HEPA filters.[69]

Vaishampayan et al. conducted a spacecraft cleanroom study utilizing propidium monoazide (PMA, an agent to mask DNA from dead cells) treatment pre-sequencing to distinguish between dead microbes and live ones and found that dead cells far outnumber living ones, suggesting that 93%- 96% of total microbial cells present are dead.[72] Mahnert et al. utilized PMA treatment coupled with PhyloChip analysis in sequence with adenosine triphosphate (ATP)-based assays, aimed at distinguishing between dead and living cells as a function of intracellular versus extracellular ATP, finding that over 90% of the cells present in SACs surveyed were dead. However, uncontrolled adjoining rooms and facilities adjacent to the SACs had even higher proportions of dead cells, suggesting that cleaning techniques employed in SACs are somewhat effective at removing dead materials.[10] Weinmayer et al. analyzed eukaryotes, prokaryotes, and viruses and found that approximately 90% of all cells in SAC facilities were dead.[108] Venkateswaran et al. used ATP-based assays and found that extracellular ATP content in the SAC was 2 to 3 orders of magnitude more than intracellular ATP content, indicating that many dead

cells have been lysed open. This process would inevitably release membrane lipids during the process of cell rupture, further contributing to molecular lipid contamination.[118]

For biomolecule life detection instruments, the viability of the cell is not important, only the presence of the molecular target. Therefore, decontamination methods to remove or eliminate dead cells and intracellular material are vital to effectively clean instruments prior to spaceflight.

2.2.4 Encapsulated Contamination

Porous materials like epoxies, polymers, and other fillers commonly used in spacecraft instruments carry a burden of encapsulated endospores that are unaffected by surface cleaning. Accurate determination of encapsulated contamination levels is difficult, but it is estimated that $4x10^3$ gene copies/ 5 g of material can be expected for some filler materials like silicon-based resins. These spores can be drawn out with organic solvents, heat, or sonication. Organic solvents are often used in lipid sample handling, and heating and sonication are experienced upon entry into a planetary atmosphere, meaning that encapsulated contamination can potentially be released and re-contaminate the instrument after landing.[119,120] These porous materials are especially incompatible with baking and harsh cleaning agents, indicating that a more creative decontamination technique is necessary.

Overall, results of these studies show that assaying for spore-formers alone (as mandated by COSPAR) is not the best metric for elucidating viable or total contamination, microbial populations in SAC environments are larger and more varied than previously estimated, SACs contain a diverse range of extremophiles able to potentially survive spaceflight, traditional methods for sampling and characterizing viable microbial contamination are less than effective, and dead cells and encapsulated contamination presents a significant contamination risk.

2.3 Contamination Control Techniques and their Efficacy

Decontamination techniques used on instruments searching for extraterrestrial life encompass PP-approved methods aimed at spore count and bioburden reduction, cleanroom techniques aimed at sterilization and particulate matter reduction, and laboratory techniques aimed at removal and/or destruction of both biological matter and organic molecules. Lipid molecules are difficult to remove, these techniques have varying efficacy, and many of the most effective laboratory protocols are incompatible with the sensitive materials used in life detection instruments. Understanding the strengths and limitations of each is important.

2.3.1 Planetary Protection Approved Techniques

To ensure compliance with bioburden limits, space missions are required to apply COSPAR-validated decontamination methods for sterilization to the whole spacecraft prior to flight. Two standard techniques have been approved, including dry heat microbial reduction (DHMR) and vapor phase hydrogen peroxide (VHP).[82,121] Other chemical and radiation-based sterilization techniques are sometimes approved if necessary, but no additional standard technique has been approved for widespread applications.

DHMR includes baking at 111.7°C for 30 hours and is the primary technique recommended. DHMR decontamination has been standard protocol since the 1970s when it was applied to Viking instruments and spacecraft and successfully reduced microbial contamination below 300 spores per square meter. This led to its integration in COSPAR regulations as the "gold-standard" for spaceflight applications.[79,122] Although DHMR can achieve a 2-8 log reduction in model *Bacillus* spores, some are heat-resistant, and some extremophiles are able to survive

treatments. Further, DHMR does not remove the "dead bodies" of the spores (i.e., their biomolecules) killed following treatment. Dry heat kills spores by damaging DNA and proteins, but it does not remove their large biomolecules, and it has no effect on the much hardier lipids constituting cell membranes (Figure 11).[96,123]

Summary of Major Penetrating Bioburden Reduction Techniques

Technique	Log Reduction Range[2]	Possible Spore Resistance?	Residual Dead Bodies
DHMR	2-8	Some	Yes
Gamma	2-8	Some	Yes
γ + Heat	2-8	Unknown	Yes

Figure 11. Efficacy of major penetrating bioburden reduction techniques, including DHMR and gamma irradiation[102]

VHP was approved as a standard PP technique in 2012, since an increasing number of sensitive instruments and spacecraft components were unable to withstand DHMR application. This method requires exposure to vapor H_2O_2 for 200 seconds at concentrations of 0.5 mg/L- 1.1 mg/L to achieve a 6-log reduction in spores.[82,102,121,124] Although VHP is successful at killing spores, it does not remove dead bodies or destroy lipids. Linley found that the sporicidal mechanism of action is through extensive DNA damage, but no peroxidation of lipids occurred following application, and only minimal damage to cell membranes was sustained, illustrated in Figure 12.[125]

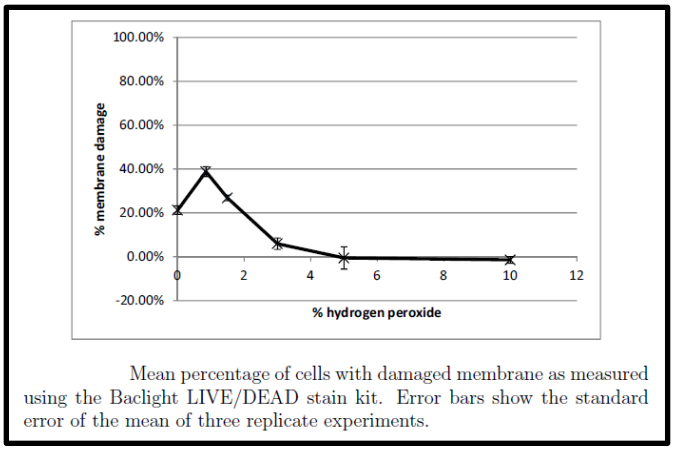

Figure 12. Membrane damage following application of VHP at varying concentrations, as reported by Linely[125]

Instead of DHMR and VHP, radiation-based techniques, including gamma and x-ray radiation, are sometimes approved for component or whole-spacecraft sterilization because they are both effective at killing microbes through double-stranded DNA breaks and space hardware-compatible.[89,90,126,127] However, effects on dead cells and molecular contaminants have not been elucidated. To determine whether these sterilization techniques can also remove biomolecules, further research is needed. In addition to the approved methods for sterilization, mission PP plans typically include fabrication and integration in a cleanroom, where controlled environmental conditions focus on controlling contamination. Ultimately, PP-approved methods are highly materials-compatible, but do not remove or destroy molecular lipid contamination below life detection analytical instrument limits of detection.[8,125]

2.3.2 Cleanroom Techniques

Spacecraft assembly cleanrooms are highly controlled environments, engineered to limit microbial and particulate contamination. Cleanrooms must maintain a sterile environment, with stringent limits on the number of airborne particles of various sizes as designated by the International Organization for Standardization (ISO). There are nine class designations, ranging

from ISO 1- ISO 9, where ISO 1 is the cleanest and ISO 9 is the least strictly controlled.[128] An alternate naming system is sometimes used; this system preceded and informed the ISO classification system and was governed by the US Federal FED-STD-209 E *Airborne Particulate Cleanliness Classes in Cleanrooms and Cleanzones*. It recognizes 6 classes, equivalent to ISO 3-ISO 8, and named by number of particles permitted, with designations for Class 1, Class 10, Class 100, Class 1,000, Class 10,000, and Class 100,000. Table 1 details particle limits by cleanroom class.

Table 1. FED STD 209E and ISO cleanroom classes with airborne particle limits by size per m^3

FED STD 209E equivalent	ISO classification	Maximum concentration of particles per m^3 of air by particle size					
		0.1 µm	0.2 µm	0.3 µm	0.5 µm	1 µm	5 µm
	ISO Class 1	10	2				
	ISO Class 2	100	24	10	4		
Class 1	ISO Class 3	1,000	237	102	35	8	
Class 10	ISO Class 4	10,000	2,370	1,020	352	83	
Class 100	ISO Class 5	100,000	23,700	10,200	3,520	832	29
Class 1,000	ISO Class 6	1,000,000	237,000	102,000	35,200	8,320	293
Class 10,000	ISO Class 7				352,000	83,200	2,930
Class 100,000	ISO Class 8				3,520,000	832,000	29,300
Room Air	ISO Class 9				35,200,000	8,320,000	293,000

It is important to note that lipids are much smaller than the smallest particles controlled by ISO regulations and are unable to be removed by HEPA filters, so while air filtration can remove larger particles containing lipids, free organics will not be removed with these filters. HEPA air filters cycle air to remove airborne particles of the designated sizes from the cleanroom, and laminar air flow is used to ensure no stagnant air can remain uncirculated. Laminar flow controls air into directed, layered paths so that there is no mixing of the air layers, which ensures that air change per hour (ACH) requirements are met. Spacecraft are typically assembled in ISO Class 5

cleanrooms, but sensitive life detection instruments are often fabricated in more stringently controlled spaces or gloveboxes.[129]

Prior to entry, any materials brought into cleanrooms must be cleaned and bagged. Human presence is kept to a minimum, as humans shed over one million particles (i.e., skin cells, bacteria, hair, etc) per hour and human-introduced microbes represents from 50% to upwards of 75% of the contamination in cleanrooms. Protective gear like bunny suits, hair nets, shoe covers, and gloves is donned prior to cleanroom entry. Hair products, aerosol products, perfumes, and makeup must be avoided because these substances can slough off as particulate matter.[122,129] However, while this can limit contamination, microbial SAC surveys show that many microbes and cells still persist.

To remove contamination that does make its way into the cleanroom, hardware, tools, floors, walls, and other surfaces are routinely cleaned with water, detergent, and isopropyl alcohol using clean swabs.[128] Cleaning agents include ethanol, 2-propanol, glutaraldehyde, iodine and

chlorine compounds, peroxyacids, hydrogen peroxide, ethylene oxide, propriolacone, and various detergents, varied to remove the maximum diversity of microbes (Figure 13).[9,83,123]

Summary of mechanisms of antibacterial action of antiseptics and disinfectants

Target	Antiseptic or disinfectant	Mechanism of action
Cell envelope (cell wall, outer membrane)	Glutaraldehyde	Cross-linking of proteins
	EDTA, other permeabilizers	Gram-negative bacteria: removal of Mg^{2+}, release of some LPS
Cytoplasmic (inner) membrane	QACs	Generalized membrane damage involving phospholipid bilayers
	Chlorhexidine	Low concentrations affect membrane integrity, high concentrations cause congealing of cytoplasm
	Diamines	Induction of leakage of amino acids
	PHMB, alexidine	Phase separation and domain formation of membrane lipids
	Phenols	Leakage; some cause uncoupling
Cross-linking of macromolecules	Formaldehyde	Cross-linking of proteins, RNA, and DNA
	Glutaraldehyde	Cross-linking of proteins in cell envelope and elsewhere in the cell
DNA intercalation	Acridines	Intercalation of an acridine molecule between two layers of base pairs in DNA
Interaction with thiol groups	Silver compounds	Membrane-bound enzymes (interaction with thiol groups)
Effects on DNA	Halogens	Inhibition of DNA synthesis
	Hydrogen peroxide, silver ions	DNA strand breakage
Oxidizing agents	Halogens	Oxidation of thiol groups to disulfides, sulfoxides, or disulfoxides
	Peroxygens	Hydrogen peroxide: activity due to from formation of free hydroxy radicals (•OH), which oxidize thiol groups in enzymes and proteins; PAA: disruption of thiol groups in proteins and enzymes

Figure 13. Summary of mechanisms of antibacterial action of selected antiseptics and disinfectants commonly used in cleanrooms[9]

While these agents can kill many microbes, some extremophiles can even subsist upon the very cleaning agents employed to destroy them. Vaishampayan et al. found that *Acinetobacter* in Mars Phoenix Lander SACs increased ~10-fold throughout spacecraft assembly, with much of this increase occurring after application of cleaning agents. *Acinetobacter* metabolize or biodegrade ethanol, 2-propanol, and Kleenol 30 (a detergent used in SACs), so cleaning actually fed the microbes instead of killing them.[71] Mogul et al. found that *Acinetobacter* are able to oxidize ethanol and 2-propanol, and use the carbon liberated as a primary energy source in low-nutrient environments, probably due to alcohol dehydrogenase enzymes in their membranes. They also found that *Acinetobacter* biodegrade Kleenol 30.[130] Although these and other chemical cleaning agents can wipe away some cells, kill microbes, and some can damage membranes and oxidize lipids, they do not remove or degrade lipid organics to levels demanded by life detection

instruments. Further, many major instrument materials are sensitive and can be damaged by these agents.[8,9]

For validation, microbial sampling from various hardware and SAC surfaces, but aforementioned studies show that sampling methods underestimate bioburden and do not detect molecular lipid contamination.[67,97,115] While SAC CC techniques do help maintain a very clean environment and typically succeed in reducing viable aerobic spores to meet PP limits, they do not reduce encapsulated, surface biological, or molecular lipid contamination to ~ppb levels required by life detection instrument LoDs.

2.4 Electron Beam Irradiation

One promising technique for decontamination is Electron Beam Irradiation (EBI). This technique has been widely used in medical, food, and wastewater treatment industries for both microbial and lipid decontamination and proposed for PP applications but it has not yet been applied to life detection instruments.

2.4.1 Electron Beam Irradiation Mechanisms

EBI uses linear accelerators (LINAC) or particle accelerators to concentrate, focus, and blast a machine-generated stream of electrons directly onto material surfaces to kill microbes and destroy contamination, shown in Figure 14.

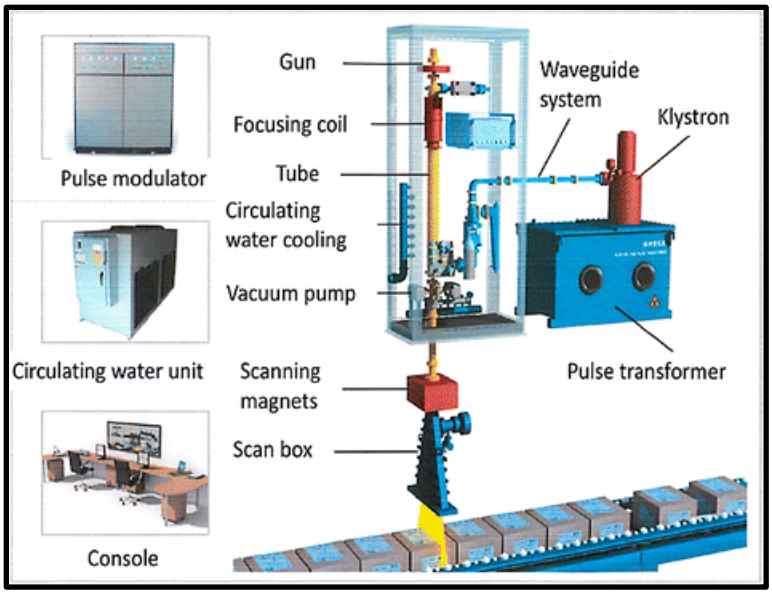

Figure 14. Electron beam irradiation setup; beam is generated from the gun, then focused and directed onto the conveyor belt below to decontaminate boxes of materials[86]

This effectively and efficiently eliminates contamination because it degrades molecules instead of simply mechanically wiping away material. EBI is measured in kilograys (kGy), a unit of absorbed energy where 1 Gray (Gy) is equal to 100 rad, and 1 rad is equal to 0.01 J/kg.[131] Electron irradiation is tunable by both dosage (1 kGy- ~100s of kGy) and depth (10 µm for 50 keV electrons- 10 cm for 10 MeV electrons) and can penetrate into materials with potential to destroy contamination encapsulated in porous materials and trapped between mated parts. EBI is safer and cheaper than gamma irradiation because it is simply a machine-generated stream of electrons, and does not require radioisotopes, whereas photon-based gamma irradiation requires cobalt-60 or cesium-137 generated in nuclear reactors.[85,127] X-ray irradiation is similar to EBI in that it uses a LINAC accelerator as a first step, however, it differs because the accelerator blasts the electrons into a

shield of tantalum or gold, which generates photons that subsequently penetrate the material undergoing irradiation (Figure 15).

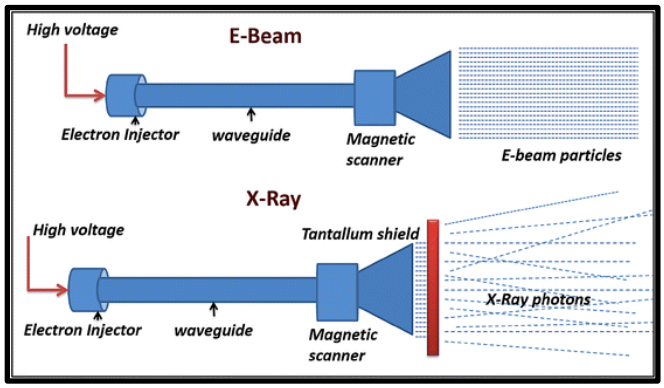

Figure 15. Electron beam irradiation compared to X-ray irradiation[86]

X-ray irradiation is similar to gamma irradiation because both use photons as the ionizing particles, but differs because it is cheaper and safer than gamma irradiation, does not require radioactive material, and can generate higher dose rates than gamma at ~100 Gy/sec as opposed to ~100 Gy/min.[86] However, compared to X-ray irradiation, EBI is cheaper, safer, more tunable, and more energetic. Additionally, electron beams are more easily focused than X-rays.[127]

2.4.2 Sterilizing Effects of EBI on Microbes

Gamma and electron beam irradiation are both widely used for microbiocidal capacities to sterilize food and medical devices. Gamma irradiation is sometimes approved for PP purposes, including on the would-be Beagle 2 Mars Lander life detection mission (unfortunately, the spacecraft crashed on the Martian surface).[132] Although EBI has not yet been approved for PP purposes, it has been proposed since its sterilization efficiency is on-par with gamma irradiation efficiency and EBI is materials-compatible.[90] Tallentire et al. compared sterilization efficiency of gamma to low and high energy electron beam irradiation on *Bacillus*, and found that the D_{10} values

(amount of radiation needed to achieve a 1-log reduction in viable spores) for each irradiation type are nearly the same.[133] Therefore, EBI should have the same PP applications as those of gamma.

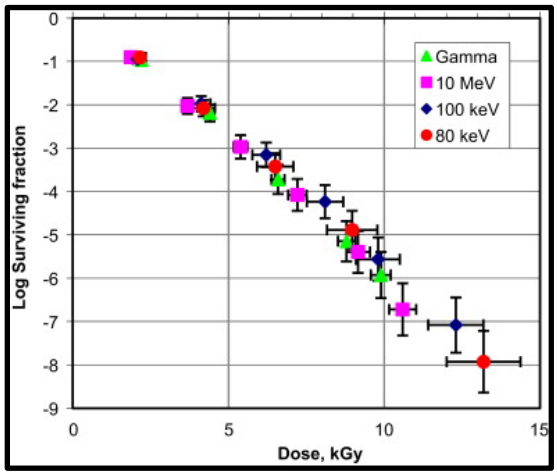

Figure 16. Sterilization efficiencies of Gamma irradiation, 10 MeV EBI, 100 keV EBI, and 80 keV EBI on Bacillus as reported by Tallentire et al.[133]

Pillai et al. irradiated several species of Bacillus spores previously isolated from SAC environments and showed them to be resilient against many CC techniques applied in those environments, including UV radiation, ionizing radiation, H_2O_2, and desiccation. Spores were inoculated onto aluminum coupons similar to materials used in spacecraft, and the setup was irradiated with EBI. They found that the D_{10} value for the species studied ranges from 2.36 kGy-4.35 kGy, doses as low as 12 kGy achieve over a 6-log reduction, and doses of 20 kGy- 40 kGy achieve over a 12-log reduction, results in Figures 17 and 18.[127]

D_{10} values of selected *Bacillus* species previously isolated from spacecraft fabrication facility on stainless steel coupons

Bacillus species	D_{10} value (kGy)
B. subtilis	2.36
B. safensis	3.50
B. megaterium	4.35
B. odyssey	2.67
B. pumilus	2.64

Figure 17. EBI D_{10} value for various Bacillus species, as reported by Pillai et al.[127]

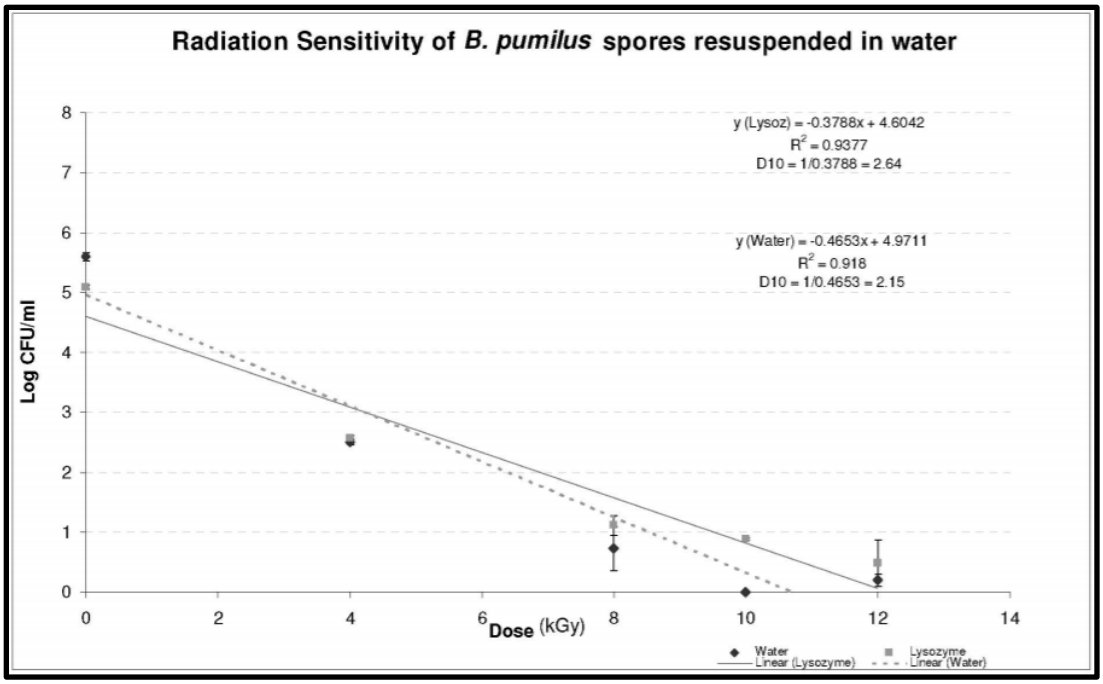

Figure 18. Radiation sensitivity of B. pumilus spores resuspended in water by log reduction and EBI dose in kGy, as reported by Pillai et al.[127]

Monk et al. found that the D_{10} value for vegetative bacteria is typically less than 1 kGy of gamma irradiation with a maximum of 10 kGy for the most radiation-resistant extremophile *Deinococcus radiodurans*, up to 4 kGy for some hardy *Bacillus* spores, and 3.5- 4.0 kGy for hardier molds.[134] Multiple other studies have recently tested EBI on various microbes and found that D_{10} values are on the same order as those for gamma irradiation.[135–138]

EBI kills microbes through a variety of chemical mechanisms, including direct hits that cause single and double stranded DNA breaks, and generation of hydroxyl radicals from radiolysis of water molecules that subsequently induce lipid peroxidation, protein denaturation, and damage to the cellular membrane, as illustrated in Figure 19.[85,139,140]

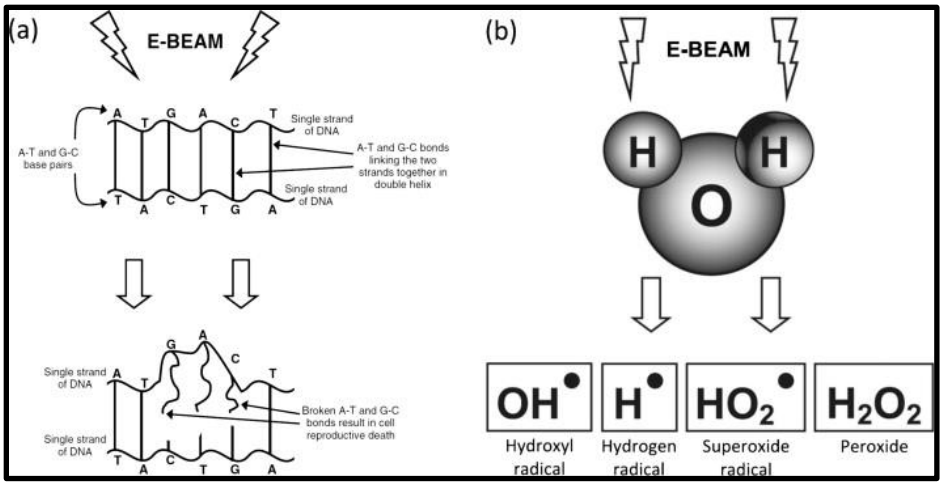

Figure 19. (a) EBI direct effects on DNA and RNA, breaking chemical bonds between base pairs and (b) EBI indirect effects on water molecules, including radiolytic breakdown into hydroxyl radical, hydrogen radical, superoxide radical, and peroxide[140]

Since EBI is highly effective at killing microbes at low doses with similar efficiency as commonly-approved gamma irradiation, it has been proposed as a potential decontamination method for spaceflight applications.[89,90]

2.4.3 Effects of Electron Beam Irradiation on Food and Wastewater Lipid Profiles

Although EBI has been shown to effectively kill microbes at low doses, effects on lipid organics have not been fully elucidated for application to spacecraft. EBI-induced lipid breakdown in foods and wastewater have been studied, but relatively low doses are typically used and applied to complex food and wastewater matrices, which are far more congested with biomolecules than the surfaces of already clean life detection instruments.

A review of the literature finds studies measuring the effects of EBI on total and proportional fatty acid content in food, but no consistent patterns are seen across or within these studies. Supriya et al. irradiated *Canavalia* seeds with EBI doses of 2.5 kGy, 5 kGy, 10 kGy, and 15 kGy, and analyzed total fatty acid profiles following exposure with several different lipid

extraction methods. They found that while some fatty acids were reduced or eliminated after irradiation, other short chain fatty acid concentrations rose with increasing EBI dose. Results varied by seed type, with individual fatty acids decreasing following irradiation in one seed species but increasing following application of the same dose in another (Figure 20).

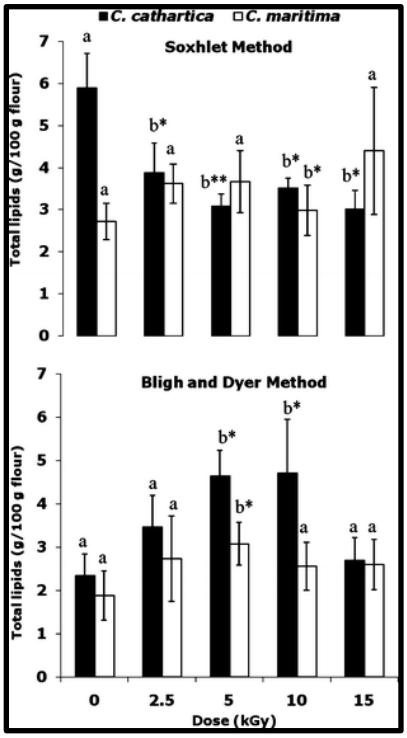

Figure 20. Total lipid yield from Canavalia seeds following irradiation at varying doses, extracted with different lipid extraction methods including the Soxhlet method (top) and Bligh and Dyer method (bottom), as reported by Supriya et al.[141]

No observable pattern was determined, and the authors hypothesize that seed material, presence of other biomolecules, food matrix, and lipid extraction technique used may have affected the ratio changes. They describe molecular changes in lipids as being due to oxidation, especially of double bonds in unsaturated fatty acids.[141]

Bhat et al. also studied fatty acid content and profiles of *Mucuna* seeds following irradiation of doses from 0 kGy- 30 kGy, finding that crude lipid content decreased with increasing EBI dose (Figure 21).

Proximate composition of *Mucuna* seeds treated with electron beam irradiation (on dry weight basis) (n = 5, mean ± SD)

Component	Dose (kGy)						
	0	2.5	5	7.5	10	15	30
Moisture (%)	9.58 ± 0.35	8.86 ± 0.56	8.87 ± 0.02	8.83 ± 0.25	8.96 ± 0.41	8.39 ± 0.02	8.18 ± 0.01
Crude protein (g/100 g)	23.04 ± 0.38	23.20 ± 0.35	23.91 ± 1.05	23.97 ± 0.57	24.17 ± 0.37	26.97 ± 1.01	27.03 ± 1.09
Crude lipid (g/100 g)	7.13 ± 0.17	6.26 ± 0.04	5.60 ± 0.01	4.84 ± 0.03	4.15 ± 0.03	4.16 ± 0.03	3.64 ± 0.01
Crude fibre (g/100 g)	7.86 ± 0.04	6.97 ± 0.03	6.62 ± 0.5	6.38 ± 0.65	6.40 ± 1.2	6.33 ± 0.54	5.76 ± 0.91
Ash (g/100 g)	4.79 ± 0.72	4.71 ± 0.09	4.75 ± 0.02	4.61 ± 0.12	4.49 ± 0.21	4.24 ± 0.75	4.14 ± 0.21
Crude carbohydrates (g/100 g)	57.18 ± 0.93	58.84 ± 0.29	58.90 ± 1.49	59.98 ± 0.80	60.67 ± 1.24	58.67 ± 1.62	59.26 ± 1.7
Gross energy (kJ/100 g)	1609 ± 10.1	1607 ± 0.9	1607 ± 3.2	1587 ± 9.1	1560 ± 7.7	1561 ± 8.6	1557 ± 23.9
In vitro protein digestibility (%)	50.65 ± 5.42	54.87 ± 6.92	54.05 ± 10.5	55.53 ± 2.75	57.33 ± 1.84	63.68 ± 7.7	47.68 ± 10.2

Figure 21. Biomolecule content of Mucuna seeds following EBI application at varying doses, as reported by Bhat et al. Crude lipid content highlighted with red box[142]

They determined that while most unsaturated fatty acids decreased following irradiation, saturated fatty acid content increased with increasing EBI dose, hypothesized because irradiation can induce oxidation of double bonds.[142]

Fernandes et al. conducted a study quantifying the effects of EBI on fatty acid profiles of *Macrolepiota procera* mushrooms, finding that overall, fatty acids tended to decrease with increasing EBI dose application, but eicosapentaenoic acid increased following irradiation. They also found that while saturated fatty acids decreased with increasing EBI doses from 0.5 kGy- 6 kGy, monounsaturated fatty acids increased, then decreased, then increased again. Polyunsaturated fatty acids increased then decreased, with a net gain for both unsaturated groups. No consistent pattern was apparent, and the authors note that further study is needed to better characterize the chemical effects of EBI on fatty acids.[143] Jo et al. conducted a similar study on smoked duck meat with different results, finding that for doses from 1.5 kGy- 4.5 kGy, total fatty acids, saturated fatty acids, monounsaturated fatty acids, and polyunsaturated fatty acids all decreased with increasing dose.[144]

Wong and Kitts expected irradiation of eggs would induce lipid breakdown through oxidation, but doses of 2 kGy- 4 kGy did not result in any formation of lipid oxidation products. While these doses did kill microbes and break down proteins, lack of lipid breakdown was hypothesized as being due to structural elements in the egg that protected the lipids from degradation and prevented them from undergoing oxidation reactions. This finding is important because it suggests that radiolytic breakdown of lipids is affected by the structure of the food matrix and not just on the lipid profile itself or interactions with other biomolecules.[145]

In addition to sterilizing food, EBI is used to treat sewage. Lim et al. studied EBI as a technique for removing crude lipid content from swine wastewater, concluding that it is relatively successful, however, irradiation was used in parallel with denitrification techniques aimed at solubilizing biomolecules for removal, so it is difficult to attribute effectiveness to one treatment versus a combinatory effect of both. Further, they used high doses of 20 kGy- 100 kGy, but reduction in lipid content via solubilization was only consistently observed up to 75 kGy- at higher doses, efficiency decreased (Figure 22).[87]

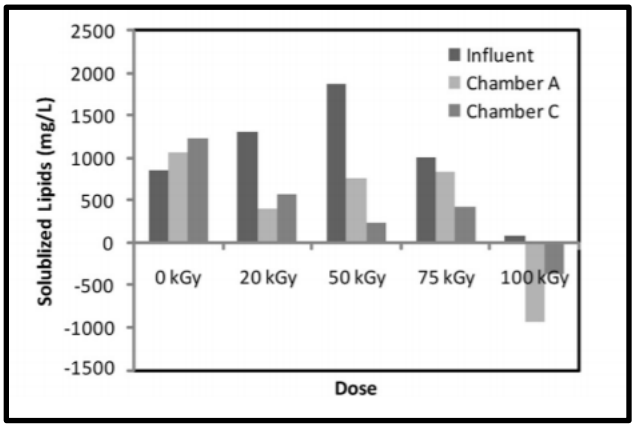

Figure 22. Solubilized lipid content in swine wastewater following EBI treatment at varying doses, as reported by Lim et al.[87]

The inconsistent results of these studies can be attributed to multiple factors, including material, presence of other biomolecules, irradiation temperature conditions, overall lipid content, individual lipid profiles, and other treatments applied in parallel with EBI.

2.4.4 Effects of Electron Beam Irradiation on Volatilized Lipids

In addition to food-based irradiation studies, a review of the literature finds an important investigation by Seo et al. on EBI-induced decomposition of volatilized fatty acids. This study irradiated aerosolized fatty acids (including acetic acid, propionic acid, butyric acid, isovaleric acid, and valeric acid) in concentrations of 12.5 ppm- 100 ppm with EBI doses of 5 kGy- 20 kGy in the presence of various gases, including He, Air, N_2, and O_2. They found that EBI was very successful in removing these fatty acids, with 100% of the 50 ppm acetic acid removed with only 5 kGy of irradiation. Results are illustrated in Figure 23.

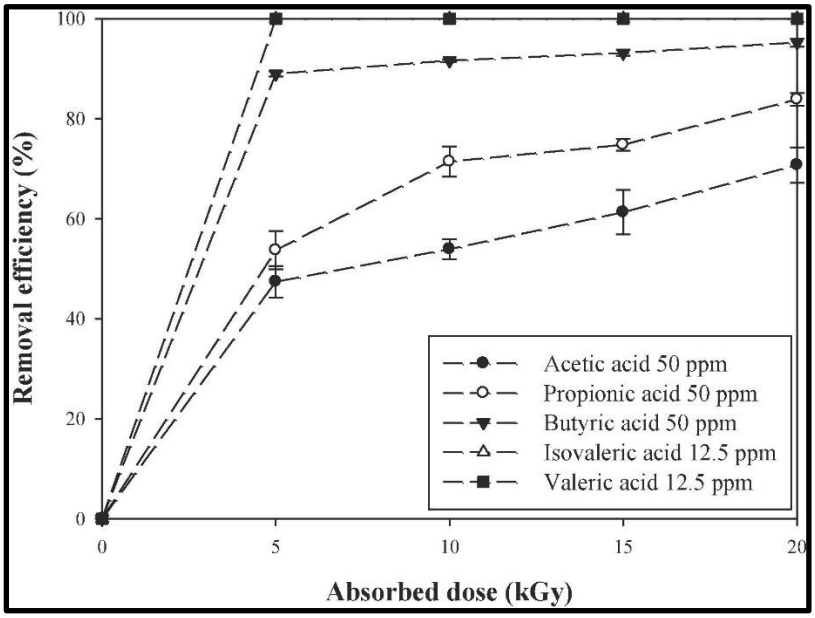

Figure 23. Removal efficiency of volatilized fatty acids for various doses of EBI, as reported by Seo et al.[146]

They found that high molecular weight fatty acids first decomposed into lower weight fatty acids, but that a range of breakdown products were created through irradiation, as illustrated in Figure 24 for valeric acid.

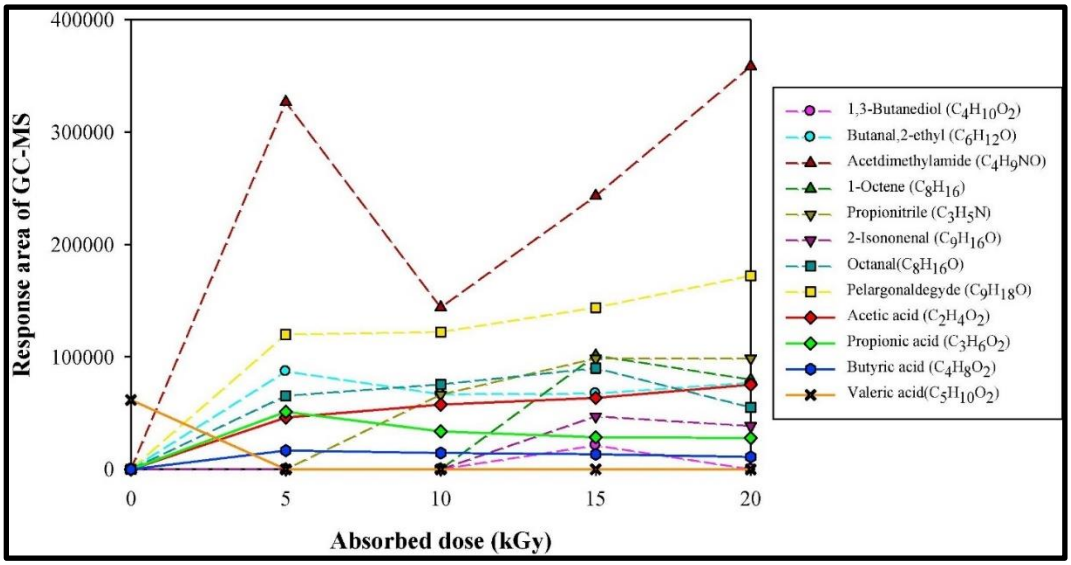

Figure 24. Breakdown products of irradiated volatilized fatty acids, detected with GC-MS by Seo et al.[146]

They also found that N_2 was an effective background gas; O_2 was not required to oxidize the lipids, and all background gases enabled removal with EBI, even those that are inert.

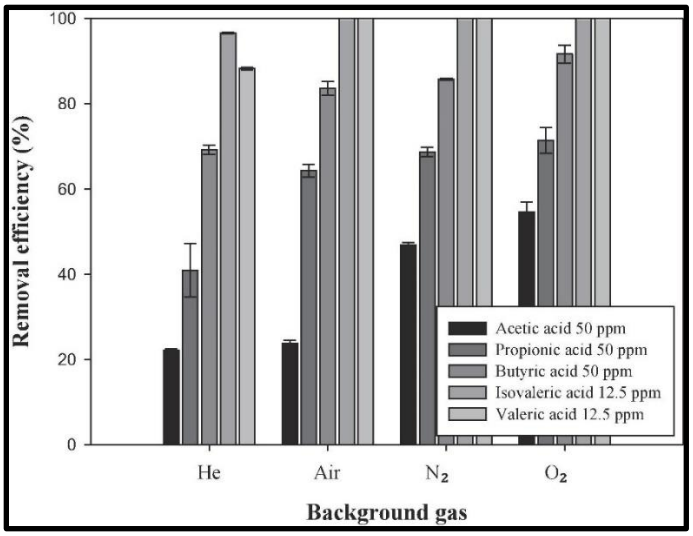

Figure 25. Removal efficiency of various volatilized fatty acids suspended in He, air, N_2, and O_2, as reported by Seo et al.[146]

This study is important because, unlike food industry studies, EBI is applied to lipids present in very low (~ppm) starting concentrations, which is akin to pre-cleaned and sterilized life detection hardware. Additionally, a range of background gases were studied and subjected higher irradiation doses than those of most food studies. However, lipids were volatilized, not seeded onto a solid substrate, and only a handful of short chain fatty acids were irradiated. The suggests that EBI may be more efficient at degrading lipids from life detection instrument hardware compared to complex food and wastewater, but further study is needed to understand how larger lipids on surfaces are affected by EBI.[146]

2.4.5 Formation of 2-Alkylcyclobutanones through Radiolysis of Lipids

Food industry studies have identified the production of 2-alkylcyclobutanones (2-ACBs) as unique radiolytic products (URPs) created after irradiation of triglycerides and fatty acids. URPs are unique compounds formed only through irradiation, with potential to serve as markers that a food has undergone radiation processing for sterilization because the compounds will not appear in the food indigenously.

A review of the literature finds a maximum of 60 kGy applied to foodstuff in a study by LeTellier and Nawar, who investigated lipids as URPs for identification of irradiated foods and discovered that 2-ACBs are URPs for triglycerides. This method of testing for past radiation processing has been accepted by the European Committee for Standardization.[147,148] During irradiation, fatty acids are cleaved and a four-carbon ring is formed at the first carbon adjacent the carboxyl group. It is hypothesized that the four-carbon ring can only form when high energy ionizing radiation is applied to the molecule for a short time (Figure 26).[92]

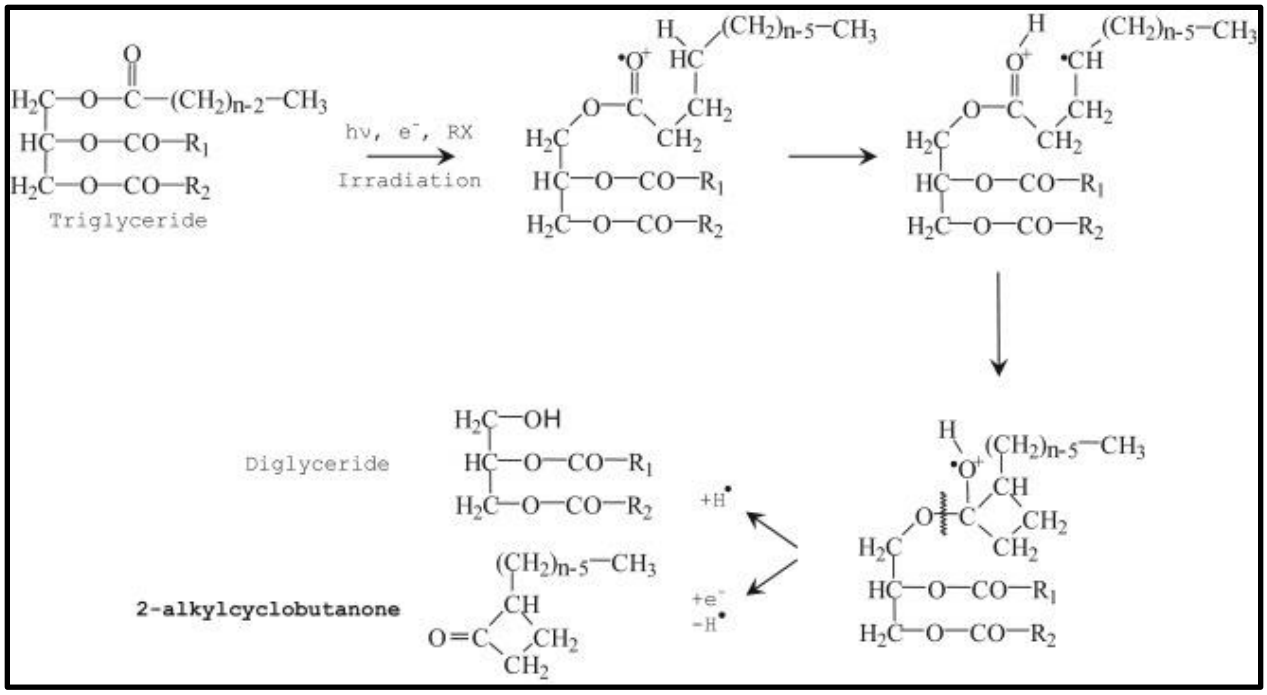

Figure 26. Reaction pathway for formation of 2-alkylcyclobutanones from triglycerides during EBI[149]

Depending on the chain length of the fatty acid, different 2-ACBs will form with corresponding chain lengths, but the butanone group is common to all. In addition to the unique 2-ACBs, volatile hydrocarbons are also produced as an irradiation byproduct.

Ndiaye et al. studied 2-ACBs produced by EBI of food, and describe a linear relationship between irradiation dose and 2-ACB yield (Figure 27)[150], but other similar studies have found inconsistent yields in production of both 2-ACBs and volatile hydrocarbons following irradiation.

Concentrations of 2-alkylcyclobutanones (nmol/mmol precursor fatty acid) in relation to the irradiation dose (kGy). Concentrations: mean of three measurements (standard deviation in parentheses); nd: not detected

	Dose	2-HCB	2-OCB	2-DCB	2-DdCB	2-TCB
Triglycerides	0.0	nd	nd	nd	nd	nd
	0.9	1.6 (0.2)	1.2 (0.2)	1.1 (0.1)	1.4 (0.2)	1.3 (0.2)
	3.1	4.1 (0.2)	4.4 (0.2)	4.0 (0.3)	4.3 (0.2)	2.6 (0.4)
	4.6	5.4 (0.4)	6.8 (0.3)	7.0 (0.2)	8.1 (0.2)	5.2 (0.3)
Cheese	0.0	nd	nd	nd	nd	nd
	0.9	1.7 (0.2)	1.5 (0.2)	1.5 (0.2)	1.5 (0.1)	1.2 (0.2)
	2.0	2.9 (0.2)	2.6 (0.2)	2.7 (0.2)	2.4 (0.2)	2.4 (0.2)
	3.1	4.8 (0.3)	4.0 (0.2)	4.7 (0.3)	4.4 (0.2)	3.2 (0.2)
Trout	0.0			nd	nd	nd
	0.9			1.0 (0.1)	1.1 (0.2)	0.8 (0.1)
	2.0			3.5 (0.3)	2.3 (0.2)	2.9 (0.2)
	3.1			4.2 (0.3)	4.1 (0.2)	3.7 (0.2)
Sardine	0.0			nd	nd	nd
	0.9			1.7 (0.2)	1.2 (0.1)	0.9 (0.1)
	2.0			2.6 (0.2)	2.1 (0.1)	1.8 (0.1)
	3.1			3.8 (0.4)	3.2 (0.2)	3.1 (0.1)
Mango (kernel)	0.0				nd	nd
	0.5				0.8 (0.2)	0.7 (0.1)
	0.9				1.4 (0.2)	1.1 (0.1)
	2.0				2.1 (0.1)	1.8 (0.1)
Chicken	0.0				nd	nd
	0.9				1.0 (0.1)	1.0 (0.1)
	2.0				2.2 (0.1)	1.7 (0.2)
	3.1				3.1 (0.1)	3.1 (0.2)
Beef	0.0				nd	nd
	0.9				0.7 (0.2)	0.4 (0.1)
	2.0				2.0 (0.2)	3.6 (0.3)
	3.1				4.6 (0.1)	5.0 (0.2)

Figure 27. Concentrations of 2-alkylcyclobutanones in various foodstuff following EBI at varying doses as reported by Ndiaye et al.[150]

Marchioni et al. measured 2-ACB yield per kGy of irradiation, and found that 2-ACB production varies for food type (Figure 28).

Formation of 2-alkylcyclobutanones in nmol/mmol precursor fatty acid/kGy in various foodstuffs

Food	2-DCB	2-dDCB	2-tDCB	2-dDeCB	2-tDeCB
Milk powder	1.31	1.65	2.79	1.34	1.16
Hazel nuts	n.d.	2.44	2.74	n.d.	1.80
Chicken meat	n.d.	1.88	2.32	1.41	1.65
Beef fillet	0.70	1.33	1.67	1.09	1.59
Goose liver paste	n.d.	1.39	1.93	n.d.	1.08
Cocoa beans	n.d.	6.14	12.21	n.d.	0.71
Hamburger	0.43	1.87	4.18	0.48	1.17
Smoked salmon	0.63	0.76	1.11	0.48	0.56
Frog's legs	n.d.	1.05	1.23	n.d.	0.20
Salmon	1.03	1.30	1.20	1.31	1.21
Avocado	n.d.	1.70	n.d.	n.d.	1.00
Liquid whole egg	n.d.	1.20	1.80	0.60	0.70

n.d.: not detected

Figure 28. Concentration of 2-alkylcyclobutanones in nmol/mmol precursor fatty acid/kGy in various foodstuffs following EBI as reported by Marchioni et al.[151]

They hypothesize that radiolytic breakdown of fatty acids depends on a variety of factors, possibly including temperature of irradiation, other biomolecules present, food matrix, total lipid content, concentration of fatty acids relative to total lipid content, etc.[151] Gadgil et al. also investigated 2-ACB formation through radiolysis of ground beef, and confirmed that 2-dodecylcyclobutanone is a URP of palmitic acid, a C_{16} unsaturated fatty acid.[94] Kim et al. also found that 2-ACBs are a URP of fatty acids and triacylglycerides and that unsaturated fatty acids yield higher 2-ACB levels than saturated fatty acids do. Individual 2-ACBs identified include 2-dodecylcyclobutanone (DCB), 2-tetradecylcyclobutanone (TCB), 2-(5′-tetradecenyl)cyclobutanone (TECB), 2-(5′,8′-tetradecadienyl)cyclobutanone (5′,8′-TCB) and 2-(5′,8′,11′-tetradecatrienyl)cyclobutanone (5′,8′,11′-TCB) as individual URCs derived from palmitic, stearic, oleic, linoleic and linolenic acids.[152]

2.4.6 Formation of Hydrocarbons through Radiolysis of Lipids

In addition to 2-alkylcyclobutanones as unique radiolytic products, hydrocarbons are also formed from triglycerides and fatty acids following EBI. While these compounds are not diagnostic of past irradiation, they represent yet another breakdown pathway and product induced by irradiation.

The previously mentioned study by Kim et al. on 2-ACB yields also examined hydrocarbons formed through 10 kGy of electron beam irradiation, and found that hydrocarbons with either one (C_{n-1}) or two (C_{n-2}) carbon atoms less than precursor fatty acids are generated (Figure 29).

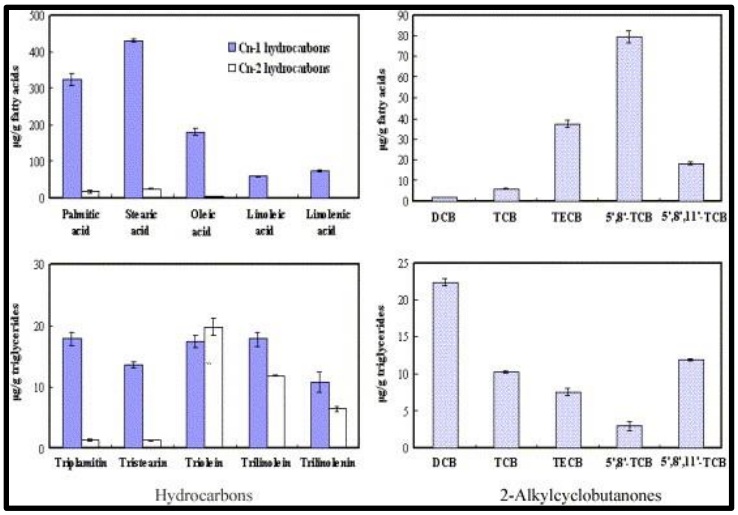

Figure 29. Comparison of C_{n-1} and C_{n-2} hydrocarbons generated from various fatty acids following EBI, as reported by Kim et al.[152]

Hydrocarbon yields do not match 2-ACB yields generated from the same sample, but represent a complementary product formed. More hydrocarbons were generated from saturated fatty acids compared to unsaturated fatty acids. Decomposition of α-carbons was higher than for the β-carbon position, and more hydrocarbons are formed from parent fatty acids compared to parent triacylglycerides.[152]

Hwang et al. irradiated ground beef at doses from 2.5 kGy- 20 kGy and found that irradiation induces formation of C_{n-1} and C_{n-2} volatile hydrocarbons from parent fatty acids (Figure 30).

Concentrations of hydrocarbons (μg/g) induced by electron beam irradiation of ground beef

	Palmitic acid ($C_{16:0}$)		Stearic acid ($C_{18:0}$)		Oleic acid ($C_{18:1}$)	
Irradiation dose (kGy)	Pentadecane ($C_{15:0}$)	1-Tetradecene ($C_{14:1}$)	Heptadecane ($C_{17:0}$)	1-Hexadecene ($C_{16:1}$)	8-Heptadecene ($C_{17:1}$)	1,7-Hexadecadiene ($C_{16:2}$)
0	0^{a} [1)]	0^{a}	0^{a}	0^{a}	0^{a}	0^{a}
2.5	$1.35^{b} \pm 0.25$ [2)]	$0.64^{b} \pm 0.29$	$0.26^{b} \pm 0.01$	$0.23^{b} \pm 0.01$	$0.68^{b} \pm 0.06$	$2.860^{b} \pm 0.15$
5	$2.51^{c} \pm 0.29$	$0.86^{c} \pm 0.28$	$0.33^{c} \pm 0.02$	$0.27^{c} \pm 0.01$	$1.60^{c} \pm 0.10$	$4.73^{c} \pm 0.25$
7.5	$2.92^{d} \pm 0.51$	$1.60^{d} \pm 0.54$	$0.71^{d} \pm 0.08$	$0.40^{d} \pm 0.08$	$2.87^{d} \pm 0.16$	$6.41^{d} \pm 0.35$
10	$4.69^{e} \pm 0.35$	$2.13^{e} \pm 0.68$	$0.77^{e} \pm 0.08$	$0.65^{e} \pm 0.06$	$3.80^{e} \pm 0.44$	$8.27^{e} \pm 0.45$
15	$7.27^{f} \pm 0.30$	$3.45^{f} \pm 0.60$	$1.06^{f} \pm 0.09$	$0.89^{f} \pm 0.08$	$6.22^{f} \pm 0.55$	$12.12^{f} \pm 0.61$
20	$11.03^{g} \pm 0.49$	$5.18^{g} \pm 0.45$	$1.60^{g} \pm 0.06$	$1.47^{g} \pm 0.06$	$9.14^{g} \pm 0.67$	$17.55^{g} \pm 0.89$

[1)] $^{a-g}$Values with different letters within a column differ significantly ($P < 0.05$).
[2)] Mean ± standard deviation ($n = 3$).

Figure 30. Concentrations of hydrocarbons generated from parent fatty acids following EBI at varying doses, as reported by Hwang et al.[93]

These shorter hydrocarbons are formed when the fatty acid carboxyl head group is cleaved from the hydrocarbon tail. They compared EBI-induced hydrocarbon formation with gamma irradiation-induced hydrocarbon formation and found similar rates of breakdown.[93] Ahn et al. also find a suite of volatile hydrocarbons formed following electron beam irradiation of pork sausages, Barba et al. find the same following irradiation of ham, and Morehouse et al. find the same following irradiation of chicken.[91,153,154]

Multiple types of breakdown appear to occur during irradiation, including oxidation of double bonds, cleavage of ester carbonyls, formation of 2-alkylcyclobutanones, and formation of volatile hydrocarbons. Ultimately, this literature review shows that EBI should induce lipid breakdown when applied to contamination on life detection instruments. However, studies on radiolytic breakdown are inconclusive and results cannot be extrapolated to EBI effects on lipid contaminants on life detection instruments, since those substrates are already quite clean compared to complex food and wastewater. Additionally, these studies use low doses compared to the ~100 kGy tolerable by life detection instruments, so further study is needed.

2.4.7 Electron Beam Irradiation Compatibility with Space Hardware Materials

Although not yet approved for use on spacecraft, EBI has been proposed for space applications and tested for compatibility with a variety of spacecraft materials. Since radiation processing is a common sterilization treatment in other industries, a growing number of radiation-resistant materials are currently being developed and manufactured and could potentially be used for life detection instrument hardware.

Pillai et al. conducted a study on EBI effects on space hardware materials, including aluminized polyethylene terephthalate, aluminized polyvinyl fluoride, spun-bonded high-density

polyethylene fiber sheets, and multilayer thermal blankets made of aluminized Mylar and Dacron nets, at doses ranging from 10 kGy- 20 kGy. Following irradiation, the materials were tested for tensile strength, load bearing capacity, stress versus strain, material extension, and total stress. Although some reduction in ability to bear stress was observed, no significant material breakdown occurred at the doses administered, suggesting that many materials will be able to withstand EBI without compromising structural integrity. Additionally, each material responded differently as a function of time following irradiation, with some only showing changes 7 days post-treatment. Further, some materials showed increased load-bearing capacity following irradiation (Figure 31).

Load bearing capacity (lbs) of 12 kGy E-beam irradiated and control (non-irradiated) epoxy (Eccobond-9®) bonded metal plates.

Sample	Load (lbs)	
	Control	Irradiated
1	229.8	146
2	188.4	337.4
3	268.3	319.2
4	225.4	296
5	302	397.4
6	277.4	177.4
7	513.6	252.8
8	351.9	447.2
9	184.4	403
Mean	282.36±102.08	308.49±102.39

Figure 31. Load bearing capacity of epoxy (Eccobond-9®) bonded metal plates following 12 kGy of EBI, as reported by Pillai et al.[127]

In the same study, Pillai et al. analyzed EBI ability to kill *Bacillus* spores, and found that 12 kGy was sufficient for a 6-log reduction in most Bacillus spores, with 15 kGy required for *B. megaterium* spores. They conclude that while some mechanical properties are compromised within 7 days following irradiation for EBI doses required to deactivate *Bacillus* spores, most mechanical properties are not significantly affected but that further study is needed to confirm their investigations on other materials.[90,127]

Spacecraft are exposed to significant amounts of irradiation during flight and while on the surface of other planets. For example, Mars has no magnetic field and experiences a high flux of solar and galactic cosmic irradiation relative to Earth, and Europa experiences a high flux of electron irradiation from Jupiter's magnetosphere. To combat these environmental conditions, space-qualified materials (e.g., polymers, solar shields, rad-hard electronics, etc.) are already engineered to withstand electron, photon, UV, and heavy particle irradiation.[155] With a wide range of materials available, compatibility with EBI could inform life detection instrument material selection during the design phase, if EBI is proven effective at decontaminating lipid organics. Since EBI is highly controllable, directable, and tunable, it can potentially be applied to instruments in a modular fashion, used only on components able to withstand contact, without harming the other portions of the instrument adjacent to the parts being irradiated (if some components are sensitive to irradiation). This is an advantage over DHMR and VHP treatments, which cannot be easily applied in a targeted fashion without impacting other regions.[127]

EBI could potentially be a final, whole-instrument decontamination technique to reduce, remove, or destroy residual organic lipid contamination not removed through other techniques. EBI could also potentially be applied as a major or primary decontamination technique for porous components that are both unable to withstand harsher treatments and have a high potential for encapsulated contamination (Figure 32). Further study is needed to assess the efficacy of EBI for decontamination and to confirm material tolerances for life detection applications.

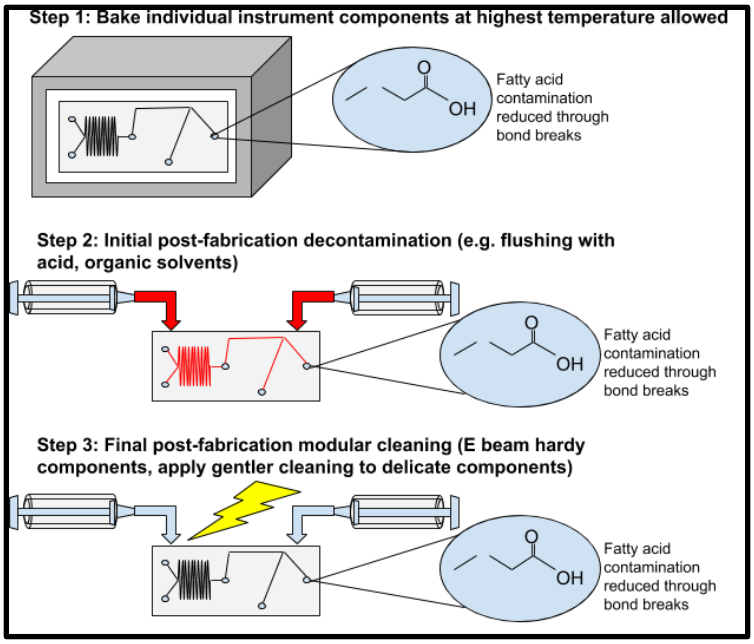

Figure 32. Hypothesized CC plan for life detection instruments, including Step 1: baking individual components at highest tolerable temps, Step 2: initial post-fabrication decontamination of sample handling stream, and Step 3: whole-instrument EBI

2.5 Knowledge Gap

In the search for extraterrestrial life, identification of molecular biomarkers is an important capability. Although this search technique has long been proposed for application to both terrestrial and icy worlds, recent advancements in the technological capabilities of life detection instrumentation have made this *in situ* analysis possible in the near future. Lipids are biomarkers of special interest because of their ubiquity in all life on Earth, vesicle-forming capability, billions of years-long preservation potential, ability to form through both biotic and abiotic processes, origin-diagnostic molecular features indicating biogenicity, and presence throughout the Solar System.

In-development lipid detection instruments for astrobiological surveys are capable of processing and analyzing samples *in situ*, can perform detailed characterization of molecular

features, couple to a variety of flight-heritage downstream analytical instruments, and have limits of detection in the ~ppb range.

Current decontamination techniques are not sufficient to meet analytical life detection instrument LoDs. PP regulations drive many CC techniques, but focus on limiting cultivable, spore-forming aerobes only, and do not address non-cultivable organisms, aerobes, dead cells, intracellular materials, or free lipids and other biomolecules. Cleanroom techniques are somewhat effective at removing whole cells (both living and dead), but analyses of contamination in SACs and on spacecraft hardware show that the problem of microbial contamination is greater than previously estimated and too high for life detection instruments.

Recent studies on CC shows that there is a gap in knowledge on how to decontaminate organic and molecular materials from life detection hardware for spaceflight. Several emerging technologies have recently been developed and used in other industries, but further study is necessary to validate their efficacy. These treatments could be applied as a complement to other techniques (i.e., cleanroom assembly, surface wipes, system flushes, baking where tolerable, etc.,) to further reduce background to lower levels than traditionally used techniques can achieve. Electron beam irradiation is one technique with promising preliminary results. EBI is tunable, machine generated, safe to use, effective for sterilization, and can be applied to both small areas and whole instruments. Further, many materials are available that are compatible with EBI. A variety of studies testing the effects of EBI on lipids suggest that it may be able to degrade these organic compounds, but there is a gap in the knowledge on how high doses of EBI would affect lipids on already relatively clean surfaces like life detection instruments.

To bridge this gap, I applied EBI, at varying doses, to a range of lipid organics identified as targets of life detection surveys in order to determine if this technique can be used for

contamination control for life detection instruments. EBI is not suggested as a standalone CC technique utilized in lieu of other treatments, but would instead represent a final, whole-system decontamination technique for reducing contamination after other cleaning treatments have been applied. EBI could also be applied to sensitive components (particularly porous materials with encapsulated contamination) that are unable to undergo other harsh but highly effective techniques (i.e., ashing, flushing/sonicating with organic solvents/acids).

CHAPTER III: METHODOLOGY

To explore electron beam irradiation as a potential lipid decontamination technique for life detection instruments, five molecular standards were selected for study from representative lipid classes identified as both targets of life detection surveys and potential terrestrial contaminants. Aliquots of these standards were prepared in triplicate at Dr. Mary Beth Wilhelm's organic biogeochemistry laboratory at NASA Ames Research Center in Mountain View, CA. The sealed lipid aliquots were subjected to varying doses of electron beam irradiation previously identified as tolerable by major materials used in life detection instruments (0 kGy, 50 kGy, and 100 kGy), at Steri-Tek Expert Sterilization Services in Fremont, CA. Post-irradiation, fatty acid, alkane, sterol, and sterane aliquots were subsampled, spiked with an internal standard, derivatized where appropriate, and analyzed with gas chromatography mass spectrometry (GC-MS) in Dr. Wilhelm's laboratory. Percent reduction in standards as a function of irradiation dose was quantified to determine whether electron beam irradiation can radiolytically degrade lipid contaminants from life detection hardware below analytical instrument limit of detection.

3.1 Experimental Setup

3.1.1 Sample Selection

Five representative molecular standards were selected from four lipid classes, including: fatty acids (i.e., carboxylic acids), alkanes (i.e., straight chain hydrocarbons), and sterols/steranes (i.e., cyclic triterpenoids). Selection criteria was based upon (1) biological and astrobiological

relevance and (2) terrestrial contamination risk for life detection instrumentation. Standards are detailed in Table 2.

Table 2. Experimental lipid standards, including identification, classification, biological and astrobiological relevance, biogenicity, and contamination potential

Molecular structure	Target compound	Chemical formula	Lipid class	Biological and astrobiological relevance	Biotic or abiotic synthesis	Contamination potential
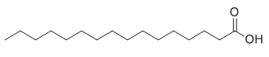	Palmitic acid (C16:0)	$C_{16}H_{32}O_2$	Saturated free fatty acid	Membrane lipid subcomponent, abundant in biology. High geologic preservation potential.	Both	High, common in cell membranes
	Oleic acid (C18:1)	$C_{18}H_{34}O_2$	Monounsaturated free fatty acid	Membrane lipid subcomponent, abundant in biology. Unsaturation lost rapidly, but the rest of the compound has high preservation potential.	Both?	High, common in cell membranes
	Heneicosane (C21)	$C_{21}H_{44}$	Saturated alkane	Common to plant waxes and as fatty acid subcomponent. Very high preservation potential.	Both	High, common in machine oils
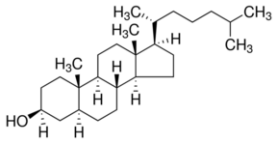	5α-cholestan-3β-ol (cholestanol)	$C_{27}H_{48}O$	Sterol	Steroid alcohol, hopanoid proxy. High preservation potential.	Biotic	Low, uncommon laboratory contaminant
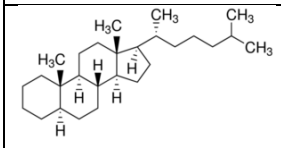	5-α-cholestane (cholestane)	$C_{27}H_{48}$	Sterane	Diagenetically degraded sterol, hopanoid proxy. High preservation potential.	Biotic (geologically processed)	Low, uncommon laboratory contaminant

1. Palmitic acid: a $C_{16:0}$ saturated free fatty acid. Free fatty acids comprise a hydrocarbon tail with a carboxyl head group and can form both biotically and abiotically. In biotic systems, palmitic acid attached to a phosphate or glycerol head group makes up cell membranes. Palmitic acid is an important biomarker because it is one of the most abundant fatty acids used by organisms. Fatty acids are relatively long-lived in the terrestrial record (~100s of millions of years [Myr]), but the carboxyl group can be cleaved during diagenesis, leaving behind a C_{n-1} alkane as a breakdown byproduct. Since fatty acids are abundant in terrestrial biology, these compounds have high potential for contaminating life detection instruments.[24,37]
2. Oleic acid: a $C_{18:1}$ monounsaturated free fatty acid. It differs from saturated free fatty acids because it contains one double bond in the hydrocarbon backbone. Unsaturations increase membrane fluidity, and are especially important membrane adaptation in cold and salty environments. Oleic acid is an important biomarker because it is one of the most abundant unsaturated fatty acids used by organisms. Unsaturations are readily oxidized, so these species are not as well-preserved compared to saturated fatty acids. However, the fatty acid skeleton is still well preserved (just without the starting unsaturation).[24,37]
3. Heneicosane: a C21 saturated *n*-alkane. This simple lipid is a sturdy hydrocarbon that forms the tail of fatty acids. Alkanes can form both biotically and abiotically. In biotic systems, heneicosane is a common leaf wax, used by plants for retaining water and protecting against cold and desiccating (i.e., dry) environments. In the geologic record, heneicosane can represent an unaltered, preserved leaf wax alkane, or it can represent a geologically reprocessed C_{22} fatty acid that has been decarboxylated through diagenesis.[24] Alkanes are commonly found in petroleum, are well-preserved for potentially billions of

years in the terrestrial record, and are important molecular targets for life detection and organic chemical surveys.[24] Saturated alkanes are abundant in biology and common to machine oils used in parts manufacturing, so they have high contamination potential, especially for instrumentation using stainless steel or other metals.[24,37]

4. 5α-cholestan-3β-ol: a sterol (i.e., polycyclic isoprenoid). This cyclic lipid is a steroid alcohol with four fused hydrocarbon rings, an aliphatic hydrocarbon side chain, and a hydroxyl functional group. Cholestanol serves as a proxy for hopanoids, which are structurally similar five-ringed compounds used by bacteria for regulating membrane fluidity (whereas cholestanol are used by eukaryotes).[156] Sterols and hopanoids are both synthesized exclusively by biotic systems and comprise linked isoprene (i.e., 2-methyl-1,3-butadiene) units that are themselves biomarker.[157] Free hopanoids and sterols are not common laboratory contaminants, but since they are present in bacteria cell membranes they could potentially present a contamination threat for life detection instruments.[24,157]
5. 5-α-cholestane: a sterane. Steranes are a diagenetic product of sterols, formed once the hydroxyl group is lost during geologic reprocessing. Steranes make up a fraction of petroleum on Earth and are stable for potentially billions of years in the geologic record, making steranes an important geologically processed biomarker.[24,157] Cholestane serves as a proxy for hopanoids, which are structurally similar to steranes and undergo similar geologic reprocessing during diagenesis. Free hopanoids and steranes are not common laboratory contaminants and are more often found in geological samples.

3.1.2 Laboratory Contamination Control Procedures

Prior to preparing samples, stringent laboratory contamination control procedures were developed. High purity lipid standards and liquid chromatography-grade solvents were used. Sample handling took place in a fume hood equipped with laminar flow, and workspace was covered in lipid-free ultra-high-vacuum (UHV) foil (All-Foils, Inc.) that was changed daily. Nitrile gloves (Sigma-Aldrich) were worn and changed frequently, and all containers holding standards, solvents, and samples were closed immediately following use.

Glassware and metal tools (i.e., tweezers, scoops, foil weigh boats) were wrapped in ultra-high-vacuum (UHV) foil and ashed by combusting at 550° C for 12 hours prior to use. To prevent re-contamination from dust particles, foil was not removed until immediately before use. Silicone-PTFE vial caps unable to be baked were sonicated for 30 minutes each in methanol (Millipore Sigma, Methanol for liquid chromatography LiChrosolv®, purity ≥99.8 %), dichloromethane (DCM, Millipore Sigma, Dichloromethane for liquid chromatography LiChrosolv®, purity ≥99.9 %), and n-hexane (Millipore Sigma, n-Hexane for liquid chromatography LiChrosolv®, purity ≥99.0 %), then placed into an ashed beaker and covered with UHV foil until use. Test tube racks were wiped with methanol-soaked KimWipes (Sigma-Aldrich) to remove dust.

Standards were weighed out into ashed foil weigh boats before being transferred into ashed glass vials. Solvents and lipid stock were transferred with syringes that were flushed 21 times each with methanol, dichloromethane, and hexane before, after, and in between each use. When a syringe was used on a new lipid compound or different irradiation dose (post-EBI), the syringe was sonicated for 30 minutes each in the same set of solvents.

Prior to GC-MS analyses, a DCM blank was injected into the instrument. When background compounds were present, blanks were repeatedly injected to pull off contaminants

from the column until a clean background was confirmed. Blanks were run in between lipid compounds to verify that no lingering compounds from previous injections were stuck on the column. To minimize any potential cross-contamination, each target lipid was analyzed as a batch, in the order of highest irradiation dose to lowest irradiation doses as follows:

1. DCM blank
2. 100 kGy 1 of 3
3. 100 kGy 2 of 3
4. 100 kGy 3 of 3
5. 50 kGy 1 of 3
6. 50 kGy 2 of 3
7. 50 kGy 3 of 3
8. control 1 of 3
9. control 2 of 3
10. control 3 of 3

3.2 Sample Preparation

3.2.1 Lipid Stock Preparation

Stock preparation took place in August 2019 at NASA Ames Research Center. Selected analytical-grade lipid standards were purchased from Sigma-Aldrich and shipped to the laboratory, and each compound was made into stock that was then portioned out into aliquots for irradiation. Creating one stock from each compound enabled precise measurements of small volumes, so each aliquot contained an equal amount of the lipid standard relative to other aliquots of the same compound.

To prepare the stock, standards were weighed out in combusted foil boats on a Satroius micro scale mass balance, transferred to ashed glass tubes, dissolved in 10 mL DCM each, vortexed for 60 seconds each to homogenize, capped with a silicone-PTFE cap (previously cleaned by sonicating for 30 min each in methanol, DCM, and n-hexane), and transferred to a -20°C freezer for storage to prevent solvent evaporation and lipid degradation. Stock shown in Figure 33.

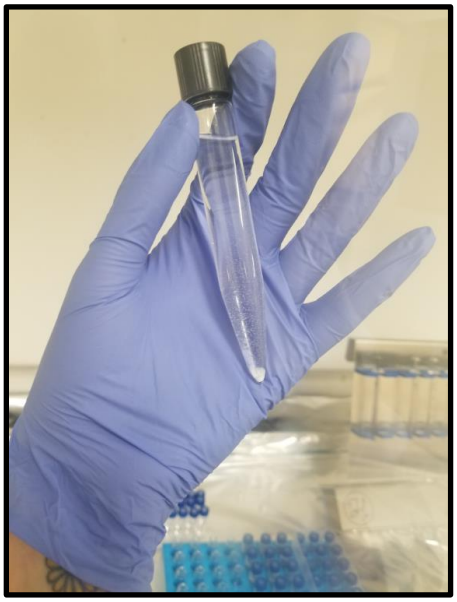

Figure 33. Lipid stock before vortexing

Stock concentrations were based on concentrations previously used by NASA Ames P.I.s Jahnke and Wilhelm for other lipid analyses. For the fatty acids, alkane, and cholestane, approximately 50 mg each (in 10 mL each of DCM) was used; for the cholestanol, approximately 100 mg was used (in 10 mL of DCM). Total stock contents are listed in Table 3.

Table 3. Lipid stocks: compounds, purities, masses, and solvent volumes

Compound	Purity	Lipid mass	DCM volume
Palmitic acid	≥99.0%	50.15 mg	10 mL
Oleic acid	≥99.0%	50.08 mg	10 mL
Heneicosane	≥99.5%	50.01 mg	10 mL
5α-cholestan-3β-ol	≥95%	100.01 mg	10 mL
5-α-cholestane	≥97.0%	50.01 mg	10 mL

3.2.2 Aliquot Preparation

Lipid stock aliquots were partitioned out into 9 aliquots each (for irradiation in triplicate at 50 kGy and 100 kGy, with a third control set) as in Table 4 by vortexing each tube for 60 seconds

to re-homogenize, drawing up aliquots (500 µL each) with solvent-cleansed Gastight syringes (Hamilton, 50 µL- 250 µL syringe volumes), and carefully depositing into tapered-bottom 1.5 mL borosilicate glass vials (Thermo Scientific), taking care to ensure no stock ran down the sides of the vials and all lipids ended up in the wells at the bottom of the vials.

Table 4. Lipid stocks: compounds, masses, solvent volumes, and number of aliquots

Compound	Lipid mass	DCM volume	Number of aliquots
Palmitic acid	2.50 mg	500 µL	9
Oleic acid	2.50 mg	500 µL	9
Heneicosane	2.50 mg	500 µL	9
5α-cholestan-3β-ol	5.00 mg	500 µL	9
5-α-cholestane	2.50 mg	500 µL	9

Equivalent volumes of stock were used for each aliquot for consistency across all compound classes and samples, and leftover stock was saved in the -20°C freezer. Vials were capped with solvent-cleaned silicone-PTFE caps (Thermo Scientific) and immediately stored in a -20°C freezer to prevent solvent evaporation and lipid degradation. This step took place in September 2019; Figure 34 shows lipid aliquots partitioned out.

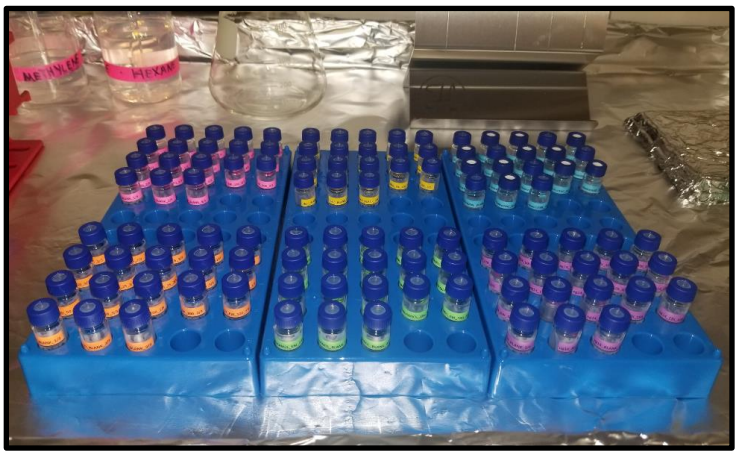

Figure 34. Lipid aliquots prepped for irradiation, including palmitic acid (pink), oleic acid (orange), heneicosane (yellow), cholestanol (green), and cholestane (blue)

3.2.3 Irradiation Preparation

Prior to irradiation, aliquots were removed from the freezer and transported to the fume hood. Caps were removed and solvent was evaporated under a gentle stream of pure N_2 blown through combusted glass pipettes (new pipette used for each aliquot), then re-capped before oxygen could enter the vials (Figure 35). Keeping the dried standards under an inert gas controlled for oxidation, particularly of the unsaturated oleic acid, ensuring that environmental factors did not cause lipid breakdown so the effects of irradiation alone could be elucidated. Seo et al. previously showed that volatilized saturated fatty acids suspended in N_2 were effectively removed with EBI at a slightly higher rate than those in a He or ambient air environment, and only marginally lower rate than those suspended in O_2.[146]

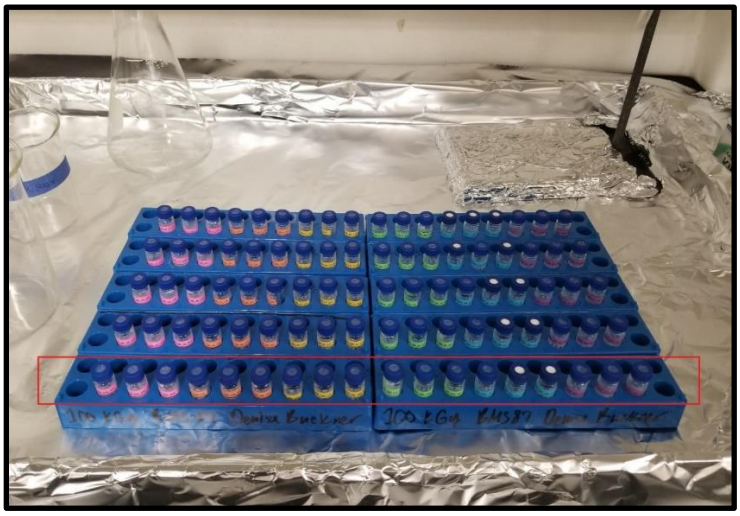

Figure 35. Aliquots dried and ready for irradiation. Red outline shows one full set of aliquots in triplicate

This thesis study included one control set and two experimental sets (hereafter control set, 50 kGy set, and 100 kGy set), so three cardboard boxes (one per irradiation dose) were prepared with triplicate aliquots of each of the five lipid compounds placed into vial racks that were 10 wells long, stacked lengthwise in two layers cushioned with paper towels (Figure 36). This was to ensure

that the electron beam, penetrating the box from the side, would hit all the vials directly and would not have to travel through one aliquot to reach the next. Boxes were sealed, then packed into a cooler filled with dry ice and driven to Steri-Tek Expert Sterilization Services in Fremont, CA.

Figure 36. Box with aliquots, pre-irradiation, with (a) first and (b) second layers stacked vertically

3.3 Irradiation Procedures

3.3.1 Steri-Tek Facilities

Steri-Tek Expert Irradiation Facilities is ISO 11136 and ISO 13485 certified, FDA registered, DEA registered, and State of California Medical Device and Drug Manufacturing licensed. Steri-Tek provides EBI and X-ray irradiation sterilization services, and EBI is performed with 10 MeV, 20 KW linear accelerators.

3.3.2 Irradiation Steps and Parameters

Steri-tek performed a "Radiation Tolerance Series Study," which includes irradiation of up to five individual sample sets at five different doses (between 5 kGy and 100 kGy, as selected by the customer) over the span of five days; for this thesis study, two sets were irradiated at 50 kGy

and 100 kGy. A Radiation Tolerance Study includes one palette of space (76" long, 36" high, 15" wide), placed on a conveyor belt that passes in front of two 10 MeV, 20 KW linear accelerators in a DualBeam™ configuration (Figure 37) on either side of the conveyor belt, so uniform doses are delivered to the palette in a single pass without requiring rotation of the boxes. Beams can penetrate through shipping boxes, paper, cardboard, plastic, and air without loss of intensity, and can penetrate up to 6.35 cm into material that has a density of 1.0 g/cm^3 (approximate density of water).

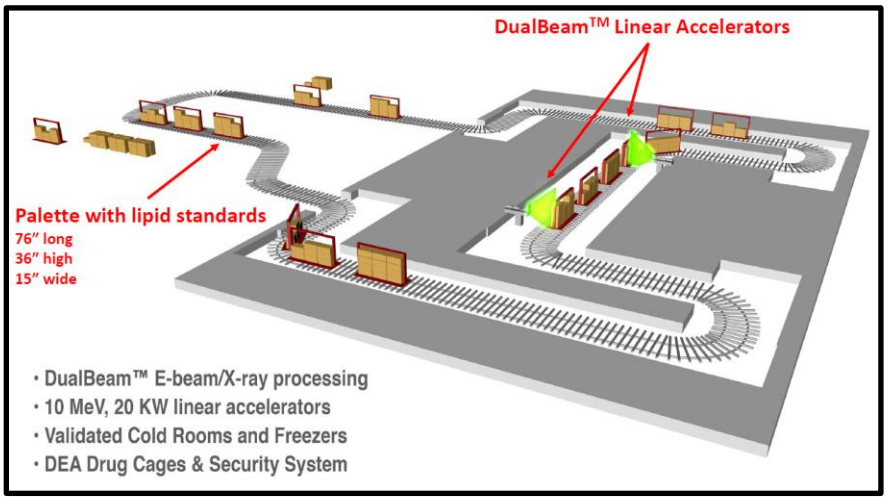

Figure 37. Steri-Tek facilities for EBI application, including illustration of the DualBeam™ Linear Accelerators configuration and palette dimensions

Samples were hand delivered to Steri-Tek (travel time from laboratory ~30 minutes) in September 2019, cooler was unpacked, and boxes were immediately placed into a temperature-controlled -26° C freezer, where they were stored for the duration of the study (7 days), except for when they were undergoing irradiation. The control set remained in the freezer the entire time. Since the beam can penetrate through the cardboard exterior, paper towel cushions, and plastic vial holder inside to reach the aliquots, the boxes were left sealed and irradiated unopened.

Each irradiation run took approximately 1 hour, including ~30 seconds spent in front of the beam. Outside of the freezer, the processing facility was temperature-controlled at 21° C, and for

each 1 kGy of irradiation, temperature increased by ~0.556° C (1° F) for the ~30 seconds spent in front of the beam. The 100 kGy set was processed twice at 50 kGy each for a cumulative 100 kGy dose, so the 50 kGy set spent 1 hour outside of the freezer and was heated to ~49° C for ~30 seconds, and the 100 kGy set spent two hours out of the freezer and was heated to ~49° C twice for ~30 seconds each time. A dosimeter (i.e., device for measuring absorbed dose of irradiation) placed on the palette validated that doses absorbed were within the ranges delivered: 0 kGy (control), 50 ±3 kGy, and 100 ±6 kGy.

Following irradiation, the samples were collected from Steri-Tek, packed into a cooler filled with dry ice, and driven back to the laboratory at Ames.

3.4 Preparation for Analysis

3.4.1 Sample Storage

Once the aliquots were back in the laboratory (September 2019), they were removed from the cooler and re-solubilized with 500 µL of DCM each, added with a solvent-cleansed 250 µL Gastight syringe. Aliquots were capped with new, solvent-cleansed silicone-PTFE caps, then stored in the -20° C freezer.

3.4.2 Chemical Preparation for GC-MS

Chemical preparation and GC-MS analysis took place at NASA Ames Research Center September 2019- March 2020.

3.4.2.1 Subsampling

Subsamples of each aliquot were taken and spiked with an internal standard for GC-MS analysis; the remainder was saved in the freezer for any future analyses. Subsample volumes are listed in Table 5.

Table 5. Subsample quantities

Target compound	Subsample volume	Fraction of total aliquot
Palmitic acid	20 µL	$1/25^{th}$
Oleic acid	20 µL	$1/25^{th}$
Heneicosane	10 µL	$1/50^{th}$
5α-cholestan-3β-ol	10 µL	$1/50^{th}$
5-α-cholestane	10 µL	$1/50^{th}$

3.4.2.2 Internal Standards

An internal standard (IS) was added to subsamples in known quantities/concentrations equivalent to the quantity/concentration of the pre-irradiated lipid, vortexed for ~60 seconds to homogenize, dried down under pure N_2, then re-solubilized with the appropriate organic solvent for either direct analysis or for derivatization and then analysis. Internal standards are used for quantification during analysis of chromatograms, whereby the pre-measured amount of the IS is compared to the quantities of other compounds present.

ISs were selected for each target lipid. For the fatty acids, alkane, and cholestane, a $C_{23:0}$ fatty acid methyl ester (FAME) was the IS, and for the cholestanol, tricosanoic acid methyl ester was used. These compounds were selected because they elute at different times relative to the target compounds without interfering with the peaks coming from the irradiated lipids. They are also unlikely to appear naturally in the aliquot as a breakdown product of any of the irradiated lipids: FAMEs are only created through a methylation reaction where a methyl group is added to the carboxyl moiety of a free fatty acid (and the C_{23} FAME hydrocarbon backbone is longer than

any of the target compounds), and aliphatic fatty alcohols are structurally unrelated to polycyclic sterols.

IS stocks were prepared, then added to the subsamples. 100.15 mg of the C23 FAME was weighed in an ashed foil boat, transferred to an ashed glass test tube, solubilized in 10 mL of DCM, vortexed for ~60 seconds, and stored in the freezer. Following the same procedures, 50.01 mg of eicanosol was solubilized in 5 mL of DCM. Using a solvent-cleansed Gastight syringe, ISs were drawn up and added to the subsamples in quantities/concentrations equivalent to the pre-irradiation lipid quantities/concentrations.

3.4.2.3 Derivatization

Fatty acids and cholestanol were derivatized via silylation with N,O-bis(trimethylsilyl) trifluoroacetamide) + 1% TMCS (trimethylchlorosilane) (BSTFA). Silylation makes polar compounds amenable to GC-MS by replacing the active hydrogen with a trimethylsilyl group, acting on the hydroxyl group in sterols and the carboxyl group in fatty acids. Silylation reaction is shown in Figure 38.[48,158,159]

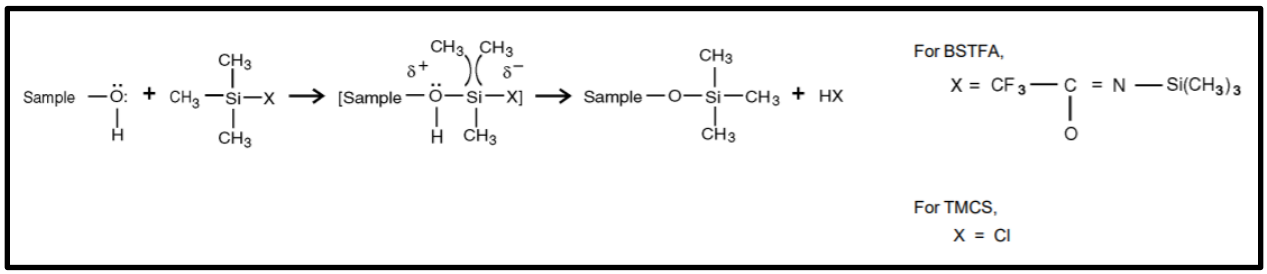

Figure 38. Illustration of silylation derivatization[160]

Silylation was performed with modified versions of the procedure described in Jahnke et al. and Wilhelm et al. with slightly different parameters for (1) cholestanol and (2) the two fatty

acids.[48,159] Procedures were modified for better recovery, and the modified steps were developed and verified in January 2020.

For the cholestanol, subsampled aliquots containing 100 µg each of lipid standard and IS were dried down under a stream of N_2 blown through combusted glass pipettes, then immediately re-capped before oxygen could enter the vials. 20 µL BSTFA (N,O-bis(trimethylsilyl) trifluoroacetamide) + 1% TMCS (trimethylchlorosilane), Regis Technologies, Inc.) and 20 µL anhydrous pyridine (Sigma-Aldrich, 99.8% purity) were added with syringes that were solvent-cleansed and flushed twice with pyridine to remove any water, as water can decompose TMS reagents and derivatized compounds. A new 1 g ampoule of BSTFA was used for each compound class. Next, N_2 was gently blown into the vials to remove air and any water vapor, then vials were re-capped, wrapped in foil and placed on a heating block for 30 minutes at 80° C to catalyze the silylation reaction. Once cooled, aliquots were diluted with the addition of another 360 µL pyridine each so that lipid concentrations were appropriate for GC-MS analysis at 0.25 µg each, given a 1 µL injection volume.

For the fatty acids, the same parameters were used, except 150 µL of BSTFA and 50 µL of anhydrous pyridine (Sigma-Aldrich, 99.8% purity) were used, aliquots were heated for 1 hour at 90° C, and 200 µL pyridine was added to dilute to appropriate volume (Table 6). Derivatization is shown in Figure 39.

Table 6. Target compound and mass, internal standard and mass, derivatization, solvent(s) and volumes, final injection volume

Target compound	Target compound starting mass in sample (pre-irradiation)	IS	IS mass	Derivatization y/n	Solvent(s)	Total solvent volume	GC-MS injection volume
Palmitic acid (C16)	100 µg	C23 FAME	100 µg	y	BSTFA:pyridine 7:1 (v/v)	400 µL	0.25µg_C16 0.25µg_IS 1µL_solvent
Oleic acid (C18)	100 µg	C23 FAME	100 µg	y	BSTFA:pyridine 7:1 (v/v)	400 µL	0.25µg_C18 0.25µg_IS 1µL_solvent
Heneicosane (C21)	100 µg	C23 FAME	100 µg	n	DCM	200 µL	0.50µg_C21 0.50µg_IS 1µL_solvent
5α-cholestan-3β-ol (stanol)	100 µg	Eicosanol	100 µg	y	BSTFA:pyridine 19:1 (v/v)	400 µL	0.25µg_stanol 0.25µg_IS 1µL_solvent
5-α-cholestane (stane)	50 µg	C23 FAME	50 µg	n	DCM	200 µL	0.25µg_stane 0.25µg_IS 1µL_solvent

Figure 39. Aliquots undergoing derivatization on a heating block

3.5 GC-MS Analysis

3.5.1 GC-MS Parameters

GC-MS analysis was performed at NASA Ames Research Center from October 2019-March 2020 on an Agilent 6890 system equipped with an Agilent DB-5MS column (60 m x 250 µm x 0.25 cm, Agilent) with helium as the carrier gas at 1 mL/min. The inlet temperature was 280°C. Initial oven temperature was 50°C, ramped to 120°C at 10°C/min, then increased from 120°C to 320°C at 3°C/min and held at this temperature for 5 min. The MS source temperature was 300°C.

3.5.2 GC-MS Interpretation

Injection volumes with lipid and IS quantities are detailed in Table 8; each GC-MS run used 1 µL total injection volume. Compounds were quantified relative to the internal standard. Results were analyzed in triplicate, using Agilent ChemStation (Agilent) software coupled to the National Institute of Standards and Technology (NIST) 2017 database. This database identifies compounds present based on *m/z* ratio and retention time of peaks. Peaks representing the starting compound and the IS were identified using the NIST. Any other major peaks were also identified with the NIST.

To determine lipid abundance post-irradiation, the ChemStation AutoIntegrate function was used to calculate peak areas for the internal standard and the starting compound in each chromatogram. Then, the concentration of the target lipid C_x was determined by comparing the target lipid peak area to the IS peak area with the following equation:

Equation 1. Lipid compound concentration in analyzed sample

$$C_x = (A_x) * (\frac{C_{IS}}{A_{IS}})$$

where

A_x is the peak area of the target lipid

C_{IS} is the known concentration of the IS in the injected sample

A_{IS} is the peak area of the IS

If lipids were degraded with EBI, those starting compounds would appear in lower concentrations relative to the control samples, but the concentration of the IS, added after irradiation, would remain the same (equivalent to the concentration of the target lipid in the control), so comparing the two can help elucidate breakdown. To determine degree of degradation, relative abundance RA in each aliquot compared to the control was determined, using the equation:

Equation 2. Relative abundance in lipid compound relative to the unirradiated control

$$RA = C_x / C_{Cavg}$$

where

C_x is the concentration of the target lipid in Equation 1

C_{Cavg} is the averaged concentration of the target lipid in the unirradiated control

CHAPTER IV: RESULTS

For the palmitic acid, oleic acid, heneicosane, cholestanol, and cholestane, significant degradation was not observed following irradiation at either 50 or 100 kGy. Two sets- palmitic acid 100 kGy and cholestanol 50 kGy- appeared to display some degradation, with 79.5% ±2.3% and 84.04% ±9.63% abundances relative to the controls, respectively. However, there was no degradation observed for palmitic acid at 50 kGy or for cholestanol at 100 kGy. Additionally, standard deviations were high for these compounds. Several minor peaks representing radiolytic products were observed, but they were only present in very low abundances.

5.1 Fatty Acids

5.1.1 Palmitic Acid

According to GC-MS analyses, the mean concentration C_x of palmitic acid in the control set was 0.33 ±0.04 µg/µL, quantitated relative to the IS. For aliquots irradiated at 50 kGy, C_x of palmitic acid was unchanged at 0.33 ±0.01 µg/µL, and for those irradiated at 100 kGy, C_x decreased to 0.26 ±0.01 µg/µL.

Palmitic acid and IS peak areas, concentrations, and percent abundances relative to the control are detailed in Table 7. Change in percent abundance across the three sample sets is illustrated in Figure 40.

Table 7. Abundance of palmitic acid by irradiation dose in control set, 50 kGy set, and 100 kGy set, as determined by GC-MS.

Grey represents averages for the triplicate aliquots in each set

Dose in kGy	Aliquot	Lipid compound (identified by NIST)	Peak area (palmitic acid)	IS (identified by NIST)	Peak area (IS)	C_{IS} in µg/µL	C_x in µg/µL (palmitic acid)	Percent abundance relative to the control (in %)
100	1 of 3	Palmitic acid	2,741,928,748	C_{23} FAME	2,667,914,533	0.25	0.26	78.64
100	2 of 3	Palmitic acid	2,762,354,083	C_{23} FAME	2,719,127,081	0.25	0.25	77.74
100	3 of 3	Palmitic acid	2,832,238,239	C_{23} FAME	2,640,093,698	0.25	0.27	82.09
100 mean			2,778,840,357		2,675,711,771		0.26 ±0.01	79.49 ±2.3
50	1 of 3	Palmitic acid	4,467,476,827	C_{23} FAME	3,375,712,432	0.25	0.33	101.27
50	2 of 3	Palmitic acid	3,016,888,596	C_{23} FAME	2,367,620,198	0.25	0.32	97.51
50	3 of 3	Palmitic acid	4,357,136,480	C_{23} FAME	3,297,834,092	0.25	0.33	101.10
50 mean			3,947,167,301		3,013,722,241		0.33 ±0.01	99.96 ±2.1
0 (control)	1 of 3	Palmitic acid	3,838,411,995	C_{23} FAME	3,364,411,961	0.25	0.29	87.30
0 (control)	2 of 3	Palmitic acid	3,106,789,527	C_{23} FAME	2,096,066,727	0.25	0.37	113.42
0 (control)	3 of 3	Palmitic acid	3,709,030,041	C_{23} FAME	2,858,812,777	0.25	0.32	99.28
0 mean			3,551,410,521		2,773,097,155		0.33 ±0.04	100.0 ±13.1

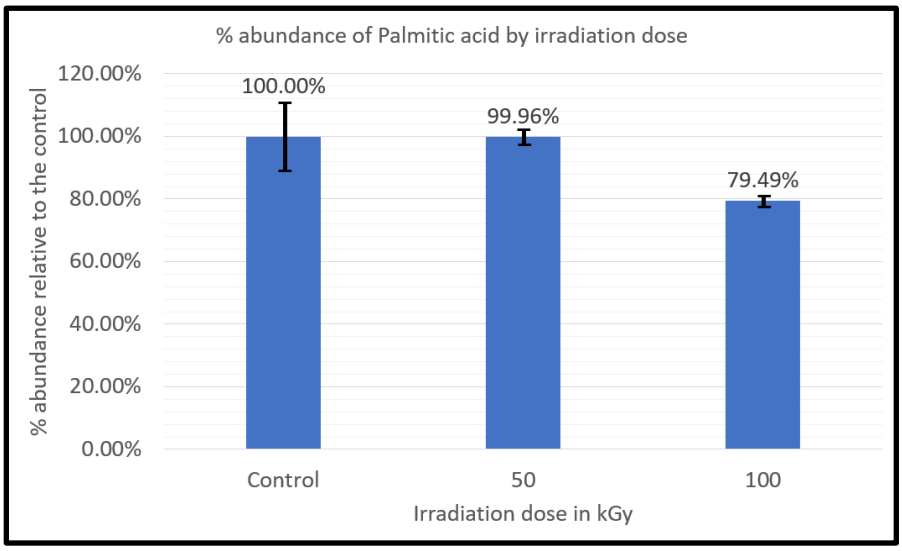

Figure 40. Percent abundance of palmitic acid by irradiation dose in kGy, averaged over triplicates in each set

Compared to the control set, the relative abundance of palmitic acid in the 50 kGy set was 99.96% ±2.1%. For the 100 kGy set, the relative abundance was 79.49% ±2.3 compared to the control set. Standard deviation between the aliquots in the control set was ±13.1%. Although the percent abundance of palmitic acid was lower for the 100 kGy set (with a low standard deviation) relative to the control, no significant reduction was observed for the 50 kGy set relative to the control.

Additionally, chromatograms from GC-MS analyses did not reveal any other compounds present in significant quantities in the sample. Figures 41-43 show representative chromatograms from each of the EBI doses and the two peaks illustrate that, for all irradiation doses, only two compounds are present in any appreciable quantities: palmitic acid and the IS.

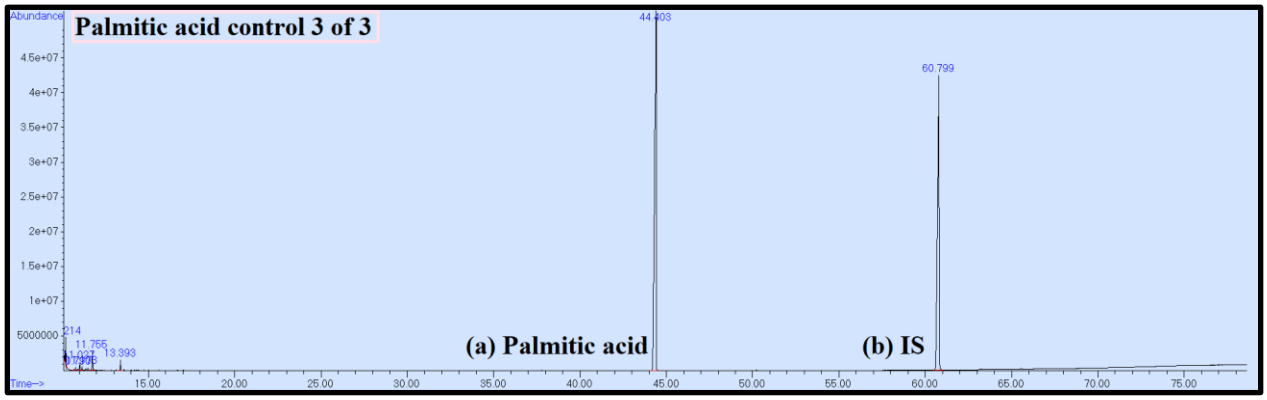

Figure 41. Chromatogram representing aliquot 3 of 3 from the palmitic acid control set. (a) represents palmitic acid, (b) represents the C_{23} FAME IS

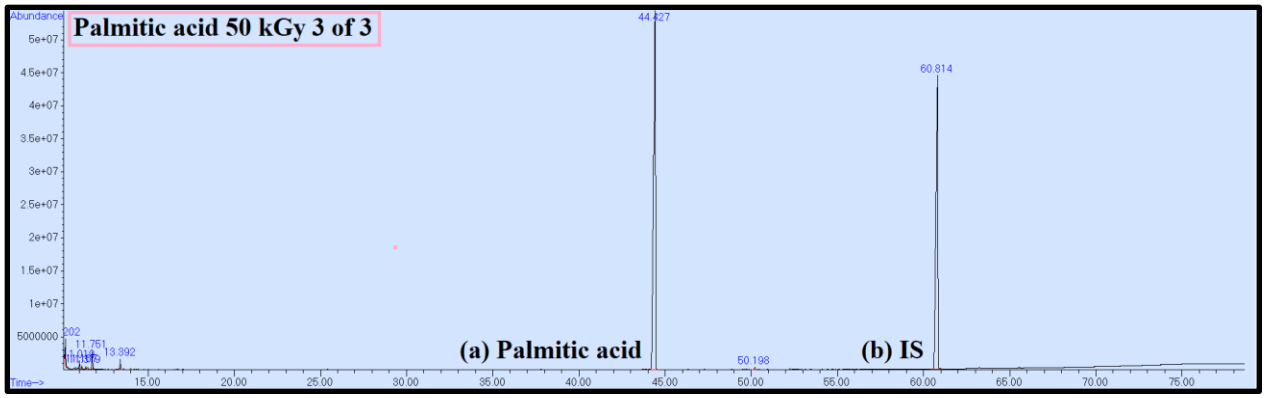

Figure 42. Chromatogram representing aliquot 3 of 3 from the palmitic acid 50 kGy irradiated set. (a) represents palmitic acid, (b) represents the C_{23} FAME IS

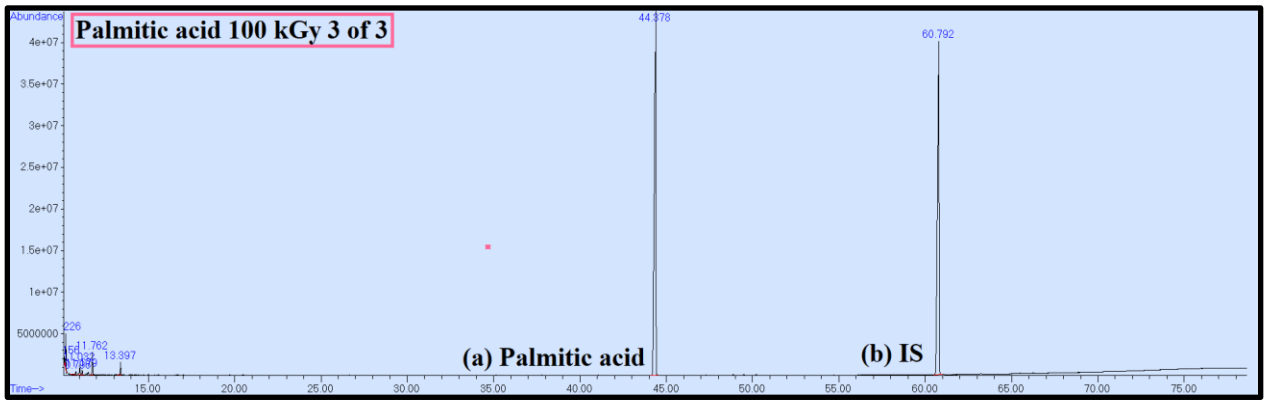

Figure 43. Chromatogram representing aliquot 3 of 3 from the palmitic acid 100 kGy irradiated set. (a) represents palmitic acid, (b) represents the C_{23} FAME IS

Although the only two major peaks belong to the palmitic acid and the IS, numerous low-abundance breakdown products are observed in both the 50 kGy and 100 kGy sets but absent the control. However, these compounds are present in small quantities and their combined abundance does not account for the degradation observed in the 100 kGy set. Products include a homologous series of unsaturated fatty acids, a homologous series of *n*-alkanes, several dicarboxylic acids, several monounsaturated fatty acids, several oxo fatty acids, several oxo dicarboxylic acids, and a furanone; all of which have chain lengths of C_{16} or shorter (Figure 44). To better visualize and

characterize minor breakdown products, a 20x concentrated aliquot was analyzed with GC-MS; upon zooming in, these products are also visible in the Figure 41-43 chromatograms.

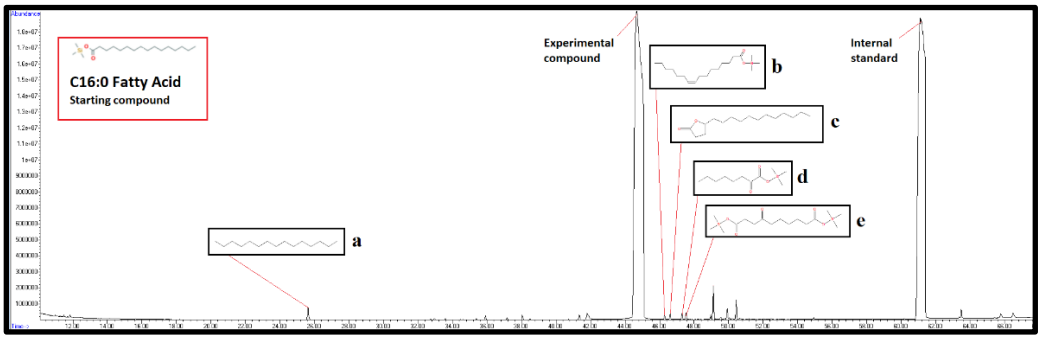

Figure 44. 20x concentrated chromatogram of a 100 kGy palmitic acid aliquot, showing selected minor breakdown products. a. C_{15} n-alkane b. $C_{16:1}$ monounsaturated fatty acid c. furanone d. oxyacid e. oxo dicarboxylic acid. Other minor peaks include n-alkanes and fatty acids

From these results, only the 100 kGy set displayed reduction in the abundance of the starting compound. While numerous breakdown products were identified, they are all present in low abundances (close to the background) and their combined quantities do not account for the reduction in the 100 kGy set.

5.1.2 Oleic acid

According to GC-MS analyses, the mean concentration C_x of oleic acid in the control set was 0.27 ±0.01 µg/µL (quantitated relative to the IS). For aliquots irradiated at 50 kGy, C_x of palmitic acid was 0.25 ±0.02 µg/µL, and for those irradiated at 100 kGy, C_x was 0.26 ±0.01 µg/µL.

Oleic acid and IS peak areas, concentrations, and percent abundances relative to the control are detailed in Table 8. Change in percent abundance across the three sample sets is illustrated in Figure 45.

Table 8. Abundance of oleic acid by irradiation dose in control set, 50 kGy set, and 100 kGy set, as determined by GC-MS. Grey represents averages for the triplicate aliquots in each set

Dose in kGy	Aliquot	Lipid compound (identified by NIST)	Peak area (oleic acid)	IS (identified by NIST)	Peak area (IS)	C_{IS} in µg/µL	C_x in µg/µL (oleic acid)	Percent abundance relative to the control (in %)
100	1 of 3	Oleic acid	1,417,657,980	C_{23} FAME	1,294,554,898	0.25	0.27	102.48
100	2 of 3	Oleic acid	1,321,765,127	C_{23} FAME	1,269,556,678	0.25	0.26	97.42
100	3 of 3	Oleic acid	1,469,870,606	C_{23} FAME	1,487,927,351	0.25	0.25	92.44
100 mean			1,403,097,904		1,350,679,642		0.26 ±0.01	97.45 ±5.02
50	1 of 3	Oleic acid	1,584,416,095	C_{23} FAME	1,781,678,351	0.25	0.22	83.22
50	2 of 3	Oleic acid	2,112,852,904	C_{23} FAME	1,975,541,299	0.25	0.27	100.08
50	3 of 3	Oleic acid	1,640,487,668	C_{23} FAME	1,674,304,746	0.25	0.25	91.69
50 mean			1,779,252,222		1,810,508,132		0.25 ±0.02	91.66 ±8.43
0	1 of 3	Oleic acid	1,546,135,017	C_{23} FAME	1,492,511,656	0.25	0.26	96.94
0	2 of 3	Oleic acid	1,755,152,131	C_{23} FAME	1,584,046,876	0.25	0.28	103.69
0	3 of 3	Oleic acid	1,630,022,747	C_{23} FAME	1,538,068,636	0.25	0.27	99.17
0 mean			1,643,769,965		1,538,209,056		0.27 ±0.01	100.00 ±3.44

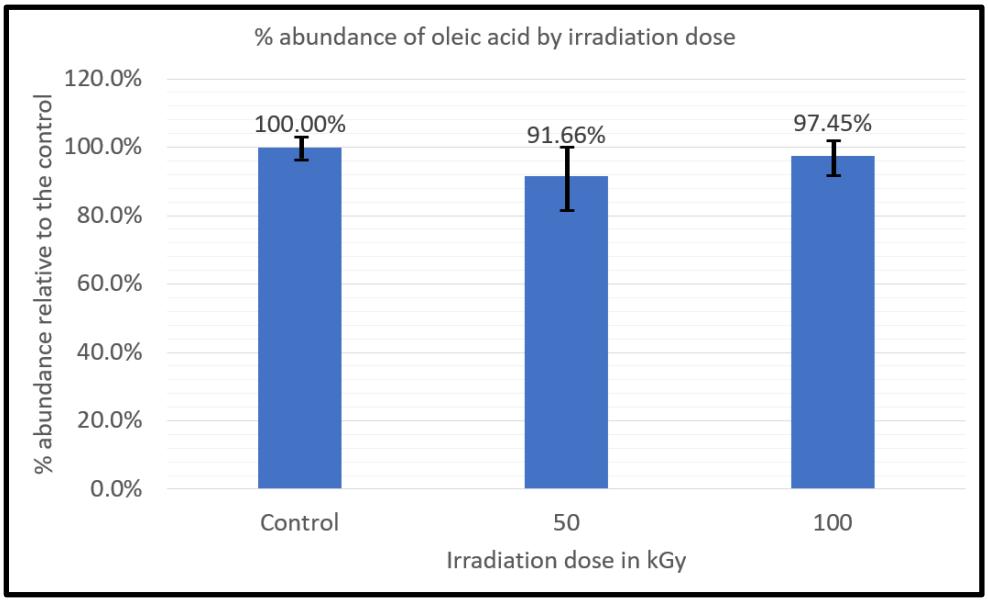

Figure 45. Percent abundance of oleic acid by irradiation dose in kGy, averaged over triplicates in each set

Compared to the control set, the relative abundance of oleic acid in the 50 kGy set was 91.66% ±8.43%. For the 100 kGy set, the relative abundance was 97.45% ±5.02% compared to the control set. Standard deviation between the aliquots in the control set was ±3.44%. From these analyses, no degradation in oleic acid was observed at either 50 kGy or 100 kGy of irradiation.

Additionally, chromatograms from GC-MS analyses did not reveal any other compounds present in significant quantities in the sample. Figures 46-48 show representative chromatograms from each of the EBI doses and the two peaks illustrate that, for all irradiation doses, only two compounds are present in any appreciable quantities: oleic acid and the IS.

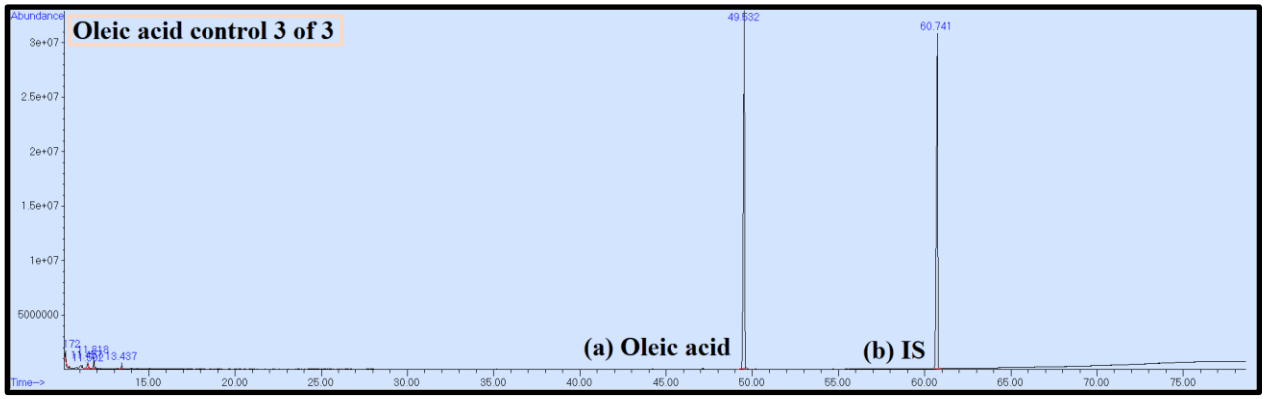

Figure 46. Chromatogram representing aliquot 3 of 3 from the oleic acid control set. (a) represents palmitic acid, (b) represents the C_{23} FAME IS

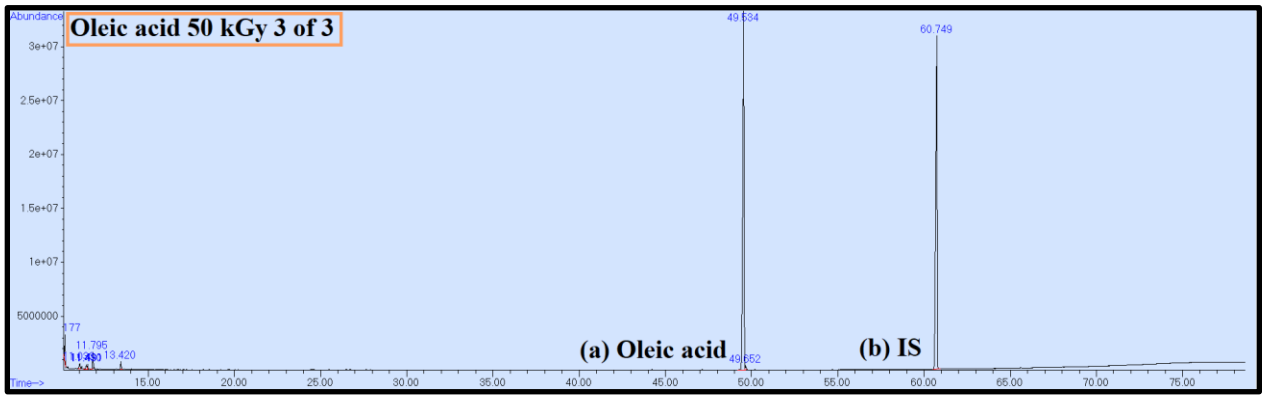

Figure 47. Chromatogram representing aliquot 3 of 3 from the oleic acid 50 kGy set. (a) represents palmitic acid, (b) represents the C_{23} FAME IS

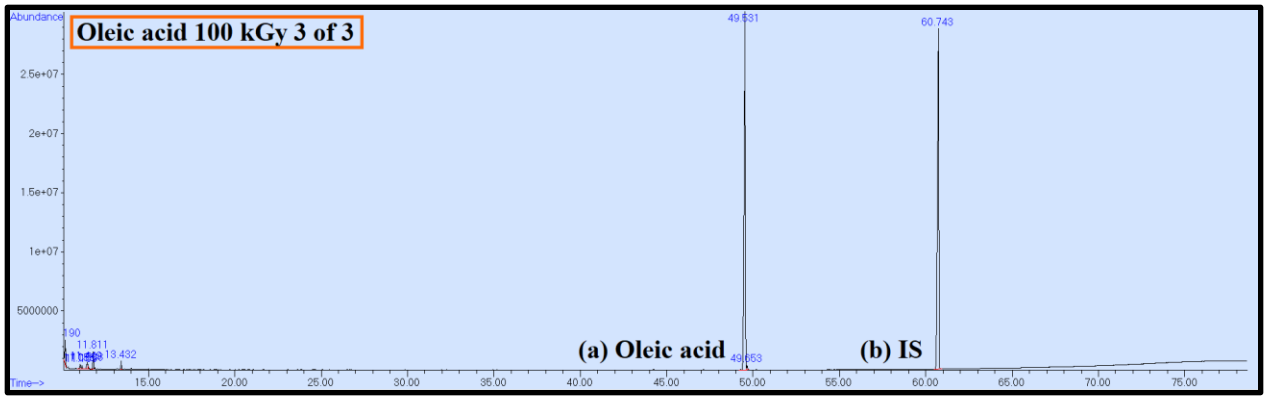

Figure 48. Chromatogram representing aliquot 3 of 3 from the oleic acid 100 kGy set. (a) represents palmitic acid, (b) represents the C_{23} FAME IS

Although the only two major peaks belong to the oleic acid and the IS, numerous low-abundance breakdown products are observed in both the 50 kGy and 100 kGy sets but absent the control. However, these compounds are present in small quantities. Products include a homologous series of unsaturated fatty acids, a homologous series of *n*-alkanes, several alkenes, several dicarboxylic acids, several oxo fatty acids, several oxo dicarboxylic acids, and a dihydroxy acid; all of which have chain lengths of C_{18} or shorter (Figure 49). To better visualize and characterize minor breakdown products, a 20x concentrated aliquot was analyzed with GC-MS; upon zooming in, these products are also visible in the Figure 46-48 chromatograms.

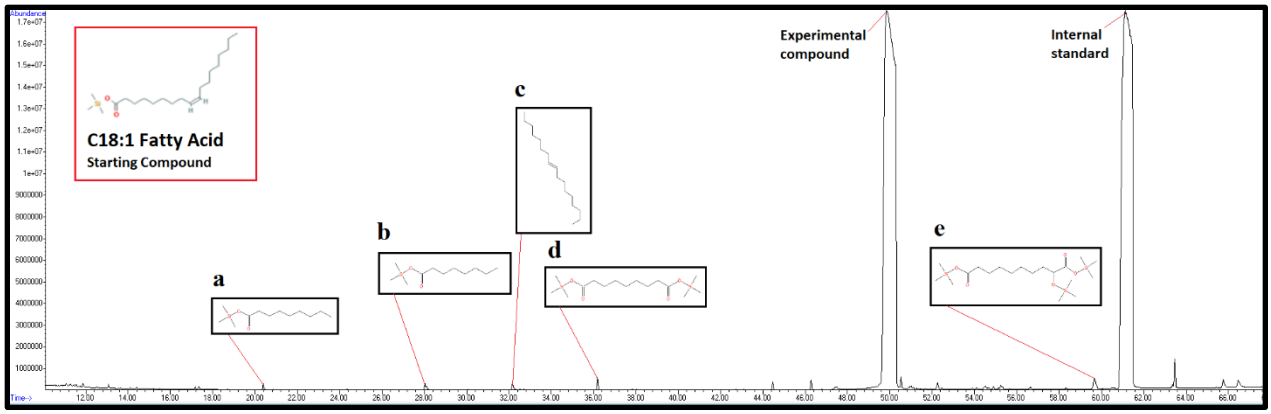

Figure 49. 20x concentrated chromatogram of a 100 kGy oleic acid aliquot, showing selected minor breakdown products. a. $C_{9:0}$ fatty acid b. $C_{8:0}$ fatty acid c. C_{17} alkene d. dicarboxylic acid e. dihydroxy acid. Other minor peaks include n-alkanes and fatty acids

From these results, neither the 50 kGy nor 100 kGy sets displayed reduction in the abundance of the starting compound. While numerous breakdown products were identified, they are all present in low abundances (close to the background).

5.2 Alkane

5.2.1 Heneicosane

According to GC-MS analyses, the mean concentration C_x of henicosane in the control set aliquots was 0.42 ±0.02 µg/µL (quantitated relative to the IS). For aliquots irradiated at 50 kGy, C_x of heneicosane was 0.42 ±0.03 µg/µL, and for those irradiated at 100 kGy, C_x was 0.43 ±0.03 µg/µL.

Heneicosane and IS peak areas, concentrations, and percent abundances relative to the control are detailed in Table 9. Change in percent abundance across the three sample sets is illustrated in Figure 50.

Table 9. Abundance of heneicosane by irradiation dose in control set, 50 kGy set, and 100 kGy set, as determined by GC-MS.

Grey represents averages for the triplicate aliquots in each set

Dose in kGy	Aliquot	Lipid compound (identified by NIST)	Peak area (heneicosane)	IS (identified by NIST)	Peak area (IS)	C_{IS} in µg/µL	C_x in µg/µL (heneicosane)	Percent abundance relative to the control (in %)
100	1 of 3	Heneicosane	471,806,074	C_{23} FAME	575,694,632	0.5	0.41	98.69
100	2 of 3	Heneicosane	539,874,866	C_{23} FAME	587,617,399	0.5	0.46	110.63
100	3 of 3	Heneicosane	429,924,651	C_{23} FAME	514,878,583	0.5	0.42	100.55
100 mean			480,535,197		559,396,871		0.43 ±0.03	103.29 ±6.43
50	1 of 3	Heneicosane	467,036,662	C_{23} FAME	598,466,176	0.5	0.39	93.97
50	2 of 3	Heneicosane	779,866,370	C_{23} FAME	872,303,484	0.5	0.45	107.66
50	3 of 3	Heneicosane	742,407,988	C_{23} FAME	856,985,823	0.5	0.43	104.32
50 mean			663,103,673		775,918,494		0.42 ±0.03	101.98 ±7.14
0	1 of 3	Heneicosane	567,461,341	C_{23} FAME	668,281,707	0.5	0.43	102.25
0	2 of 3	Heneicosane	776,246,630	C_{23} FAME	985,835,422	0.5	0.40	94.82
0	3 of 3	Heneicosane	833,187,689	C_{23} FAME	974,699,500	0.5	0.43	102.93
0 mean			725,631,887		876,272,210		0.42 ±0.02	100.00 ±4.50

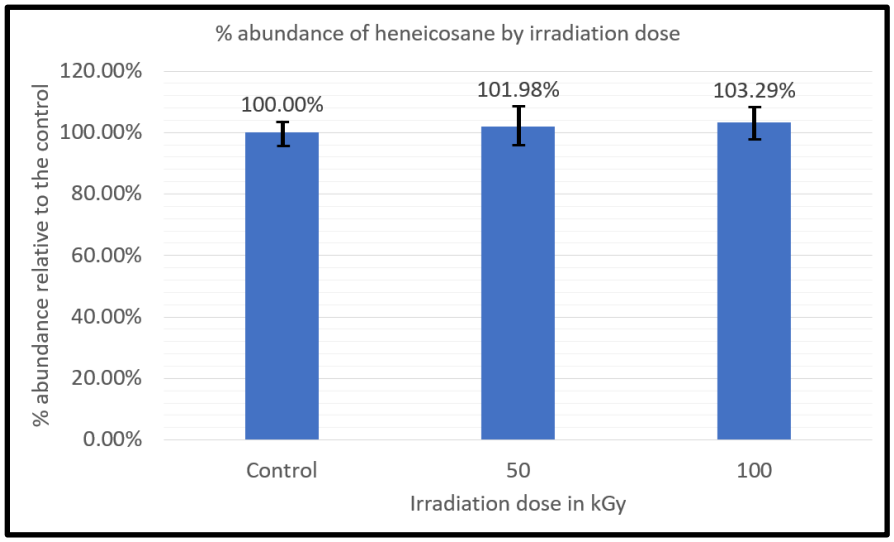

Figure 50. Percent abundance of heneicosane by irradiation dose in kGy, averaged over triplicates in each set

Compared to the control set, the relative abundance of heneicosane in the 50 kGy set was 101.99% ±7.14%. For the 100 kGy set, the relative abundance was 103.29% ±6.43% compared to the control set. Standard deviation between the aliquots in the control set was ±4.50%. From these analyses, no degradation in heneicosane was observed at either 50 kGy or 100 kGy of irradiation.

Additionally, chromatograms from GC-MS analyses did not reveal any other compounds present in significant quantities in the sample. Figures 51-53 show representative chromatograms from each of the EBI doses and the two peaks illustrate that, for all irradiation doses, only two compounds are present in any appreciable quantities: heneicosane and the IS.

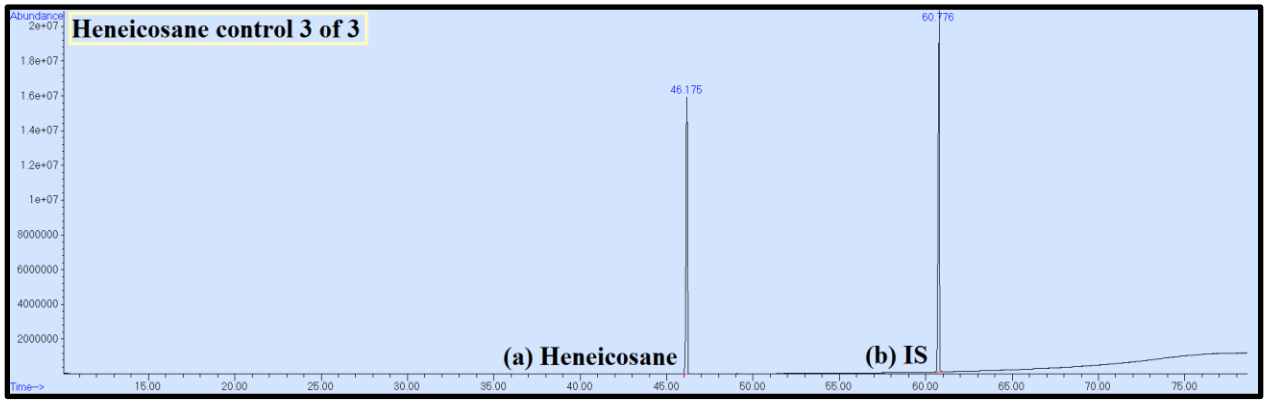

Figure 51. Chromatogram representing aliquot 3 of 3 from the heneicosane control set. (a) represents palmitic acid, (b) represents the C_{23} FAME IS

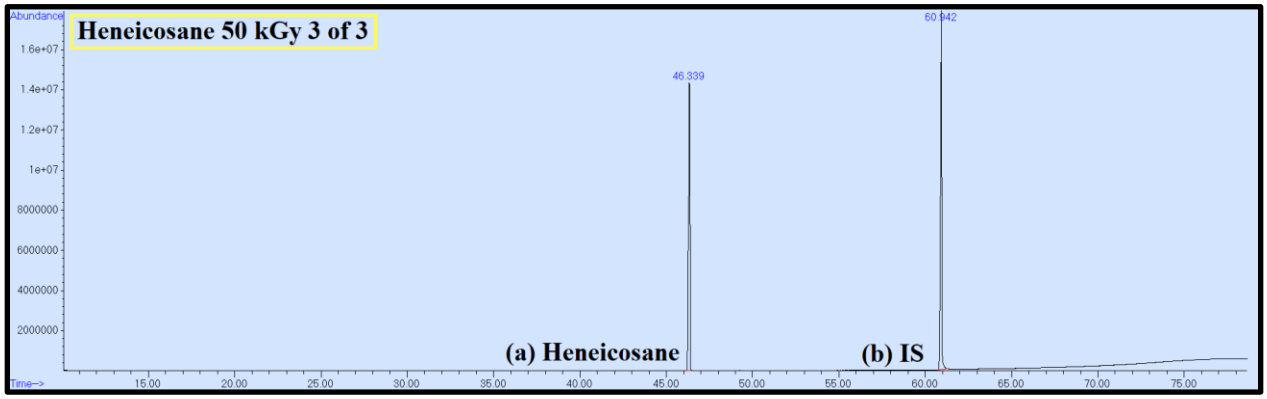

Figure 52. Chromatogram representing aliquot 3 of 3 from the heneicosane 50 kGy set. (a) represents palmitic acid, (b) represents the C_{23} FAME IS

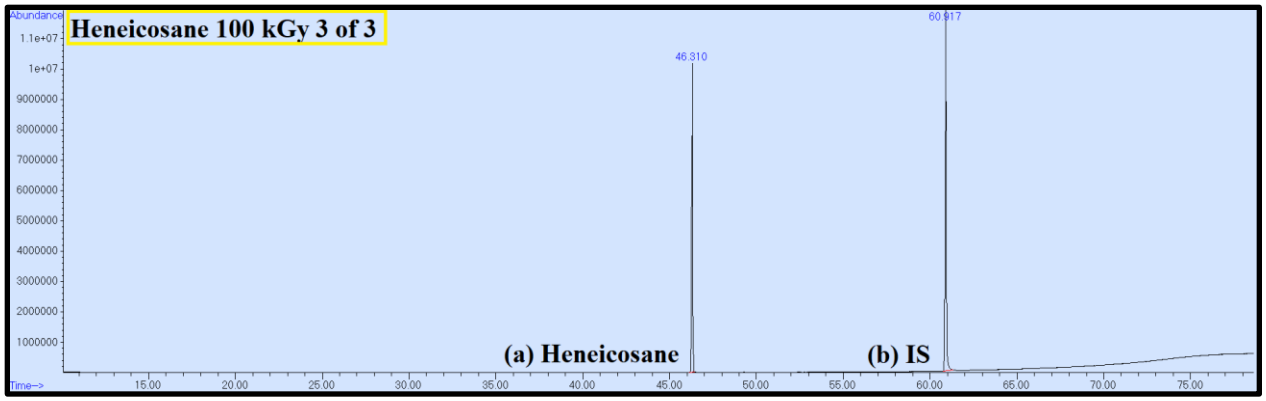

Figure 53. Chromatogram representing aliquot 3 of 3 from the heneicosane 100 kGy set. (a) represents palmitic acid, (b) represents the C_{23} FAME IS

Although the only two major peaks belong to the heneicosane and the IS, several low-abundance breakdown products are observed in both the 50 kGy and 100 kGy sets but absent the control. However, these compounds are present in small quantities. Products include a homologous series of *n*-alkanes with chain lengths of C_{20} or shorter (Figure 54). To better visualize and characterize minor breakdown products, a 20x concentrated aliquot was analyzed with GC-MS; upon zooming in, these products are also visible in the Figure 51-53 chromatograms.

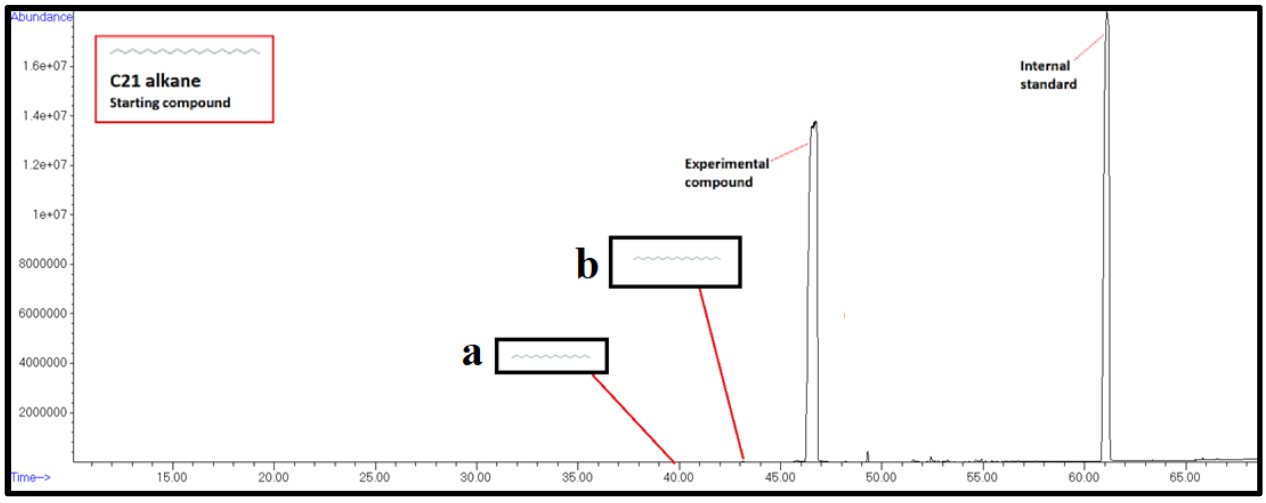

Figure 54. 20x concentrated chromatogram of a 100 kGy heneicosane aliquot, showing selected minor breakdown products. a. C_{17} n-alkane b. C_{19} n-alkane. Other minor peaks include n-alkanes of various chain lengths less than C_{21}

From these results, neither the 50 kGy nor 100 kGy sets displayed reduction in the abundance of the starting compound. While several breakdown products were identified, they are all present in low abundances (close to the background).

5.3 Polycyclic Isoprenoids

5.3.1 Cholestanol

According to GC-MS analyses, the mean concentration C_x of cholestanol in the control set aliquots was 0.36 ±0.11 µg/µL (quantitated relative to the IS). For aliquots irradiated at 50 kGy, C_x of cholestanol decreased 0.30 ±0.04 µg/µL, and for those irradiated at 100 kGy, C_x increased to 0.39 ±0.10 µg/µL.

Cholestanol and IS peak areas, concentrations, and percent abundances relative to the control are detailed in Table 10. Change in percent abundance across the three sample sets is illustrated in Figure 55.

Table 10. Abundance of cholestanol by irradiation dose in control set, 50 kGy set, and 100 kGy set, as determined by GC-MS.

Grey represents averages for the triplicate aliquots in each set

Dose in kGy	Aliquot	Lipid compound (identified by NIST)	Peak area (cholestanol)	IS (identified by NIST)	Peak area (IS)	C_{IS} in µg/µL	C_x in µg/µL (cholestanol)	Percent abundance relative to the control (in %)
100	1 of 3	Cholestanol	3,363,297,369	Eicosanol	2,318,040,620	0.25	0.36	100.60
100	2 of 3	Cholestanol	2,657,424,890	Eicosanol	2,176,165,987	0.25	0.31	84.66
100	3 of 3	Cholestanol	1,319,050,172	Eicosanol	657,720,872	0.25	0.50	139.04
100 mean			2,446,590,810		1,717,309,160		0.39 ±0.10	108.10 ±27.96
50	1 of 3	Cholestanol	2,548,940,546	Eicosanol	1,863,726,190	0.25	0.34	94.82
50	2 of 3	Cholestanol	1,292,379,035	Eicosanol	1,174,350,601	0.25	0.28	76.30
50	3 of 3	Cholestanol	1,781,138,858	Eicosanol	1,524,383,722	0.25	0.23	81.01
50 mean			1,874,152,813		1,520,820,171		0.30 ±0.04	84.04 ±9.63
0	1 of 3	Cholestanol	2,205,210,376	Eicosanol	1,923,718,639	0.25	0.29	79.48
0	2 of 3	Cholestanol	2,101,762,939	Eicosanol	1,731,879,266	0.25	0.30	84.14
0	3 of 3	Cholestanol	2,396,635,300	Eicosanol	1,218,322,773	0.25	0.49	136.39
0 mean			2,234,536,205		1,624,640,226		0.36 ±0.11	100.00 ±31.60

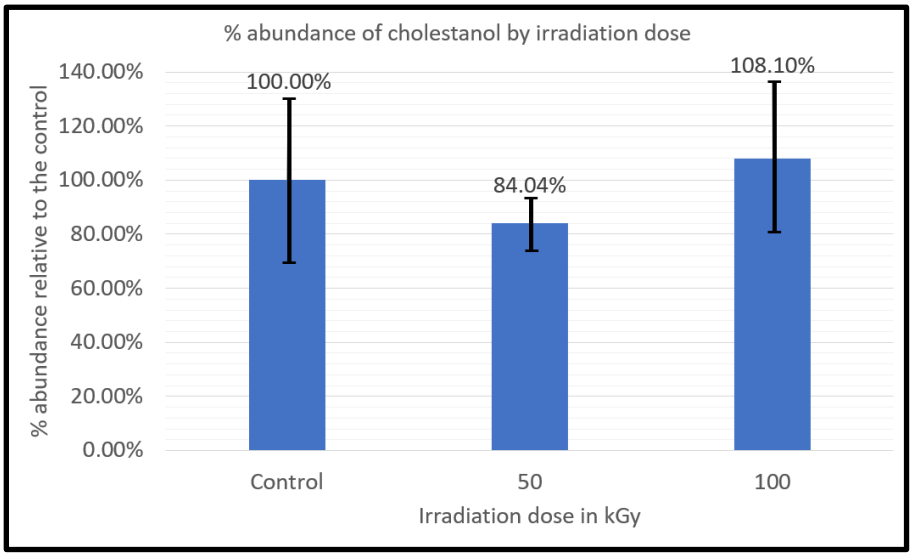

Figure 55. Percent abundance of cholestanol by irradiation dose in kGy, averaged over triplicates in each set

Compared to the control set, the relative abundance of cholestanol in the 50 kGy set decreased to 84.04% ±9.63%. For the 100 kGy set, the relative abundance increased to 108.10% ±27.96% compared to the control set. Standard deviation between the aliquots in the control and 100 kGy sets were high relative to other standards analyzed, at ±31.60% and ±27.96%, respectively.

Although the percent abundance of cholestanol was lower for the 50 kGy set relative to the control set, there was no significant reduction in the percent abundance in the 100 kGy set relative to the control, and the standard deviations for the control and 100 kGy sets were high.

Additionally, chromatograms from GC-MS analyses did not reveal any compounds present in the irradiated samples that were not also present in the control. If radiolytic breakdown had occurred, smaller peaks representing those species would have appeared. Figures 56-58 show representative chromatograms from each of the EBI doses and illustrate that, for all irradiation doses, only two compounds are present in any appreciable quantities: cholestanol and the IS. While cholestane is present in all of the aliquots, quantities are similar for the control, 50 kGy, and 100 kGy sets. The cholestanol standard purity was ≥95%, which explains the presence of cholestane.

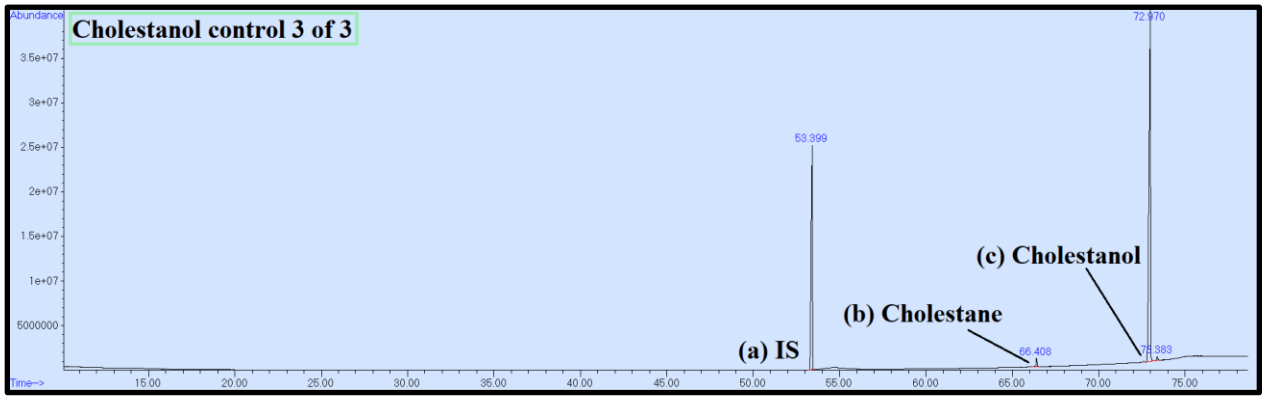

Figure 56. Chromatogram representing aliquot 3 of 3 from the cholestanol control set. (a) represents the eicosanol IS, (b) represents cholestane, a likely contaminant, and (c) represents cholestanol

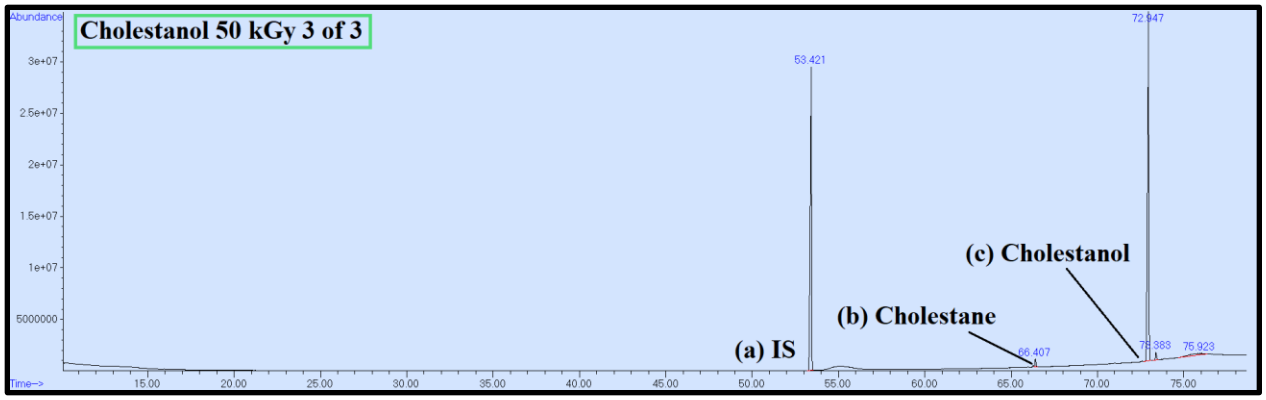

Figure 57. Chromatogram representing aliquot 3 of 3 from the cholestanol 50 kGy set. (a) represents the eicosanol IS, (b) represents cholestane, a likely contaminant, and (c) represents cholestanol

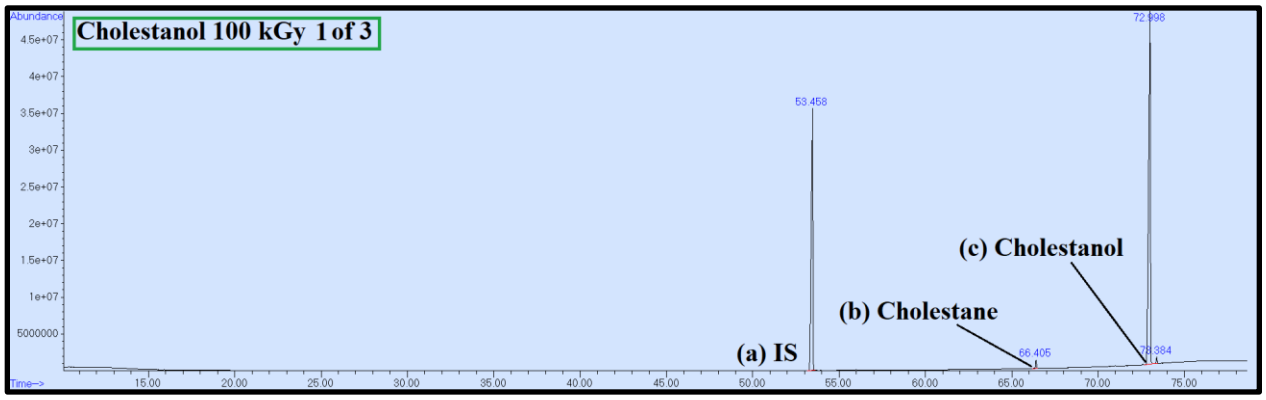

Figure 58. Chromatogram representing aliquot 1 of 3 from the cholestanol 100 kGy set. (a) represents the eicosanol IS, (b) represents cholestane, a likely contaminant, and (c) represents cholestanol

From these results, neither the 50 kGy nor 100 kGy sets displayed reduction in the abundance of the starting compound. No breakdown products were identified in any of the chromatograms.

5.3.1 Cholestane

According to GC-MS analyses, the mean concentration C_x of cholestane in the control set aliquots was 0.41 ±0.03 µg/µL (quantitated relative to the IS). For aliquots irradiated at 50 kGy,

C_x of cholestane was 0.43 ±0.05 µg/µL, and for those irradiated at 100 kGy, C_x was 0.44 ±0.04 µg/µL.

Cholestane and IS peak areas, concentrations, and percent abundances relative to the control are detailed in Table 11. Change in percent abundance across the three sample sets is illustrated in Figure 59.

Table 11. Abundance of cholestane by irradiation dose in control set, 50 kGy set, and 100 kGy set, as determined by GC-MS. Grey represents averages for the triplicate aliquots in each set

Dose in kGy	Aliquot	Lipid compound (identified by NIST)	Peak area (cholestanol)	IS (identified by NIST)	Peak area (IS)	C_{IS} in µg/µL	C_x in µg/µL (cholestane)	Percent abundance relative to the control (in %)
100	1 of 3	Cholestane	3,588,895,041	C_{23} FAME	1,868,449,274	0.25	0.48	116.65
100	2 of 3	Cholestane	3,174,676,614	C_{23} FAME	1,893,738,995	0.25	0.42	101.81
100	3 of 3	Cholestane	2,754,544,301	C_{23} FAME	1,654,674,866	0.25	0.42	101.10
100 mean			3,172,705,319		1,805,621,045		0.44 ±0.04	106.52 ±8.78
50	1 of 3	Cholestane	3,588,895,041	C_{23} FAME	1,868,449,274	0.25	0.48	116.65
50	2 of 3	Cholestane	2,844,091,503	C_{23} FAME	1,695,845,051	0.25	0.42	101.85
50	3 of 3	Cholestane	3,112,289,429	C_{23} FAME	2,017,684,257	0.25	0.39	93.68
50 mean			3,181,758,658		1,860,659,527		0.43 ±0.05	104.06 ±11.65
0	1 of 3	Cholestane	2,828,270,035	C_{23} FAME	1,593,779,832	0.25	0.44	107.77
0	2 of 3	Cholestane	2,646,598,260	C_{23} FAME	1,632,204,800	0.25	0.41	98.48
0	3 of 3	Cholestane	2,640,700,850	C_{23} FAME	1,710,628,050	0.25	0.39	93.75
0 mean			2,705,189,715		1,645,537,561		0.41 ±0.03	100.0 ±7.14

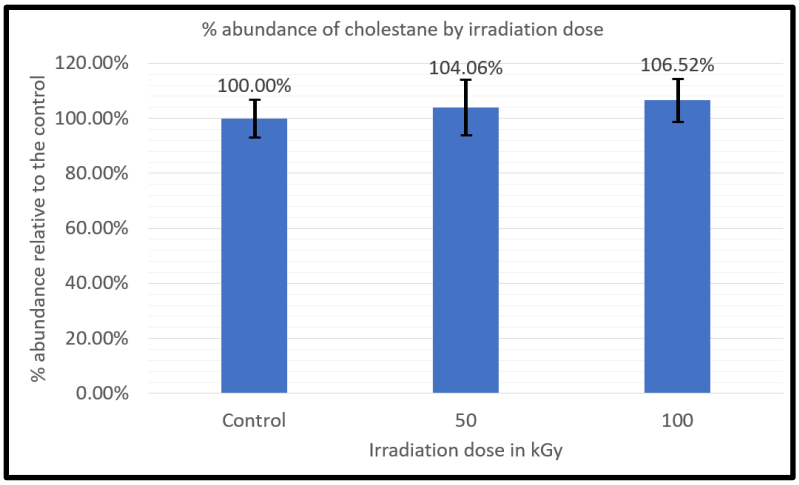

Figure 59. Percent abundance of cholestane by irradiation dose in kGy, averaged over triplicates in each set

Compared to the control set, the relative abundance of cholestane in the 50 kGy set was 104.06% ±11.65%. For the 100 kGy set, the relative abundance was 106.52% ±8.78% compared to the control set. Standard deviation between the aliquots in the control set was ±7.14%.

From these analyses, no significant degradation in cholestane was observed at either 50 kGy or 100 kGy of irradiation.

Additionally, chromatograms from GC-MS analyses did not reveal any other compounds in the sample. If radiolytic breakdown had occurred, smaller peaks representing those species would have appeared. Figures 60-62 show representative chromatograms from each of the EBI doses and illustrate that, for all irradiation doses, only two compounds are present in any appreciable quantities: cholestane and the IS.

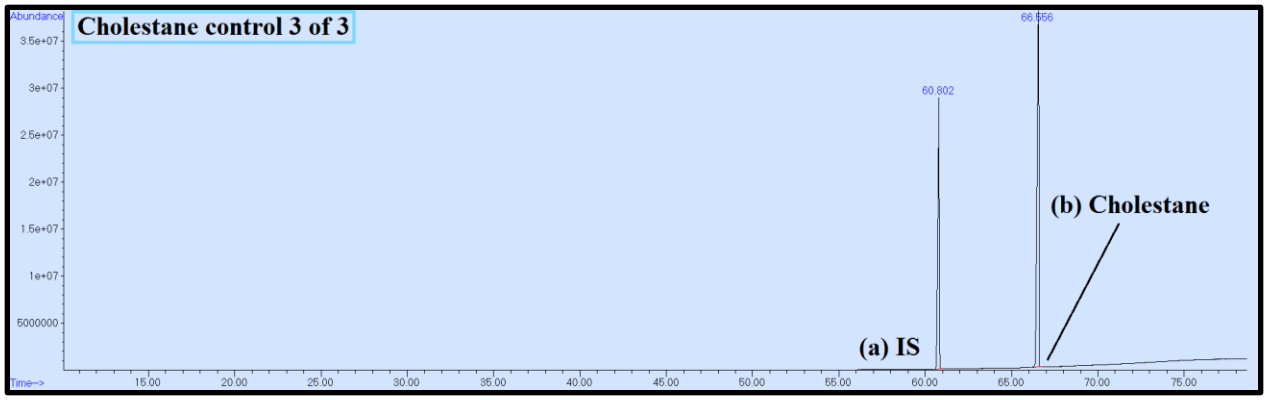

Figure 60. Chromatogram representing aliquot 3 of 3 from the cholestane control set. (a) represents the C23 FAME IS, (b) represents cholestane

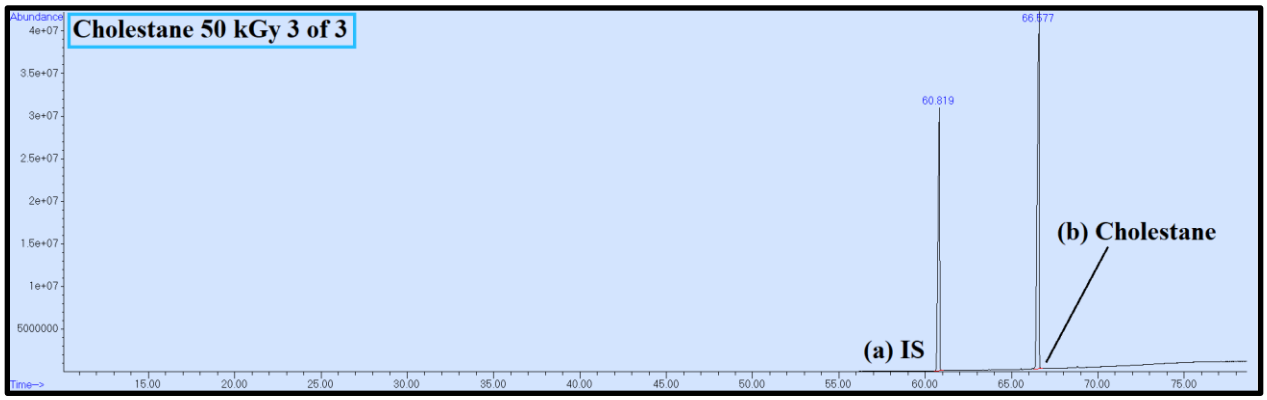

Figure 61. Chromatogram representing aliquot 3 of 3 from the cholestane 50 kGy set. (a) represents the C23 FAME IS, (b) represents cholestane

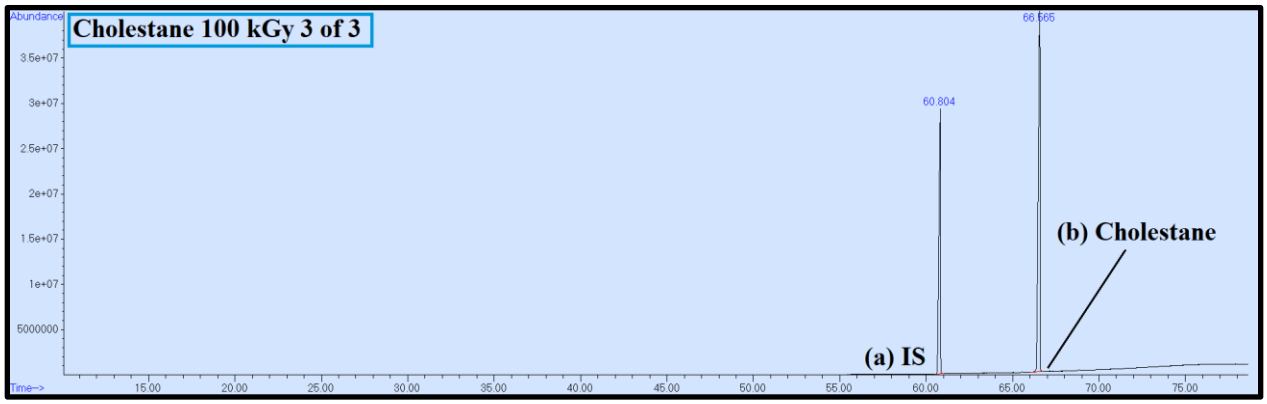

Figure 62. Chromatogram representing aliquot 3 of 3 from the cholestane 100 kGy set. (a) represents the C23 FAME IS, (b) represents cholestane

From these results, neither the 50 kGy nor 100 kGy sets displayed reduction in the abundance of the starting compound. No breakdown products were identified in any of the chromatograms.

CHAPTER V: DISCUSSION

5.1 Lipid Breakdown Following Irradiation

It was expected that EBI applied at 50 kGy and 100 kGy would effectively degrade fatty acids, alkanes, and polycyclic isoprenoids, but results of this study did not confirm the hypothesis, as no consistent degradation was observed across irradiation doses for any of the lipid classes tested. For two of the sample sets (palmitic acid 100 kGy and cholestanol 50 kGy), the percent abundance in the experimental standard compared to the control did decrease, but further analyses show that no significant quantity breakdown products were formed. Minor breakdown products were identified in the palmitic acid, oleic acid, and heneicosane 50 kGy and 100 kGy sets, which confirms that EBI did slightly degrade the lipid standards, but these low abundance products are not present in significant quantities. Further, abundances of breakdown products are so low that they do not account for any reduction observed in the palmitic acid 100 kGy set. No breakdown products were observed in any of the irradiated polycyclic isoprenoid aliquots, even the 50 kGy cholestane set that displayed a reduction relative to the control.

Since lipid standards were not degraded significantly following EBI and since breakdown products are themselves smaller lipids that would still cause false positives in life detection surveys, the results of this study suggest that this technique should not be used to decontaminate lipids from life detection instruments.

5.1.1 Fatty Acids

5.1.1.1 Palmitic Acid

Palmitic acid was not effectively degraded with EBI, but a decrease in compound abundance was observed following the highest irradiation dose applied. The relative abundance following 100 kGy irradiation was 79.50% ±2.3% compared to the control, but no corresponding decrease in abundance was observed in the 50 kGy set, which displayed a relative abundance of 99.96% ±2.1%.

A suite of low-abundance breakdown products was observed, which includes both degraded compounds and recombinants. This suggests that irradiation breaks down these compounds at numerous points and does not necessarily preferentially attack specific bonds in the molecule compared to others.

Saturated fatty acids and *n*-alkanes of every chain length shorter than C_{16} were observed in irradiated samples, which represent degraded compounds. The presence of both fatty acids and *n*-alkanes indicates that EBI cleaved the carboxyl group in some molecules, and broke C-C bonds in the hydrocarbon backbone in others. Dicarboxylic acids, oxoacids, and hydroxy oxoacids were also observed, which represent recombinants. Since the starting palmitic acid is a monocarboxylic acid, these other compounds necessarily make up fatty acid fragments that were broken and then recombined during or after irradiation.

The presence of monounsaturated fatty acids suggests that for some molecules, EBI cleaved hydrogens from the hydrocarbon chain, and those bonds re-formed as C=C double bonds. During geological diagenesis processes, unsaturations are lost and not formed, which suggests that irradiation is transforming these molecules through different mechanisms than occur during geologic reprocessing.[24]

No 2-ACBs were detected, but a structurally similar furanone was observed (Figure 63).

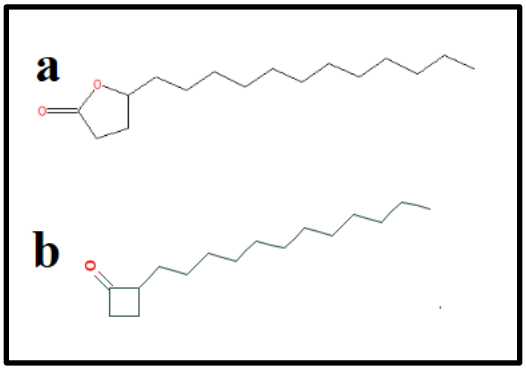

Figure 63. a. 2(3H)-Furanone, 5-dodecyldihydro-, a low-abundance breakdown product of palmitic acid observed in the 100 kGy set, b. 2-dodecyclobutanone, a 2-ACB not observed in these samples but reported in the literature as a unique radiolytic product of the C_{16} fatty acid components of triglycerides, formed following EBI application

Mansour et al. found that furanones were created following gamma irradiation of *Moringa oleifera* seeds, and Bhatia et al. found similar compounds following EBI of beef, but formation mechanisms have not been constrained.[161,162] Food irradiation studies on 2-ACB formation hypothesize that these compounds can only be created through ionizing radiation applied to a specific point in the fatty acid portion of a triglyceride molecule for a short period of time, causing cyclization of the tail.[150] Further work is needed to elucidation formation of furanones and 2-ACBs, but similar breakdown could be occurring during creation of each of these compounds.

Although a reduction of palmitic acid in the 100 kGy set is observed, lack of significant abundance breakdown products could suggest that this is due to either GC-MS response or operator variance in precisely handling extremely small fluid volumes; or that the molecules were broken down into smaller, volatile fragments. Since the palmitic acid was a pure standard irradiated in the presence of N_2 and since recombinants were observed in other lower radiation doses, it is hypothesized that EBI-induced breaks re-formed or combined with other fragments during or shortly following irradiation. This is likely because there was no oxygen atmosphere and no

reactive species present for any cleaved molecules to further react with. Seo et al. found that volatilized fatty acids were degraded with EBI under N_2, but recombinants were also observed, including those larger than the starting compounds; it is hypothesized that a similar phenomenon is occurring here. Seo et al. also found that removal efficiency decreased with increasing molecular weight (up to 100% removal at the ~ppm level for the smallest fatty acids at a maximum of 20 kGy irradiation), but valeric acid (a C_5 compound) was the largest studied. Finally, they studied volatilized fatty acids instead of ones deposited on glass, so molecular weight and state could both contribute to the lack of removal observed in this thesis study.[146]

5.1.1.2 Oleic Acid

Oleic acid was not degraded with EBI. For the 50 kGy set, percent abundance relative to the control was 91.66% ±8.43%, placing variance from 100% within the margin of error. For the 100 kGy set, percent abundance relative to the control was 97.45% ±5.02%, which also places variance from 100% within the margin of error.

Like with the palmitic acid, tens of low-abundance breakdown products were observed, including both degraded molecules and recombinants.

For the oleic acid, degraded products include saturated fatty acids and *n*-alkanes of every chain length shorter than C_{18}, along with a $C_{18:1}$ alkene. Of all the short-chain fatty acids, a $C_{8:0}$ fatty acid is the most abundant; this suggests that while the hydrocarbon tail can be cleaved at any point, it is slightly more likely to break at the position of the unsaturation, since the double bond in oleic acid occurs between C_8 and C_9. This follows trends observed in food irradiation studies that also find unsaturated fatty acids tend to break at double bonds.[141–143] However, these bonds are sometimes unaffected in molecules that have the carboxyl group cleaved, as illustrated by the presence of 8-heptadecene (Figure 64).

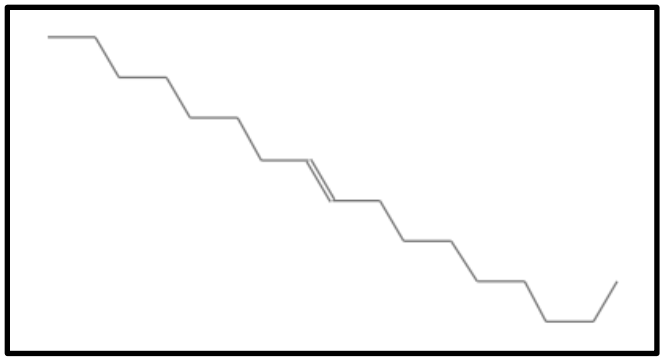

Figure 64. 8-heptadecene, a radiolytic product of oleic acid observed in the 100 kGy set

As with the palmitic acid, recombinants are observed in the 50 kGy and 100 kGy irradiated oleic acid sets, including several dicarboxylic acids and oxoacids.

Lack of breakdown in oleic acid following irradiation can be explained by the lack of reactive species available to further degrade or transform the molecules following bond cleavage by electron impact. As with the palmitic acid, it is hypothesized that any broken bonds simply re-formed, and occasionally bonded to other fragments.

5.1.2 Alkanes

5.1.2.1 Heneicosane

Heneicosane was not effectively degraded with EBI. For the 50 kGy set, percent abundance relative to the control was 101.29% ±7.14%, placing variance from 100% within the margin of error. For the 100 kGy set, percent abundance relative to the control was 103.29% ±6.43%, which also places variance from 100% within the margin of error.

As with the fatty acids, a homologous series of *n*-alkanes of every chain length shorter than C_{21} was observed following irradiation. However, no additional breakdown products were observed, and those present were extremely low in abundance.

Since heneicosane contains only carbon and hydrogen, fewer possible breakdown products can form relative to oxygen-containing fatty acids. Further, *n*-alkanes are made up of C-C and C-H bonds, making them extremely recalcitrant species, as evidenced by their longevity in the geologic record (~Gyr).[24] Although irradiation does not appear to degrade lipids by the same mechanisms that occur during diagenetic degradation, where double bonds and carboxyl groups are lost/cleaved/oxidized first, it does appear that the recalcitrance of n-alkanes relative to fatty acid holds for both geologic and radiolytic processing. Finally, it is hypothesized that lack of reactive species or oxygen present during irradiation is the main reason that heneicosane did not break down significantly.

5.1.3 Polycyclic Isoprenoids

5.1.3.1 Cholestanol

Cholestanol was not effectively degraded with EBI. Although the relative abundance following 50 kGy irradiation was 84.04% ±9.63% compared to the control, no corresponding decrease in abundance was observed in the 100 kGy set. The standard deviation was high across the control and 100 kGy sets at ±31.60% and ±27.96%, respectively, and low for the 50 kGy set at ±9.63%.

Unlike the aliphatic compounds, cholestanol yielded no breakdown products in the GC-MS that were distinguishable from the background. However, following irradiation, a white crystalline structure was visible on the inside surface of the vials holding the cholestanol, and a white ring was present around the lips of some of these vials, but not in the controls (Figure 65).

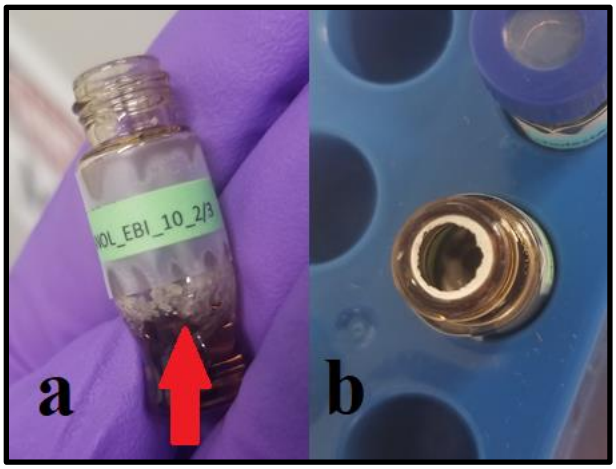

Figure 65. Cholestanol following EBI. a. shows a white residue found around the lip of some of the irradiated vials, and b shows a white crystalline structure apparent on the inside walls of all the vials

Additionally, when DCM was added to re-solubilize the cholestanol, ~mm in diameter white chunks were present that did not visibly disappear until the solution was warmed to room temperature and vortexed for ~60 seconds. The chunks in the 100 kGy set appeared larger than those in the 50 kGy set and appeared to take longer to dissolve. Further exploration is needed to determine the nature of these structures, but since no additional compounds were present in the GC-MS analyses, no reduction was observed in the 100 kGy set, and only minor reduction was observed in the 50 kGy set, it is unlikely that the cholestanol was degraded into smaller compounds. Standard deviation was high across all sets, so the apparent degradation is hypothesized as being due to either GC-MS response or operator variance in precisely handling extremely small fluid volumes.

Although cholestanol contains a potentially reactive hydroxyl group (like fatty acids do), its polycyclic hydrocarbon structure is extremely stable- even more stable than the recalcitrant aliphatic hydrocarbon structure of n-alkanes.[24,163] This combined with the N_2 within the irradiated vials and lack of oxygen or other reactive species likely contributed to the lack of significant breakdown.

5.1.3.2 Cholestane

Cholestane was not effectively degraded with EBI. For the 50 kGy set, percent abundance relative to the control was 104.06% ±11.65%, placing variance from 100% within the margin of error. For the 100 kGy set, percent abundance relative to the control was 106.53% ±8.78%, which also places variance from 100% within the margin of error.

As with the cholestanol, no breakdown products were observed in any of the GC-MS chromatograms. Unlike cholestanol, no reduction was observed in any of the aliquots and standard deviation is low. Like *n*-alkanes, cholestane contains only carbon and hydrogen, so .[24,163] N_2, lack of reactive species with which to recombine, and stability of the cyclic structures likely all contributed to the lack of breakdown observed here.

5.2 Implications for Life Detection Instruments

It was hypothesized that EBI would be highly effective at removing lipids from life detection instruments through radiolytic degradation, but lack of breakdown in standards at the high doses tested suggests that EBI is not an effective lipid decontamination technique. No compound was significantly degraded across all irradiation doses, and minor breakdown products identified are themselves smaller lipids that would still present a contamination concern for life detection surveys. Although previous studies show that EBI can effectively kill microbes, this study suggests that it cannot remove/destroy lipid molecules found in biological and industrial contaminants.

CHAPTER VI: Conclusion and Future Work

6.1 Implications for Life Detection Missions

Although the results of this study do not support implementation of EBI as a lipid decontamination technique, lack of breakdown reinforces the claim that lipids are ideal biomarkers for life detection surveys. If lipid standards can survive concentrated, direct streams of ionizing electrons, they could potentially resist degradation on other planetary surfaces/subsurfaces that receive high radiation fluxes, at least for timescales that accrue cumulative doses equivalent to those tested in this study. Organic lifetimes would increase with burial depth since regolith or ice covering lipids would help shield them.[64] Understanding lipid biomarker longevity and potential breakdown products in high radiation environments, like Mars and Europa, is essential for crafting life detection investigations.

The experimental conditions (lipids kept cold under an oxygen-free environment on borosilicate glass) share some qualities with Mars and Icy Moon environments. Those bodies have no or very thin atmospheres,[164,165] and Martian regolith is rich in silicates.[166] Oher conditions on these bodies do vary (i.e., perchlorates on Mars, water on Icy Moons), so further research is needed to simulate these other conditions (in addition to those used in this study)

6.1.1 Implications for Mars

Mars has no magnetic field and a thin atmosphere, so it receives a high radiation flux relative to Earth. The Mars Science Laboratory's (MSL) Radiation Assessment Detector (RAD)

onboard the Curiosity rover found that the average flux on the surface due to galactic cosmic radiation (GCR) is ~76 mGy/year. At a 10 cm depth in the subsurface, the dose increases to ~96 mGy/year, but then drops with depth as described in Figure 64.

Depth below surface	Effective shielding mass (g/cm^2)	GCR dose rate (mGy/year)	GCR dose-equivalent rate (mSv/year)
Mars surface (RAD)	0	76	232
−10 cm	28	96	295
−1 m	280	36.4	81
−2 m	560	8.7	15
−3 m	840	1.8	2.9

Figure 66. Mars subsurface radiation estimates from Hassler et al. calculated from surface measurements taken with the MSL RAD instrument and the HZETRN model[167]

GCRs are mostly made up of protons (85%) and alpha particles (14%), with a small amount of heavy particles and electrons, so the results of this thesis study are not directly applicable, as GCR irradiation may interact with organic molecules differently than smaller particle electron irradiation. However, small size means that electrons can penetrate solid materials deeper than heavier particles can, with greater potential to impact buried material. Additionally, GCRs striking the surface generate secondary radicals (including neutrons, gamma particles, and electrons) in a cascading effect that penetrates the surface further than the primary particles themselves (Figure 65).[168,169]

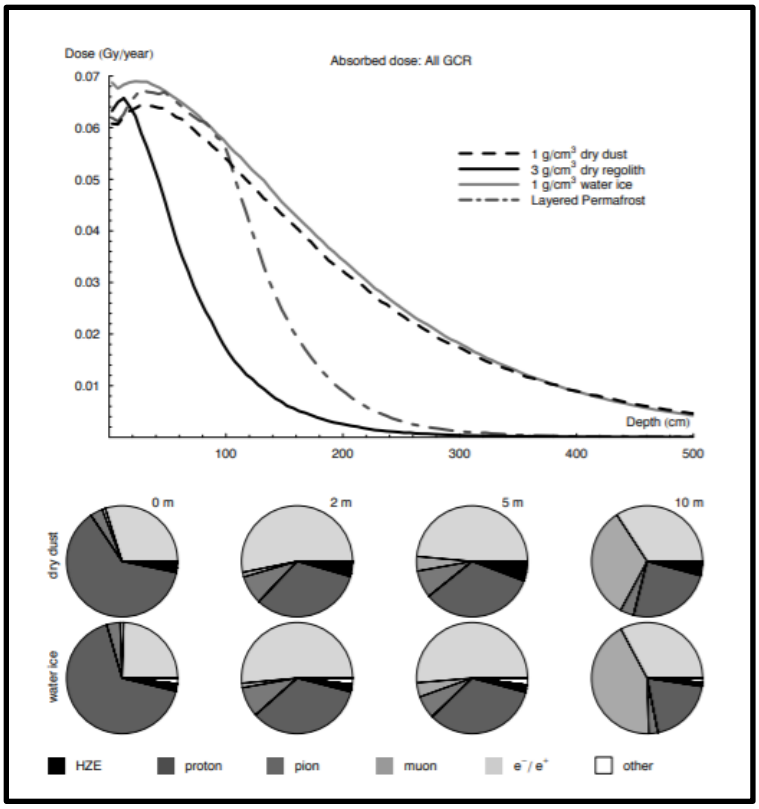

Figure 67. (top) GCR dose profile in the Martian subsurface and (bottom) the changing composition of the ionizing radiation field with depth, compared between 1g/cm³ dry dust and water ice. Light grey fraction is electrons, which increase with depth[170]

Hassler et al. report that organics approximately 100 atomic mass units in size could survive for ~650 million years on Mars at 4-5 cm surface depth at doses measured by RAD, but note that the Martian subsurface radiation environment is dynamic and unlike any found on Earth, so further study is needed to elucidate effects on other, smaller biomolecules like lipids.[167] Radiation flux estimates vary drastically within the literature,[64,167,169,170,170] so further research is needed to determine true flux and environmental effects (i.e., subsurface interactions with perchlorates, shielding, etc.) to estimate lipid lifetimes.

6.1.2 Implications for Europa

Although Mars' radiation environment primarily consists of GCR, UV, and Solar Energetic Particles (SEP), Europa is dominated by electron and heavy ion radiation from within Jupiter's magnetosphere.[171,172] Paranicas et al. show that the flux of energetic electrons delivered to Europa's surface could penetrate up to one meter into its solid ice shell (Figure 66).

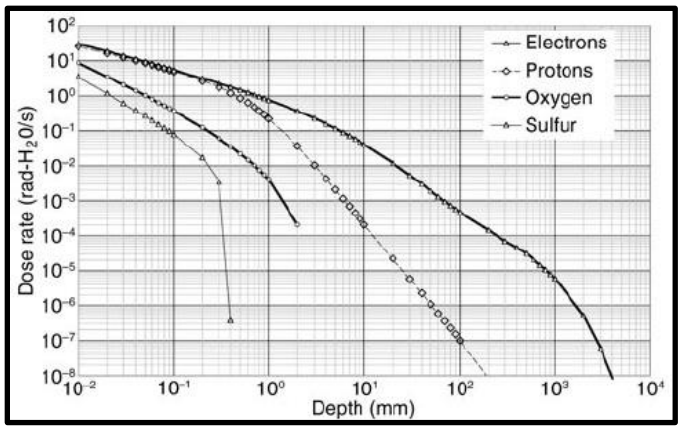

Figure 68. Dose rate in rad-H_2O/sec versus depth curves for ion and electron irradiation into the Europan subsurface[171,173]

Although any life native to Europa would almost certainly live within the shielded subsurface ocean, organic matter contained within liquid water plumes is frequently ejected from the subsurface. These molecules are proposed targets of life detection surveys, as they could provide evidence of organisms that live deep within an ocean otherwise inaccessible to spacecraft.[18,23] Additionally, organics sourced from the ocean migrate upwards through the ice shell over long timescales, and Johnson and Sundvist estimate that as these molecules near the surface (where they could potentially be detected and analyzed by future astrobiology missions), they could be degraded by penetrating electron irradiation and removed by surface sputtering (i.e., when a solid surface is impacted by ions or other energetic particles, causing microscopic particles from that surface to be excavated and ejected), with an estimated ~10 year lifetime to ejection for a particle buried at ~10 μm.[174] Future research is needed to determine how electron (and ion) irradiation

would impact lipids in these environments, but the robustness that lipids displayed against 100 kGy EBI in this study suggest that they also may be able to withstand radiation on Europa's surface for long periods of time.

To characterize lipid lifetimes, future work is needed that replicates multiple environmental conditions and exposes lipids to EBI in conjunction with other types of relevant radiation at higher doses than tested in this thesis to effectively drive life detection search techniques.

6.2 Implications for CC

Although this study found that EBI did not degrade lipids at the doses tested, further work is needed to establish doses of irradiation that would destroy these compounds. Lack of breakdown even at 100 kGy suggests that to remove lipid contaminants below the ~ppb range, extremely high doses would likely be required. EBI up to 100 kGy is compatible with many major materials used in life detection instruments but may not be compatible at doses required to destroy lipids. Further work is needed to identify and test an effective lipid decontamination protocol for life detection instruments; instead of radiation-based methods or heat-based methods, chemical degradation is the next logical step.

Additionally, apparent longevity of lipids under EBI suggests that these compounds could be long-lived on Mars and Europa as well, so further work is needed to replicate environmental conditions to greater fidelity and expose lipids to greater doses of EBI in conjunction with other types of radiation to determine how and when lipid biomarkers might degrade in these environments; this could help determine potential biomarker ages and constrain life detection search techniques.

APPENDIX A: GC-MS Chromatograms (palmitic acid)

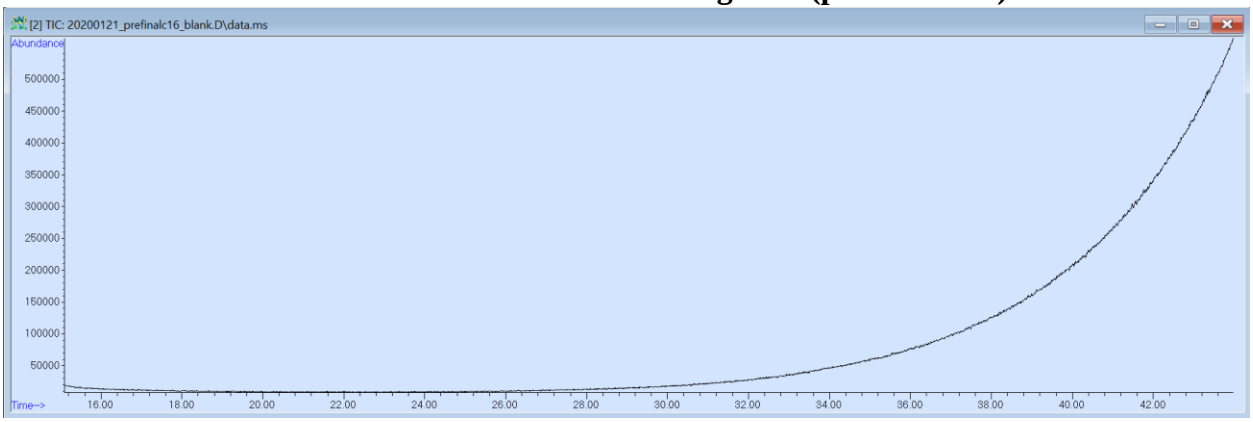

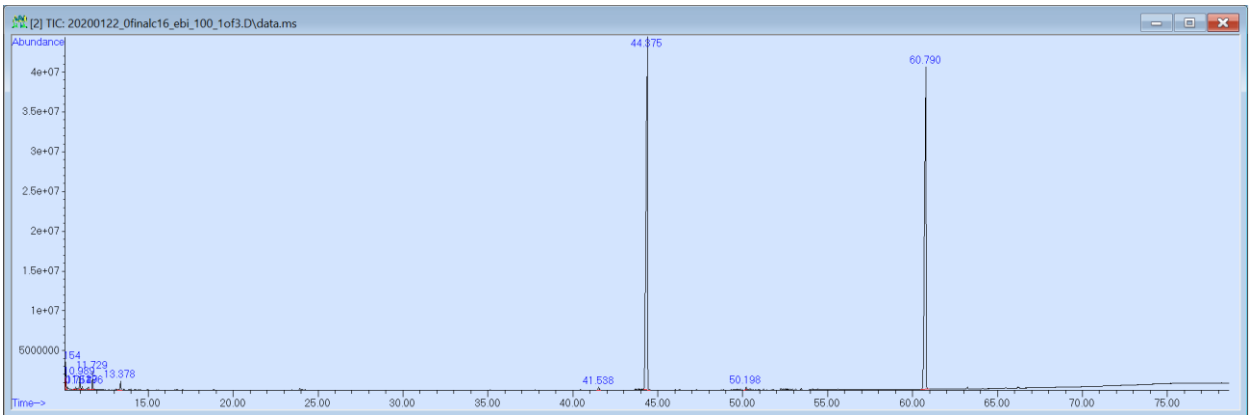

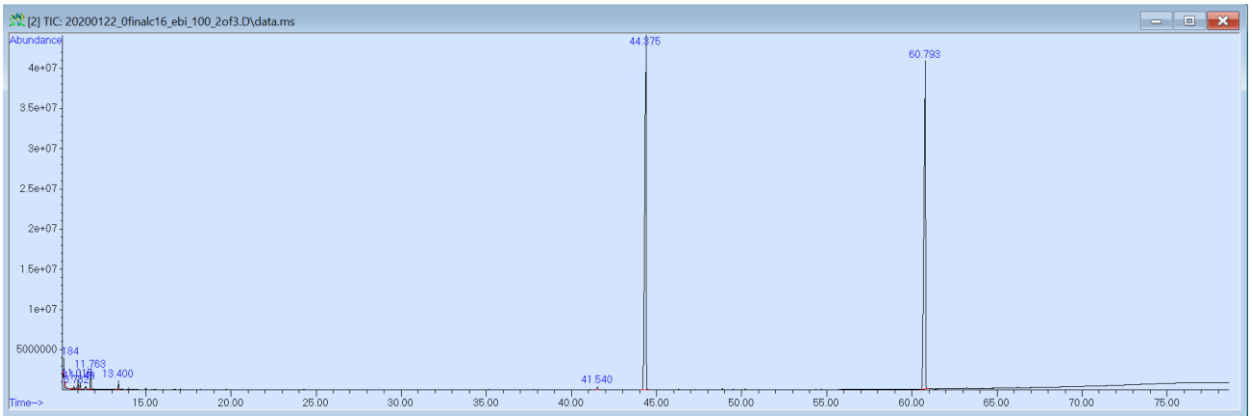

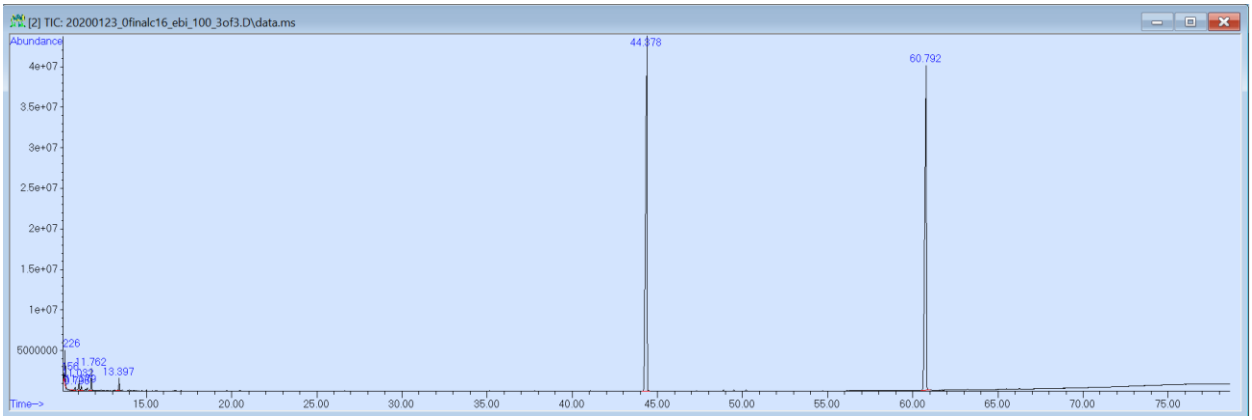
[2] TIC: 20200123_0finalc16_ebi_100_3of3.D\data.ms
Abundance
44.378
60.792
226
11.762
13.397
Time-->
15.00
20.00
25.00
30.00
35.00
40.00
45.00
50.00
55.00
60.00
65.00
70.00
75.00

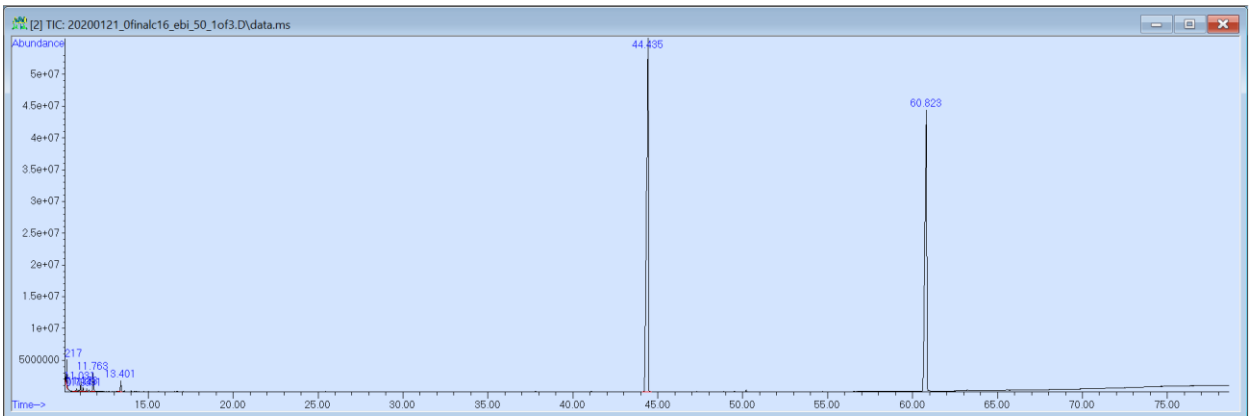
[2] TIC: 20200121_0finalc16_ebi_50_1of3.D\data.ms
Abundance
44.435
60.823
217
11.763
13.401
Time-->
15.00
20.00
25.00
30.00
35.00
40.00
45.00
50.00
55.00
60.00
65.00
70.00
75.00

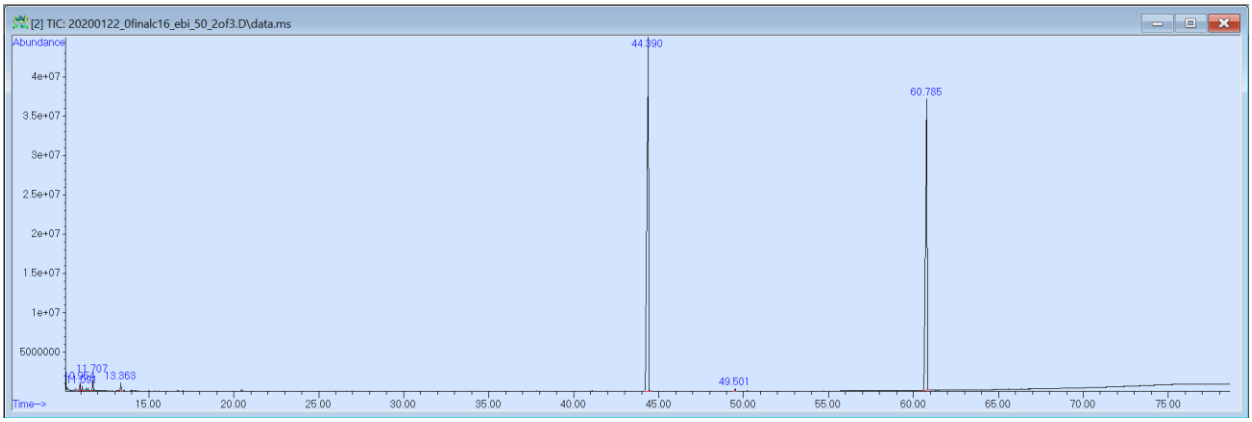
[2] TIC: 20200122_0finalc16_ebi_50_2of3.D\data.ms
Abundance
44.390
60.785
11.707
13.368
49.501
Time-->
15.00
20.00
25.00
30.00
35.00
40.00
45.00
50.00
55.00
60.00
65.00
70.00
75.00

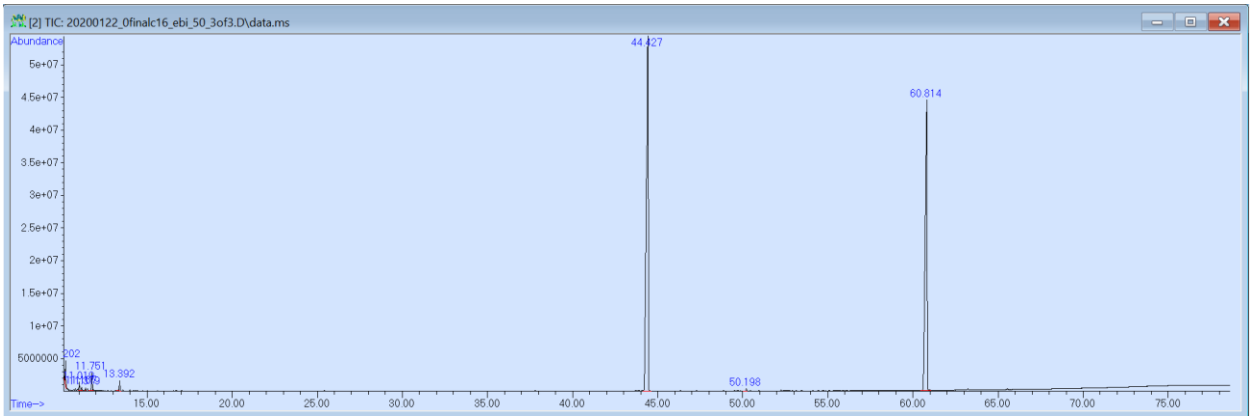
[2] TIC: 20200122_0finalc16_ebi_50_3of3.D\data.ms
Abundance
44.427
60.814
50.198
11.751
13.392
Time-->

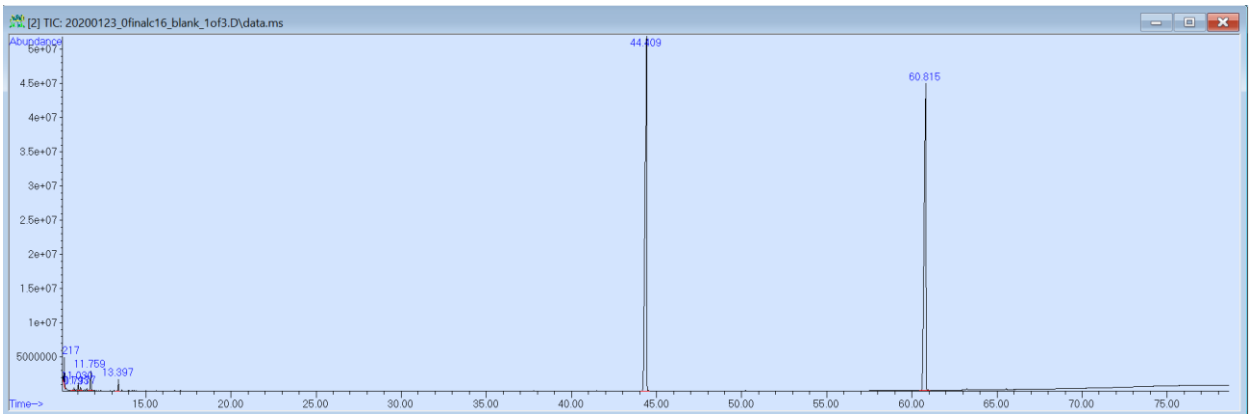
[2] TIC: 20200123_0finalc16_blank_1of3.D\data.ms
Abundance
44.409
60.815
11.759
13.397
Time-->

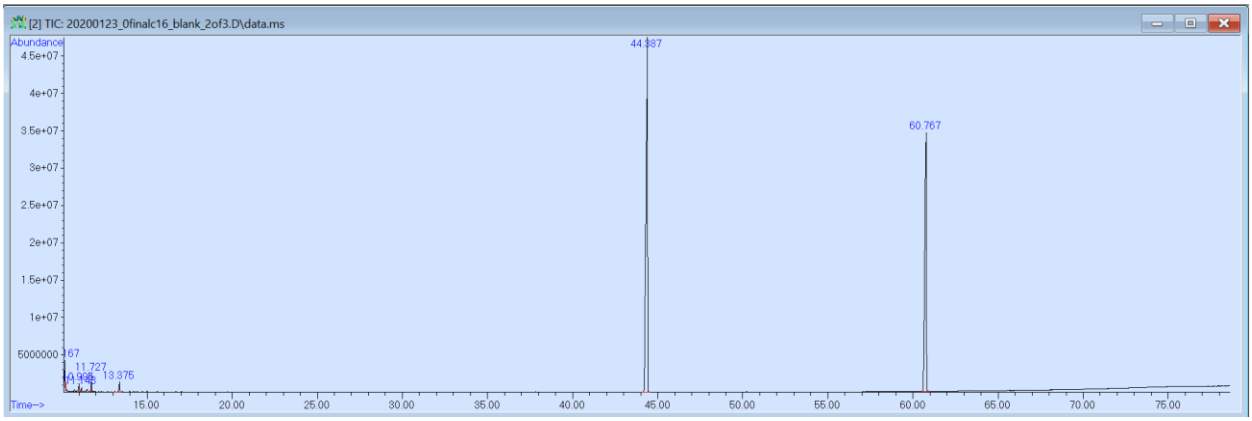
[2] TIC: 20200123_0finalc16_blank_2of3.D\data.ms
Abundance
44.387
60.767
11.727
13.375
Time-->

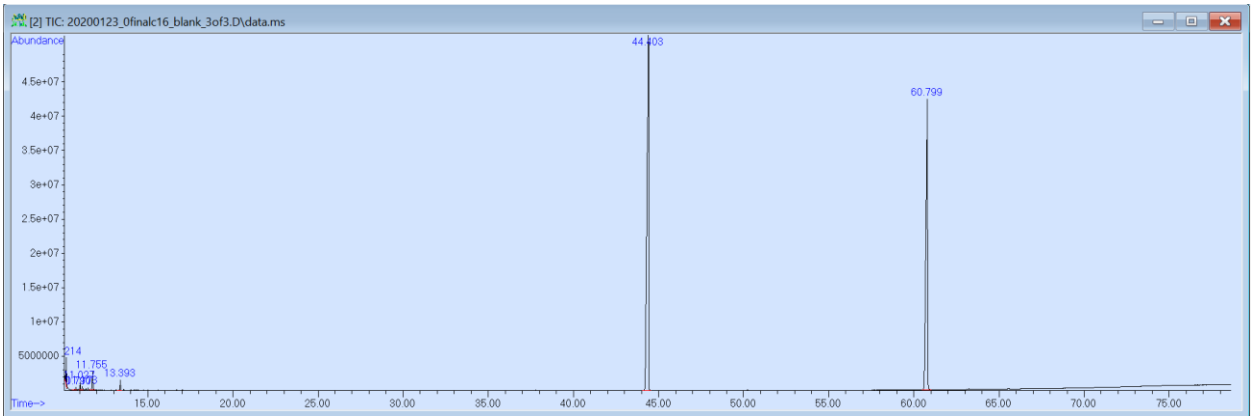
[2] TIC: 20200123_0finalc16_blank_3of3.D\data.ms
Abundance
44.403
60.799
4.5e+07
4e+07
3.5e+07
3e+07
2.5e+07
2e+07
1.5e+07
1e+07
5000000
214
11.755
13.393
Time-->
15.00
20.00
25.00
30.00
35.00
40.00
45.00
50.00
55.00
60.00
65.00
70.00
75.00

APPENDIX B: GC-MS Chromatograms (oleic acid)

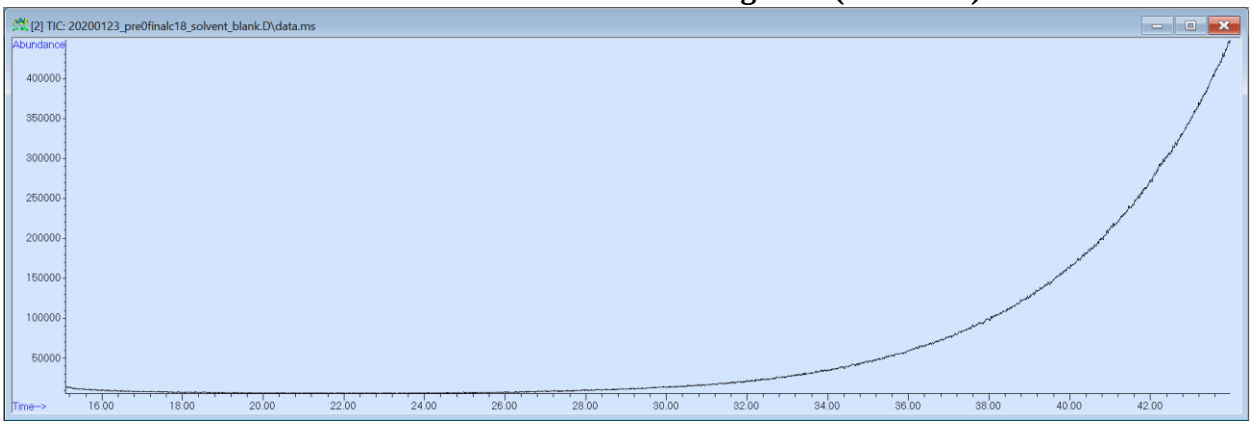

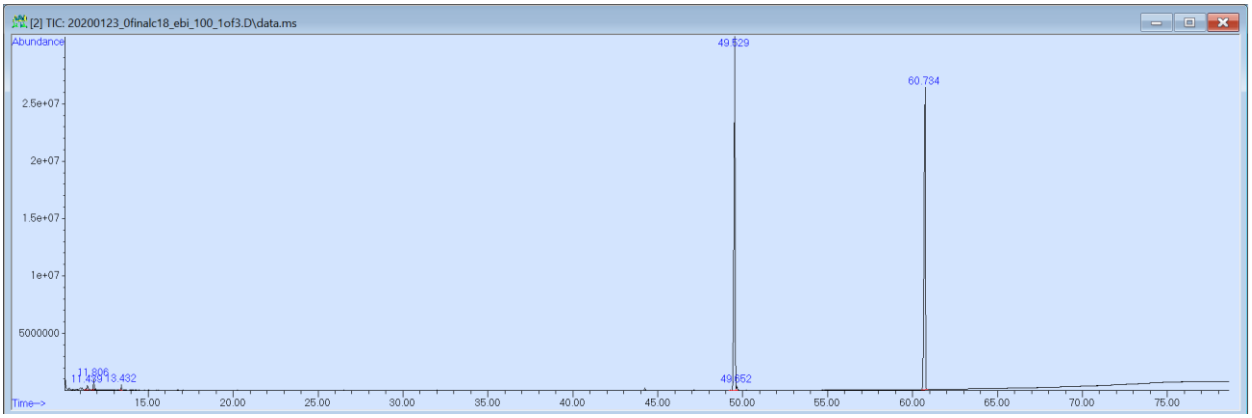

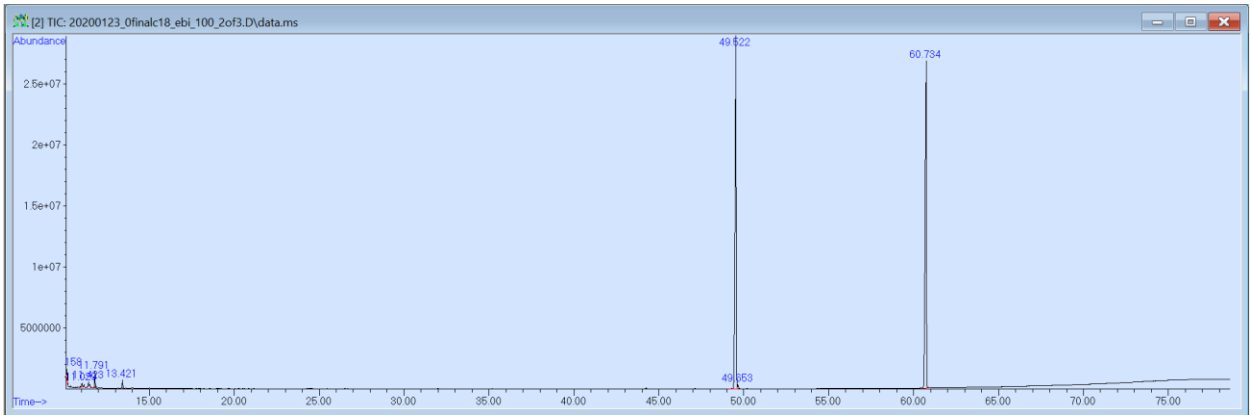

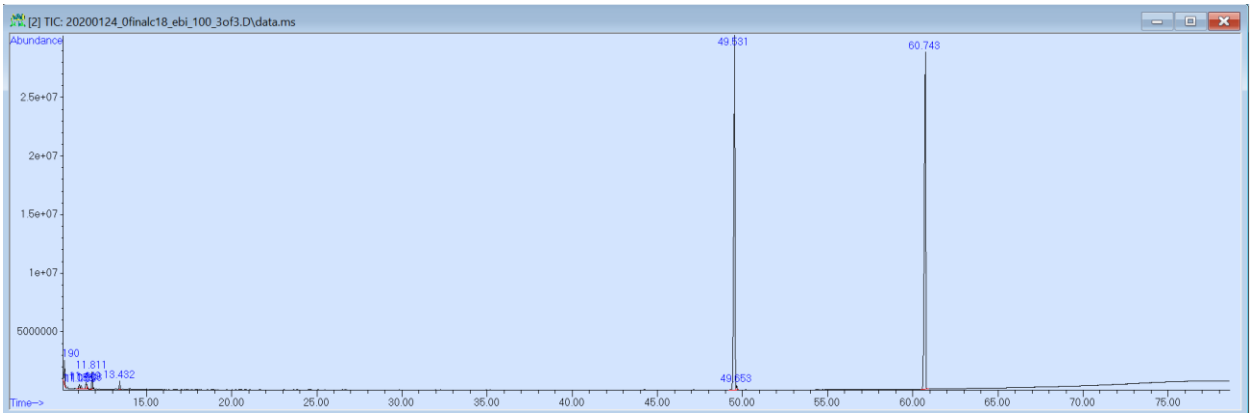
[2] TIC: 20200124_0finalc18_ebi_100_3of3.D\data.ms
Abundance
49.631
60.743
11.811
13.432
49.653
Time-->

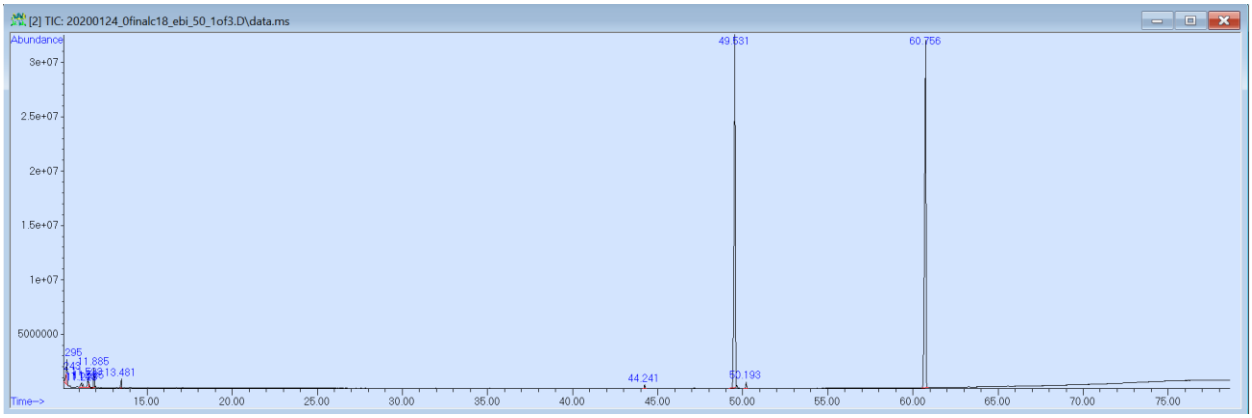
[2] TIC: 20200124_0finalc18_ebi_50_1of3.D\data.ms
Abundance
49.631
60.756
11.885
13.481
44.241
50.193
Time-->

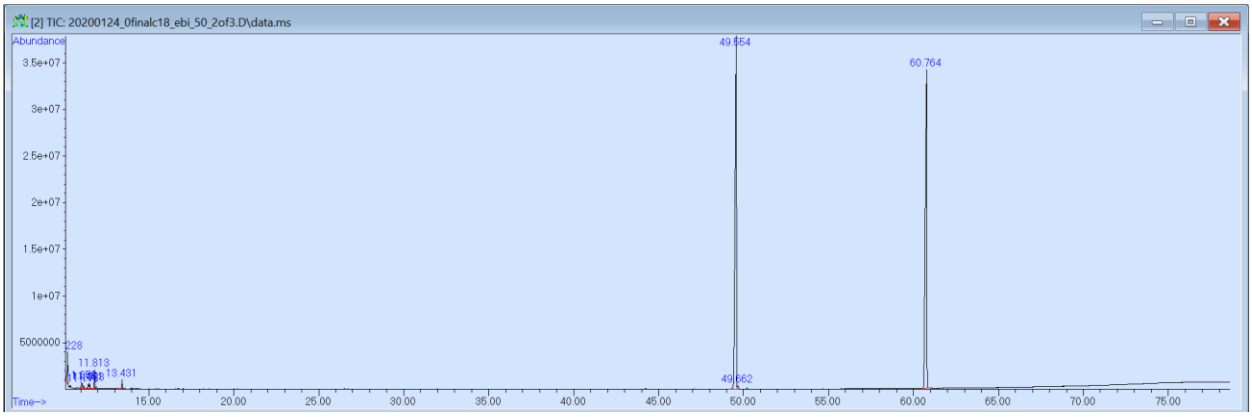
[2] TIC: 20200124_0finalc18_ebi_50_2of3.D\data.ms
Abundance
49.654
60.764
11.813
13.431
49.662
Time-->

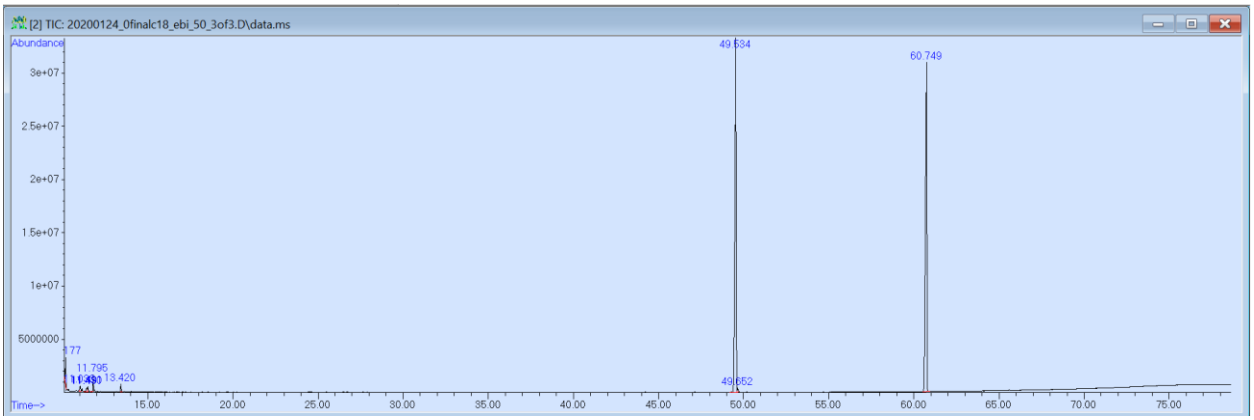
[2] TIC: 20200124_0finalc18_ebi_50_3of3.D\data.ms
Abundance
49.634
60.749
11.795
13.420
49.652
Time-->

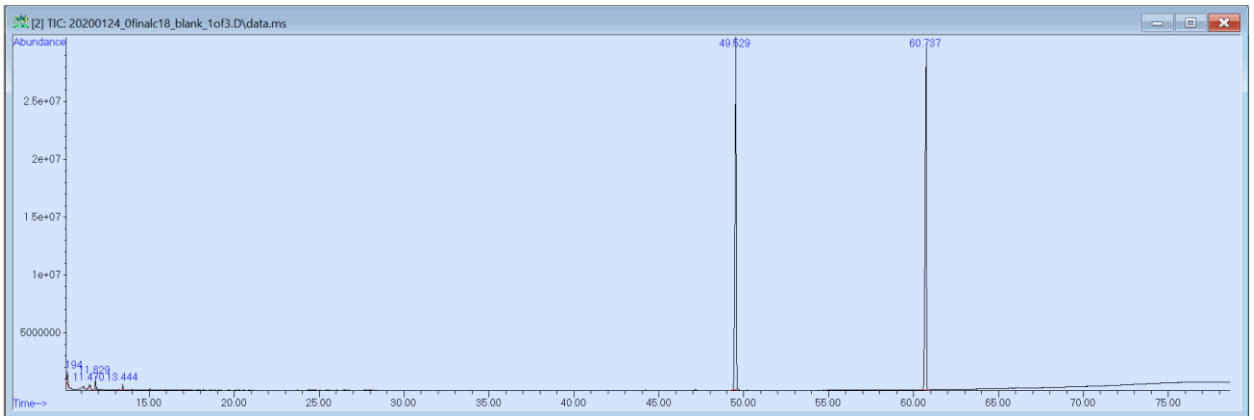
[2] TIC: 20200124_0finalc18_blank_1of3.D\data.ms
Abundance
49.629
60.737
11.829
13.444
Time-->

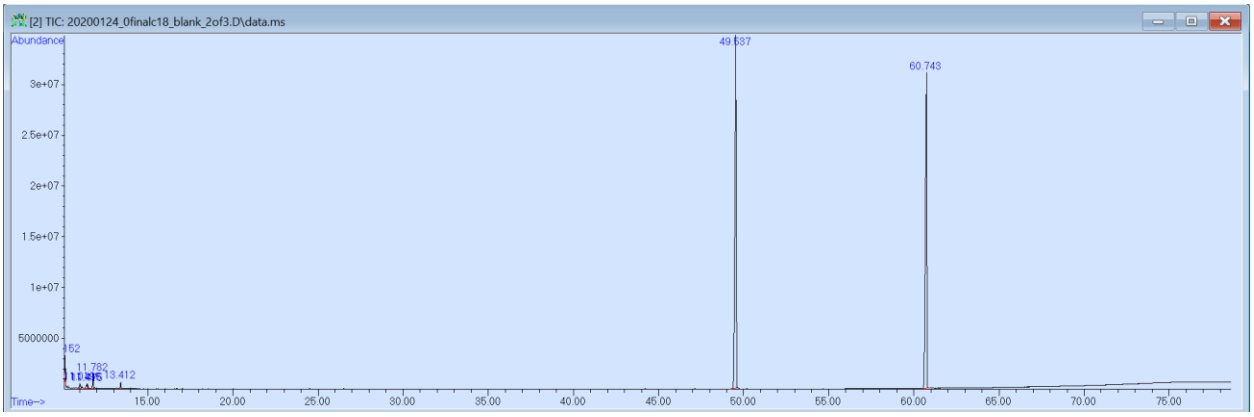
[2] TIC: 20200124_0finalc18_blank_2of3.D\data.ms
Abundance
49.637
60.743
11.782
13.412
Time-->

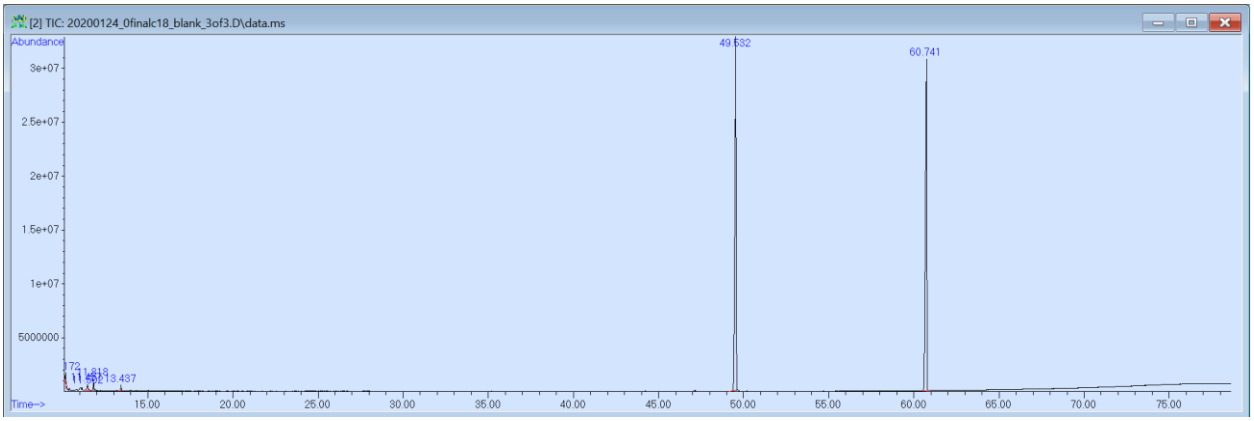
[2] TIC: 20200124_0finalc18_blank_3of3.D\data.ms
Abundance
3e+07
2.5e+07
2e+07
1.5e+07
1e+07
5000000
49.632
60.741
Time-->
15.00
20.00
25.00
30.00
35.00
40.00
45.00
50.00
55.00
60.00
65.00
70.00
75.00

APPENDIX C: GC-MS Chromatograms (heneicosane)

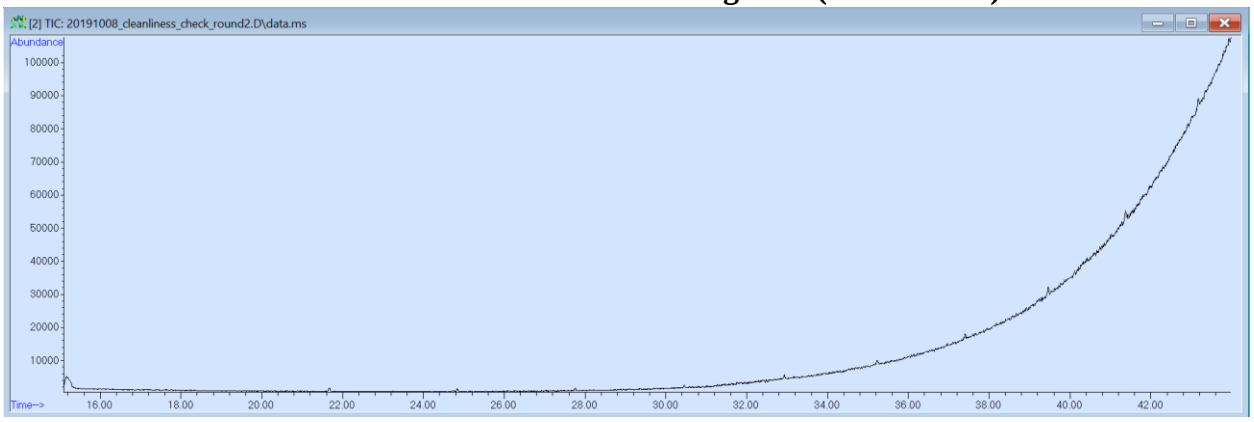

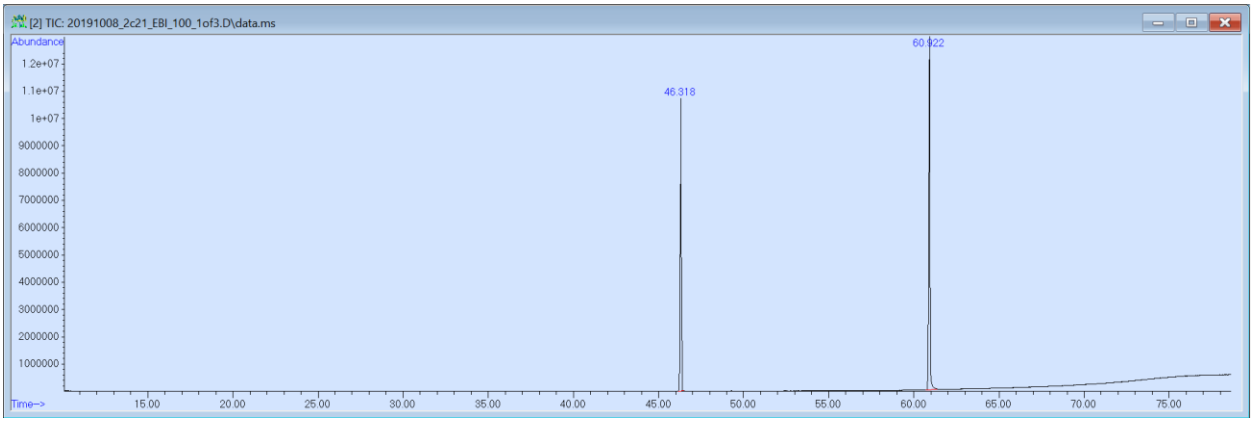

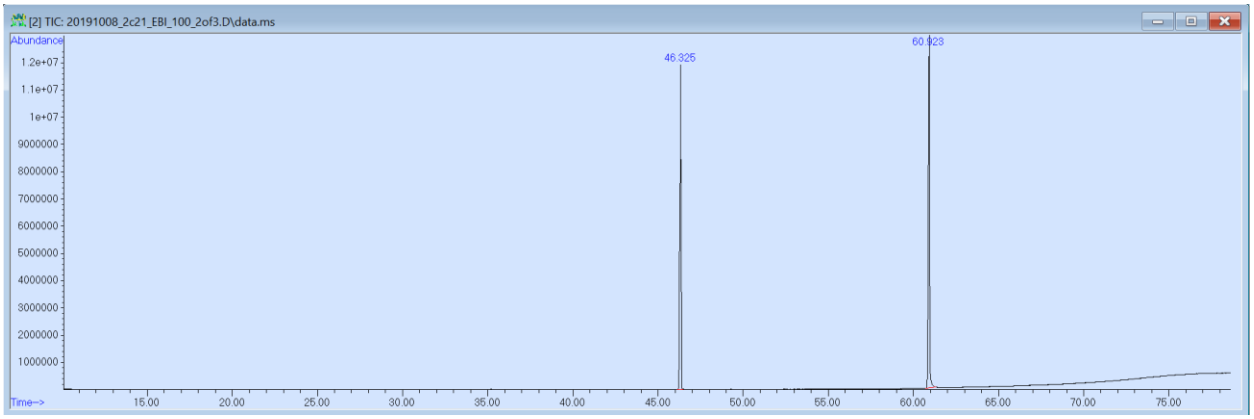

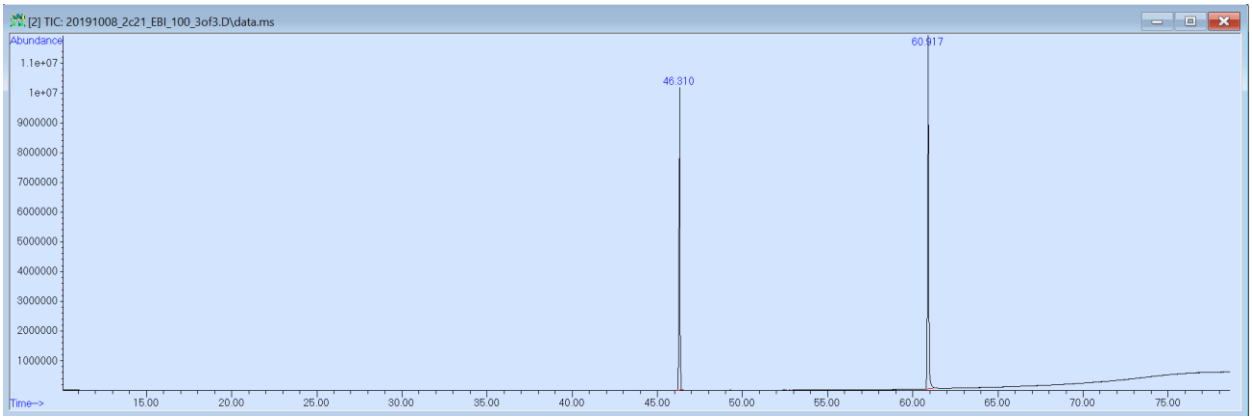
[2] TIC: 20191008_2c21_EBI_100_3of3.D\data.ms
Abundance
46.310
60.917
Time-->

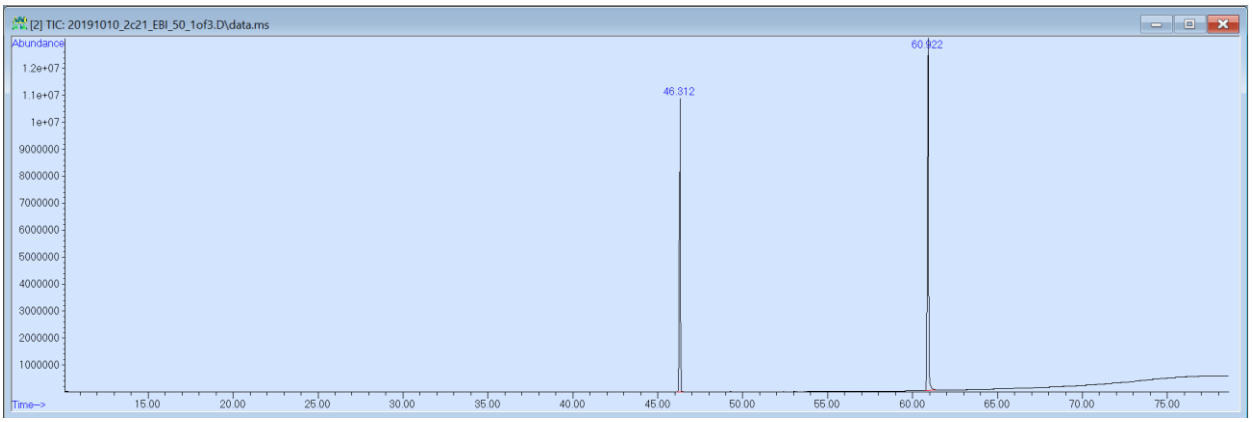
[2] TIC: 20191010_2c21_EBI_50_1of3.D\data.ms
Abundance
46.312
60.922
Time-->

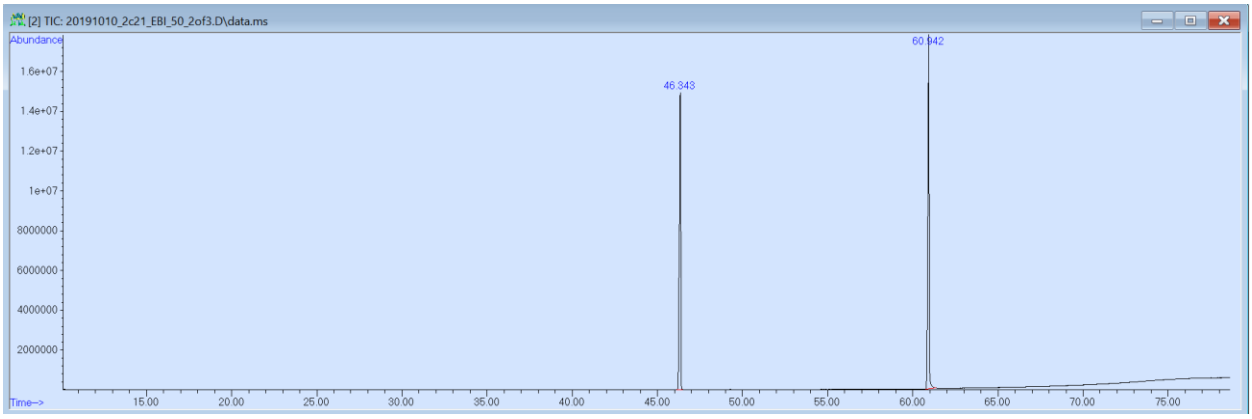
[2] TIC: 20191010_2c21_EBI_50_2of3.D\data.ms
Abundance
46.343
60.942
Time-->

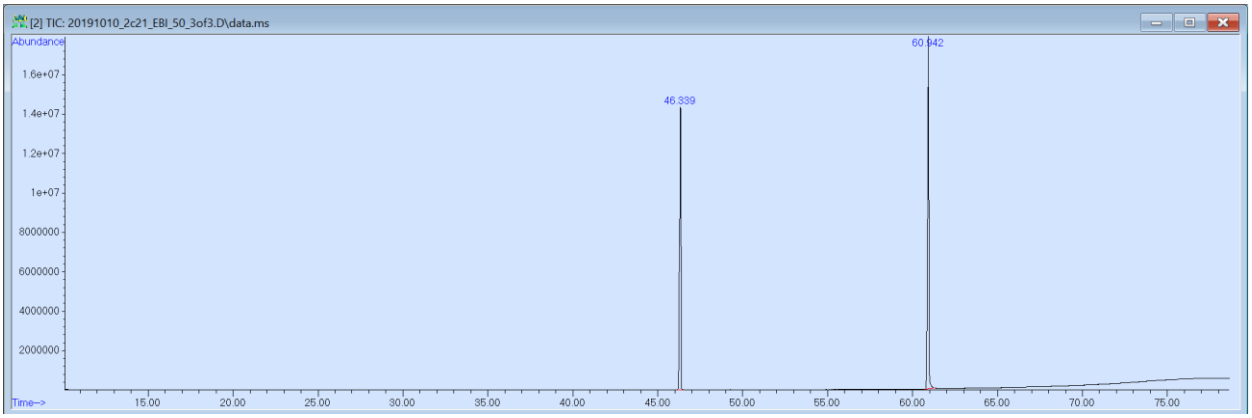
[2] TIC: 20191010_2c21_EBI_50_3of3.D\data.ms
Abundance
1.6e+07
1.4e+07
1.2e+07
1e+07
8000000
6000000
4000000
2000000
46.339
60.942
Time-->
15.00
20.00
25.00
30.00
35.00
40.00
45.00
50.00
55.00
60.00
65.00
70.00
75.00

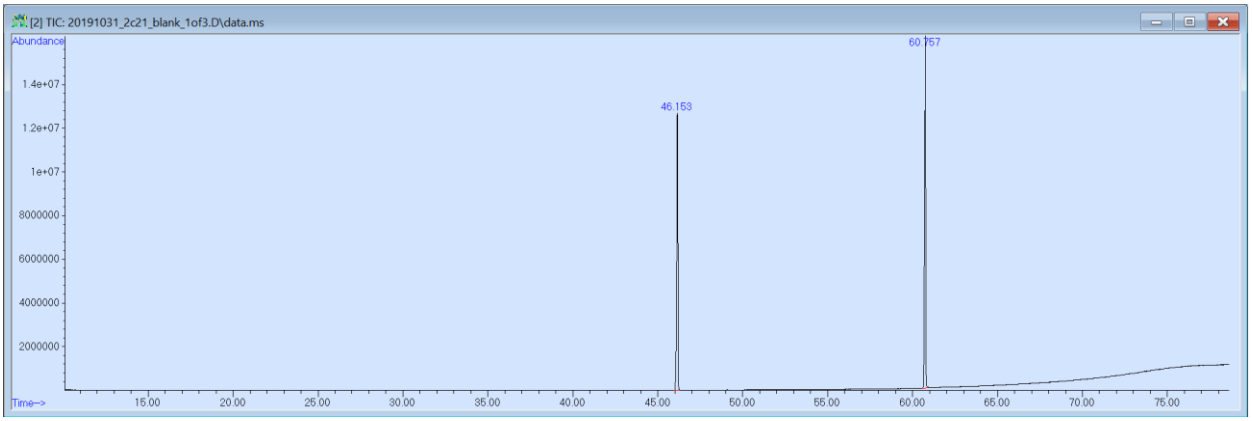
[2] TIC: 20191031_2c21_blank_1of3.D\data.ms
Abundance
1.4e+07
1.2e+07
1e+07
8000000
6000000
4000000
2000000
46.153
60.757
Time-->
15.00
20.00
25.00
30.00
35.00
40.00
45.00
50.00
55.00
60.00
65.00
70.00
75.00

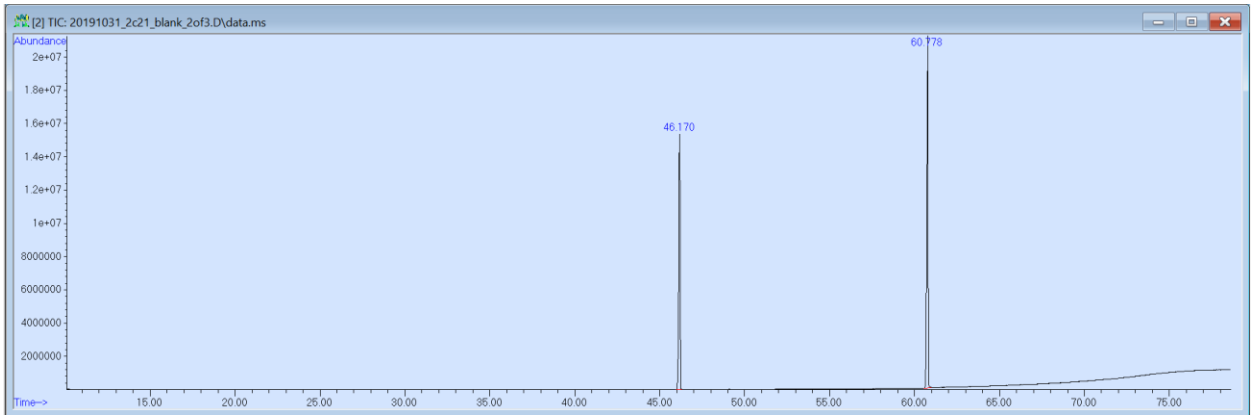
[2] TIC: 20191031_2c21_blank_2of3.D\data.ms
Abundance
2e+07
1.8e+07
1.6e+07
1.4e+07
1.2e+07
1e+07
8000000
6000000
4000000
2000000
46.170
60.778
Time-->
15.00
20.00
25.00
30.00
35.00
40.00
45.00
50.00
55.00
60.00
65.00
70.00
75.00

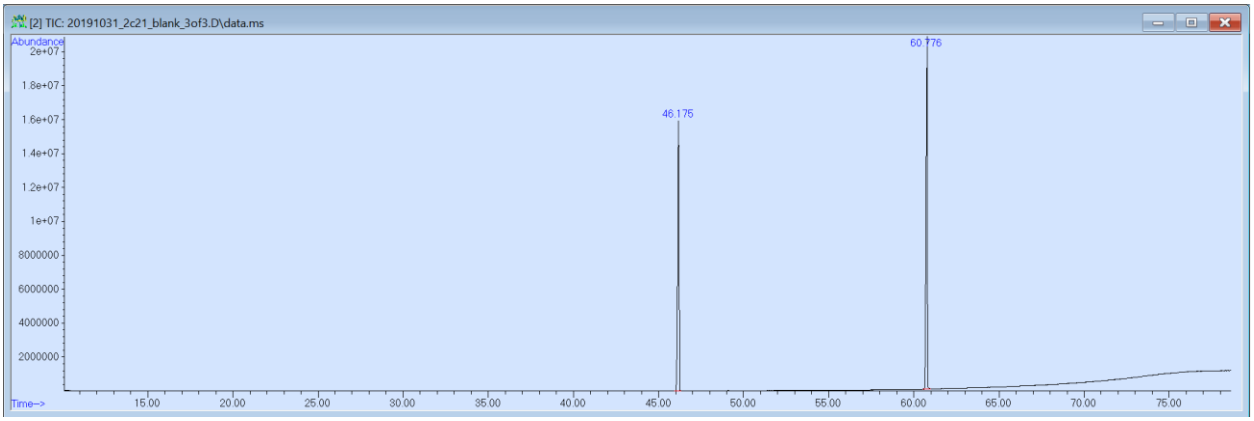
[2] TIC: 20191031_2c21_blank_3of3.D\data.ms
Abundance
2e+07
1.8e+07
1.6e+07
1.4e+07
1.2e+07
1e+07
8000000
6000000
4000000
2000000
46.175
60.776
Time-->
15.00
20.00
25.00
30.00
35.00
40.00
45.00
50.00
55.00
60.00
65.00
70.00
75.00

APPENDIX D: GC-MS Chromatograms (cholestanol)

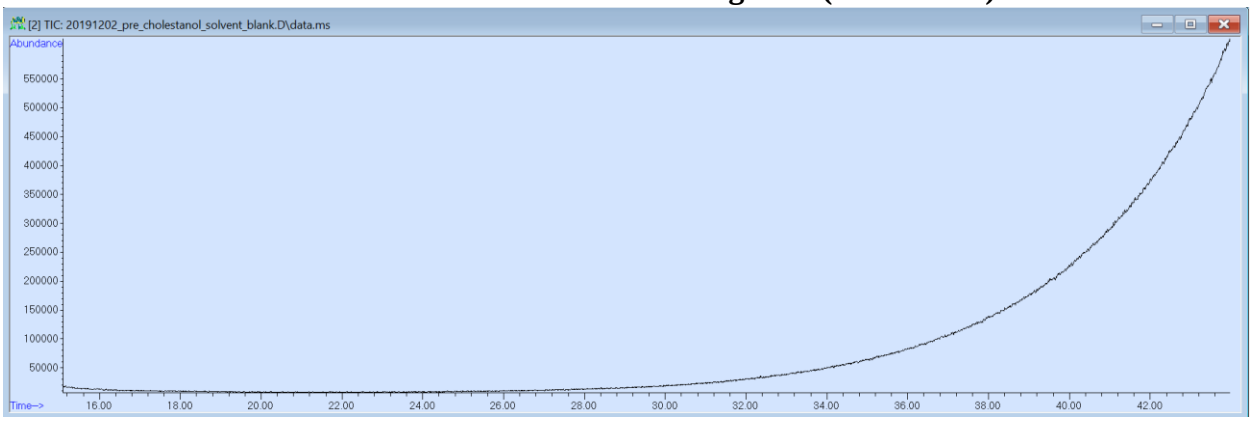

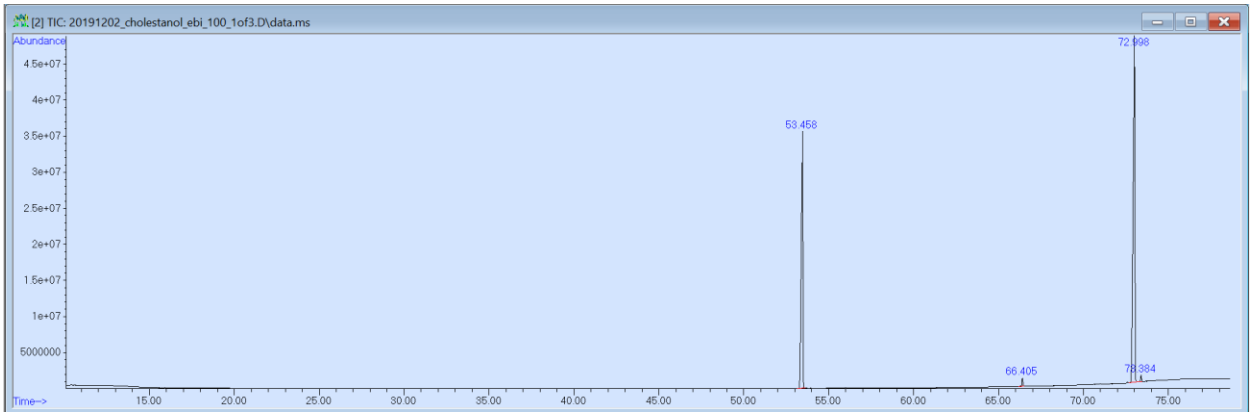

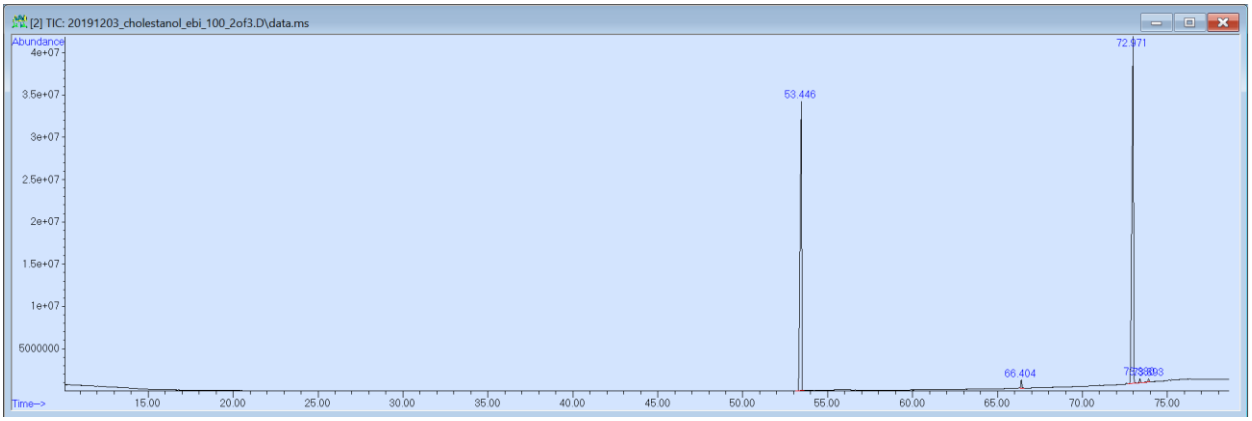

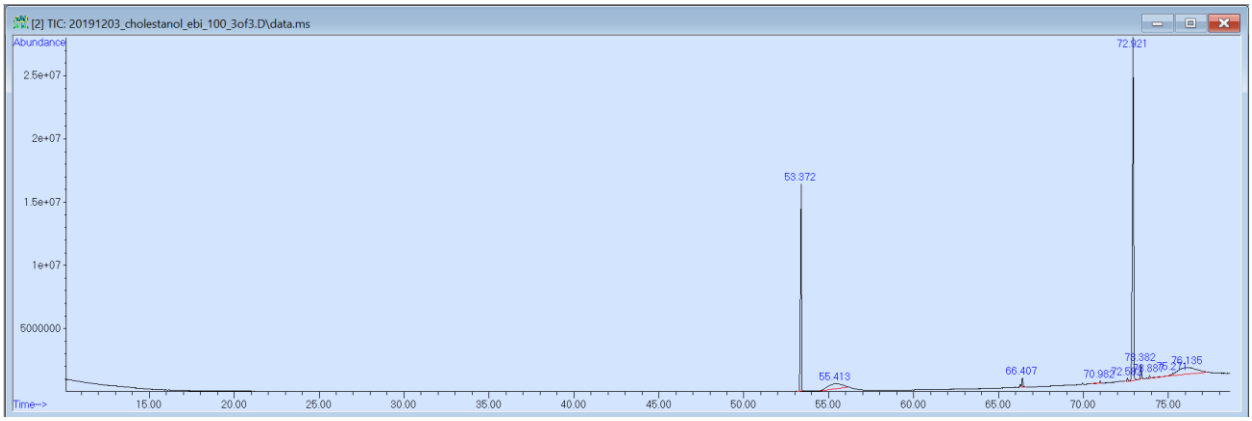
[2] TIC: 20191203_cholestanol_ebi_100_3of3.D\data.ms
Abundance
Time-->
72.921
53.372
55.413
66.407
70.982
73.382
76.135

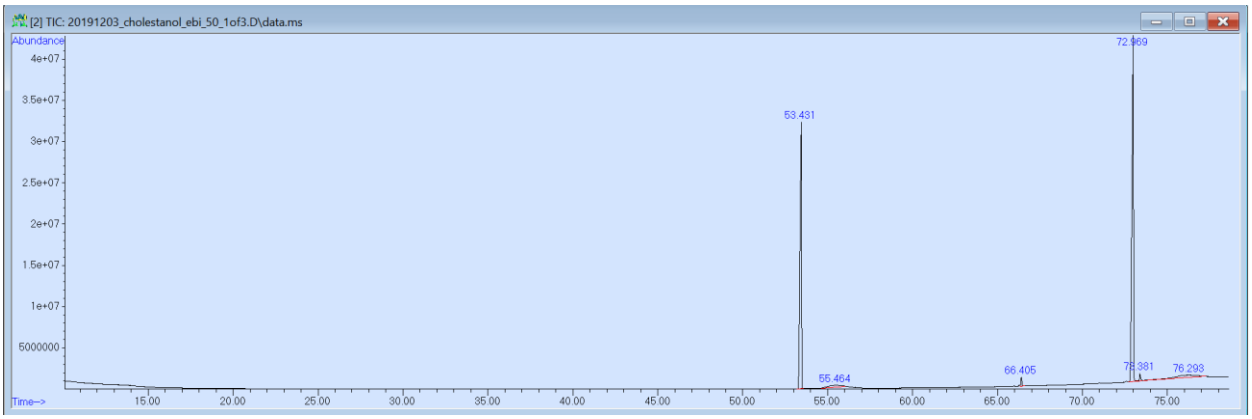
[2] TIC: 20191203_cholestanol_ebi_50_1of3.D\data.ms
Abundance
Time-->
72.969
53.431
55.464
66.405
73.381
76.293

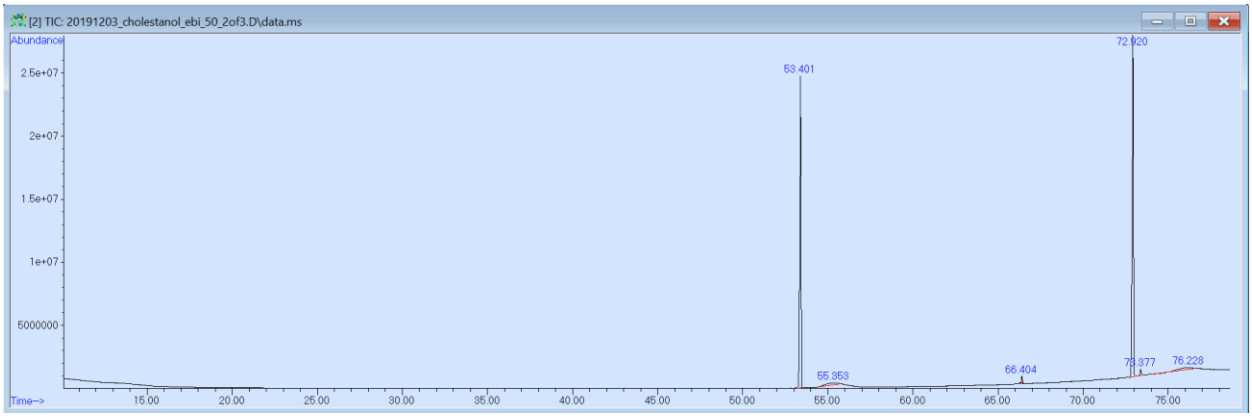
[2] TIC: 20191203_cholestanol_ebi_50_2of3.D\data.ms
Abundance
Time-->
72.920
53.401
55.353
66.404
73.377
76.228

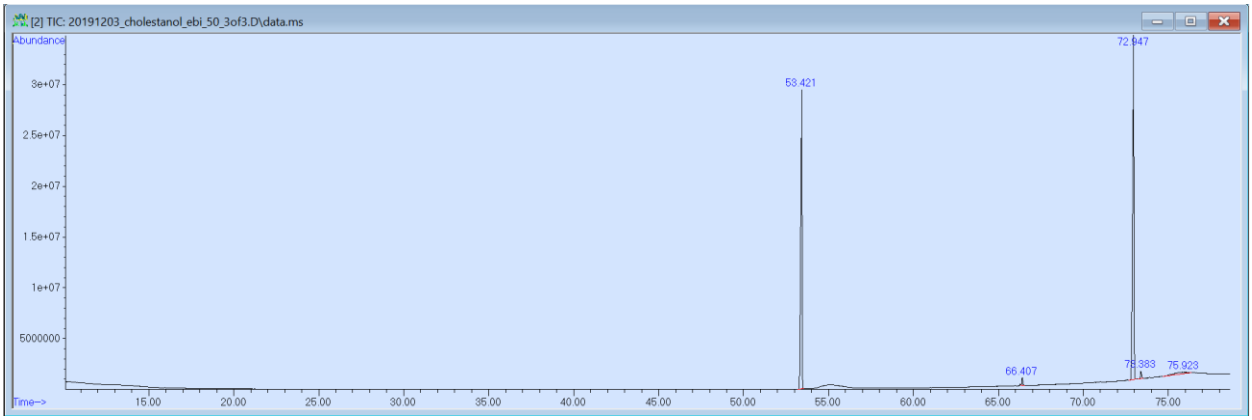
[2] TIC: 20191203_cholestanol_ebi_50_3of3.D\data.ms
Abundance
3e+07
2.5e+07
2e+07
1.5e+07
1e+07
5000000
53.421
72.947
66.407
73.383
75.923
Time-->
15.00
20.00
25.00
30.00
35.00
40.00
45.00
50.00
55.00
60.00
65.00
70.00
75.00

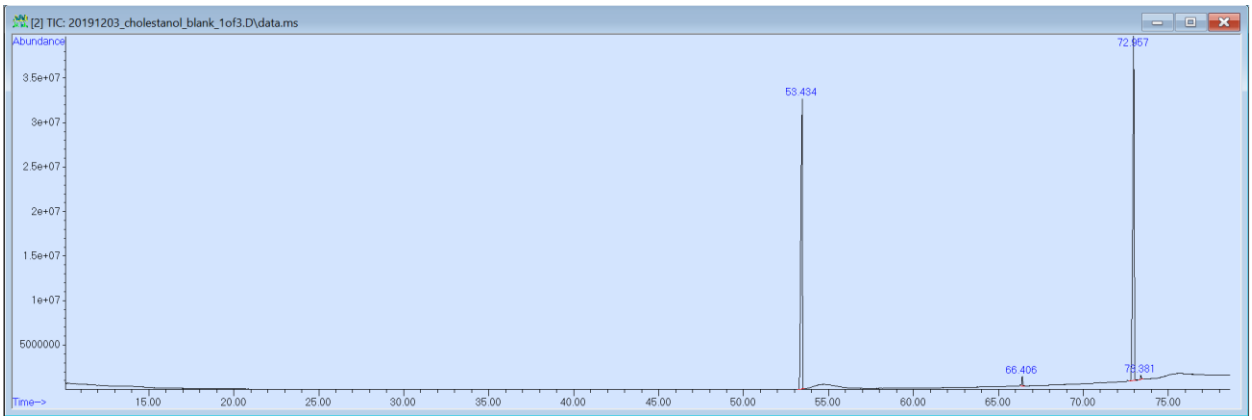
[2] TIC: 20191203_cholestanol_blank_1of3.D\data.ms
Abundance
3.5e+07
3e+07
2.5e+07
2e+07
1.5e+07
1e+07
5000000
53.434
72.967
66.406
73.381
Time-->
15.00
20.00
25.00
30.00
35.00
40.00
45.00
50.00
55.00
60.00
65.00
70.00
75.00

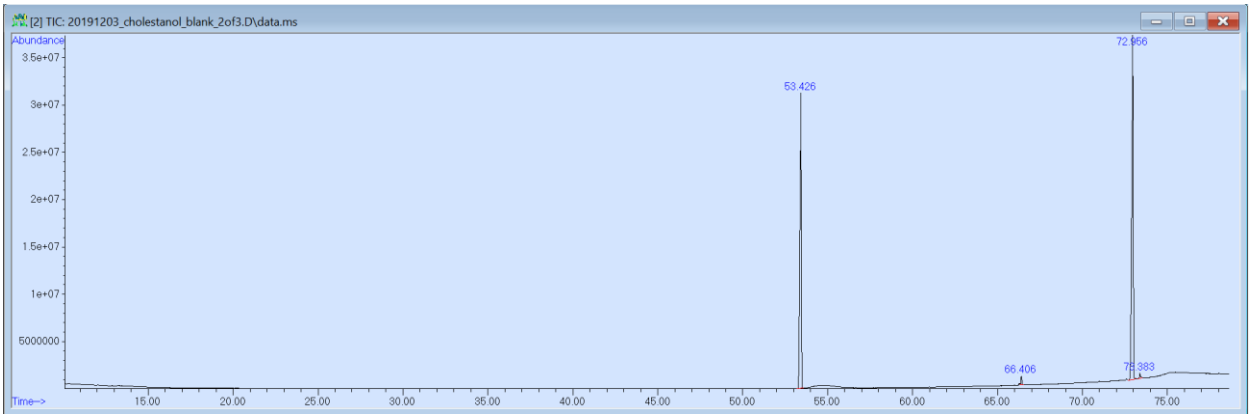
[2] TIC: 20191203_cholestanol_blank_2of3.D\data.ms
Abundance
3.5e+07
3e+07
2.5e+07
2e+07
1.5e+07
1e+07
5000000
53.426
72.966
66.406
73.383
Time-->
15.00
20.00
25.00
30.00
35.00
40.00
45.00
50.00
55.00
60.00
65.00
70.00
75.00

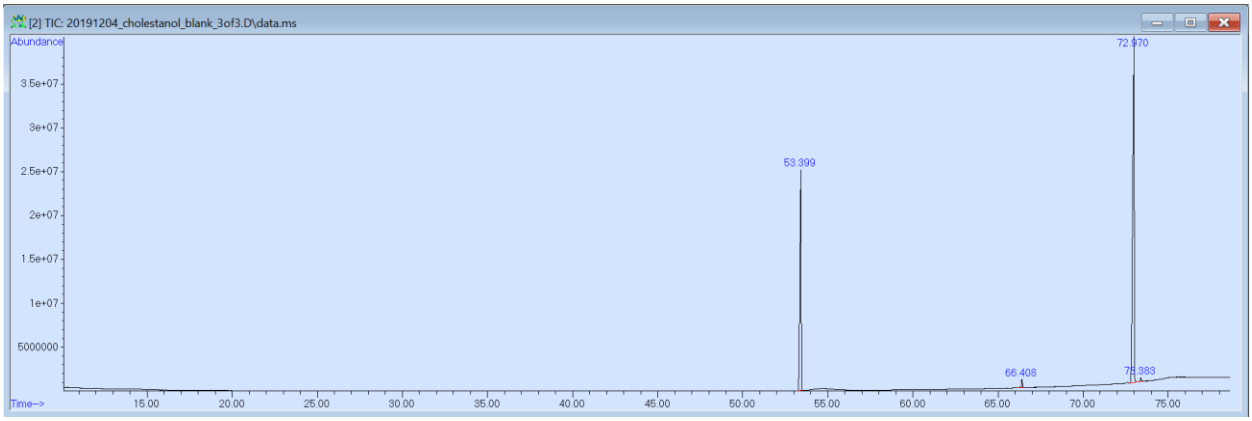
[2] TIC: 20191204_cholestanol_blank_3of3.D\data.ms
Abundance
3.5e+07
3e+07
2.5e+07
2e+07
1.5e+07
1e+07
5000000
Time-->
15.00
20.00
25.00
30.00
35.00
40.00
45.00
50.00
55.00
60.00
65.00
70.00
75.00
53.399
66.408
72.970
75.383

APPENDIX E: GC-MS Chromatograms (cholestane)

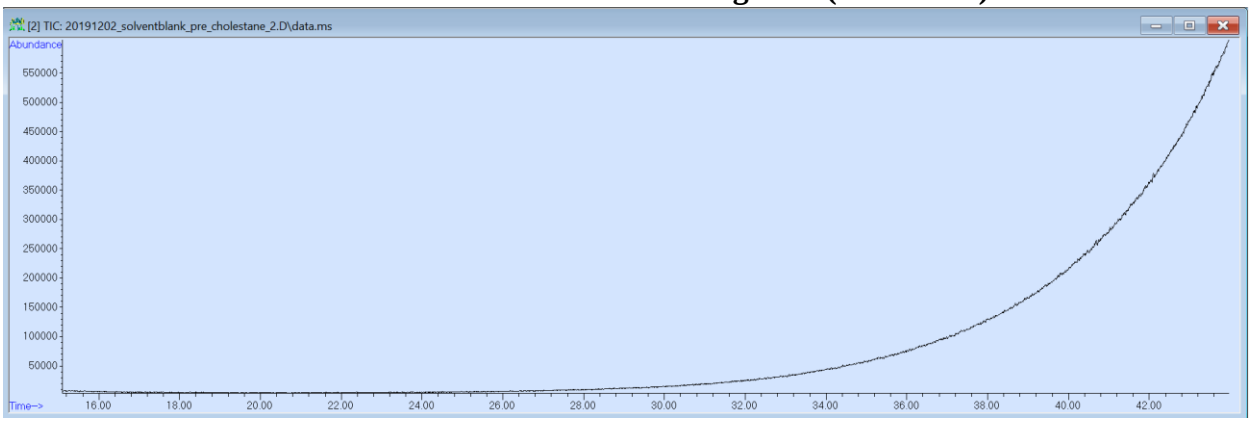

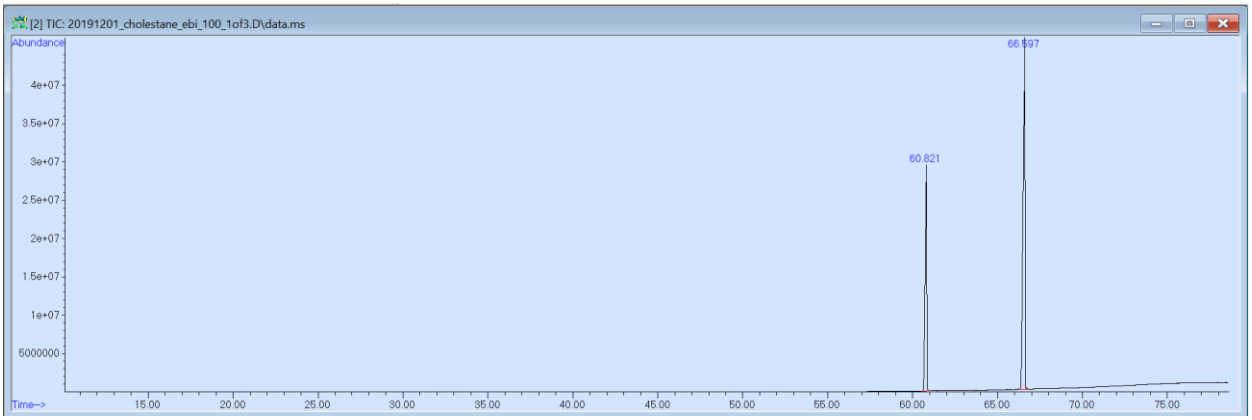

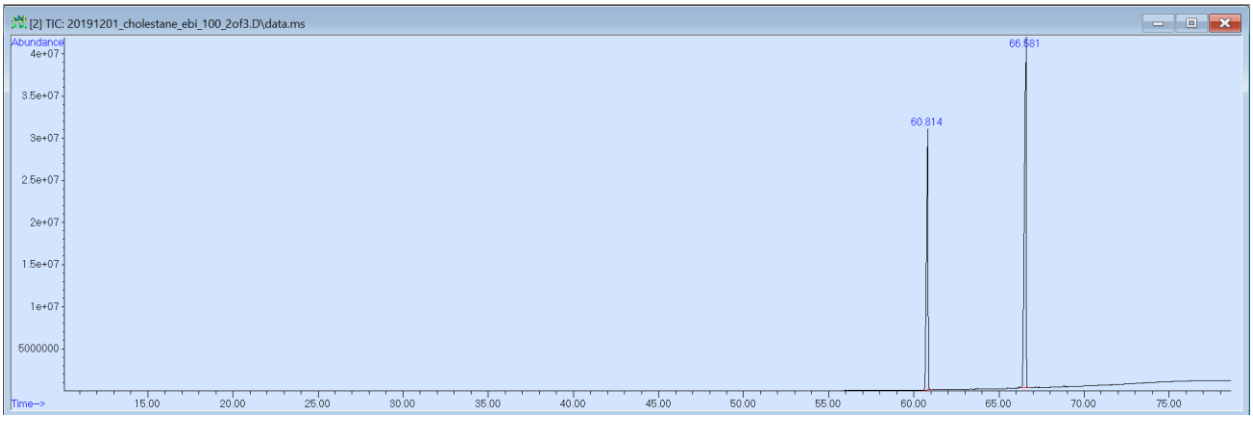

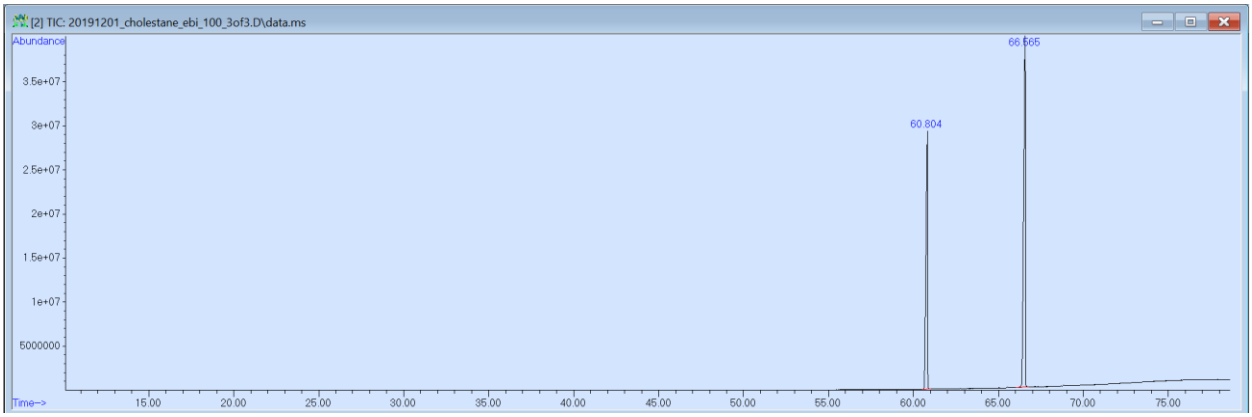
[2] TIC: 20191201_cholestane_ebi_100_3of3.D\data.ms
Abundance
66.665
60.804
Time-->

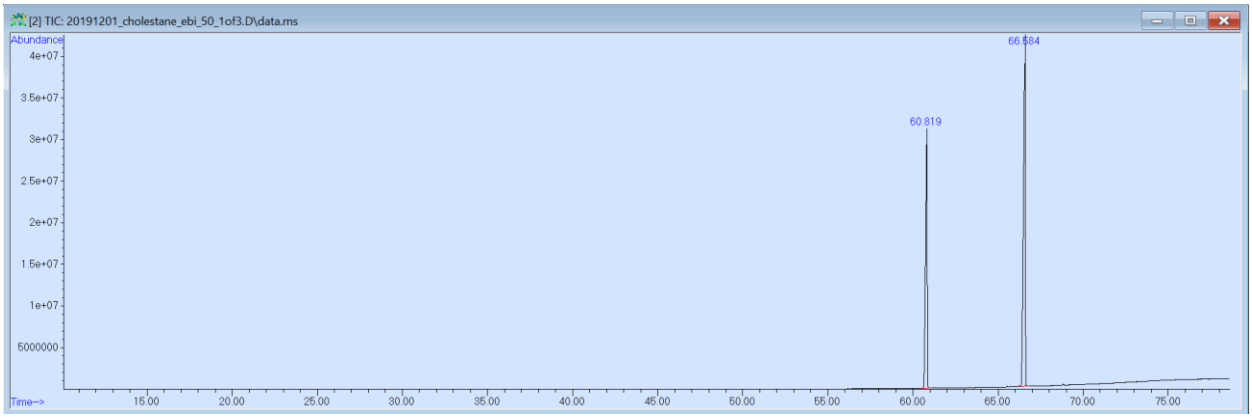
[2] TIC: 20191201_cholestane_ebi_50_1of3.D\data.ms
Abundance
66.684
60.819
Time-->

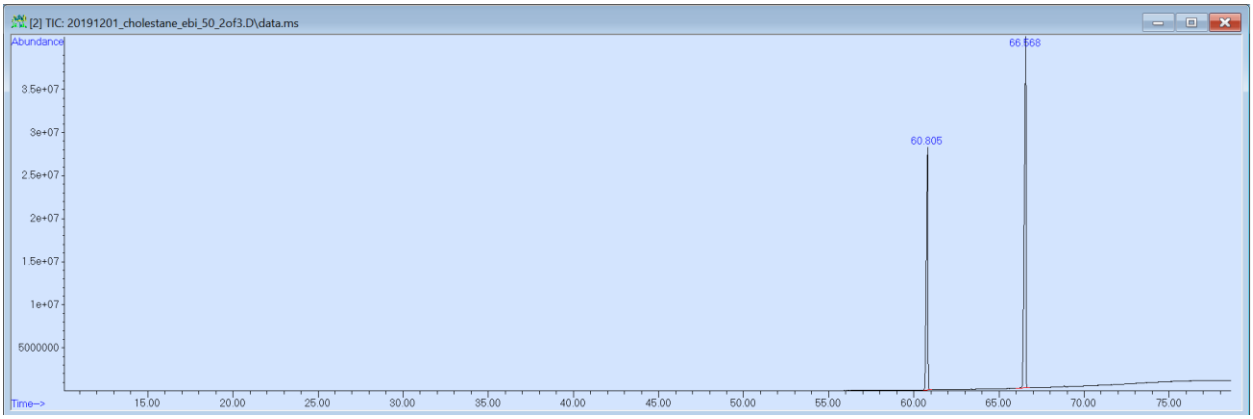
[2] TIC: 20191201_cholestane_ebi_50_2of3.D\data.ms
Abundance
66.668
60.805
Time-->

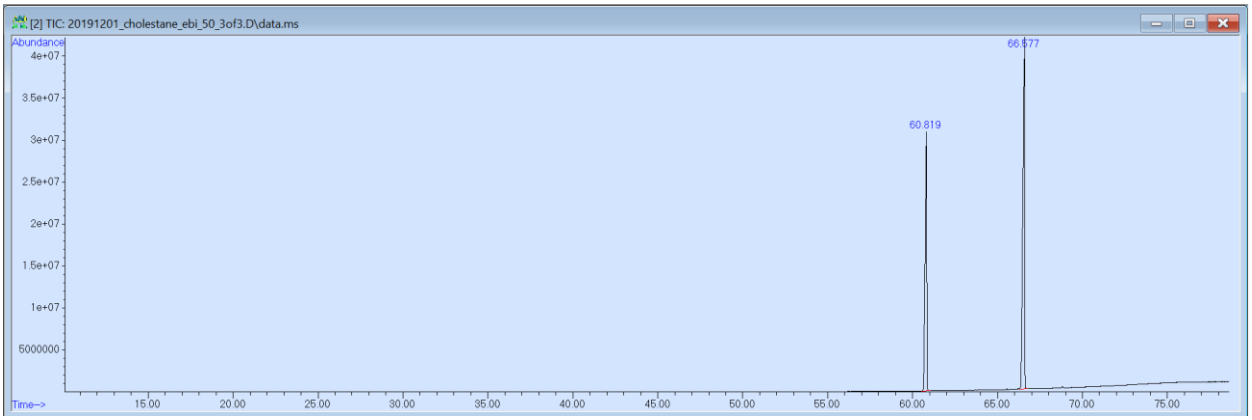
[2] TIC: 20191201_cholestane_ebi_50_3of3.D\data.ms
Abundance
4e+07
3.5e+07
3e+07
2.5e+07
2e+07
1.5e+07
1e+07
5000000
60.819
66.577
Time-->
15.00
20.00
25.00
30.00
35.00
40.00
45.00
50.00
55.00
60.00
65.00
70.00
75.00

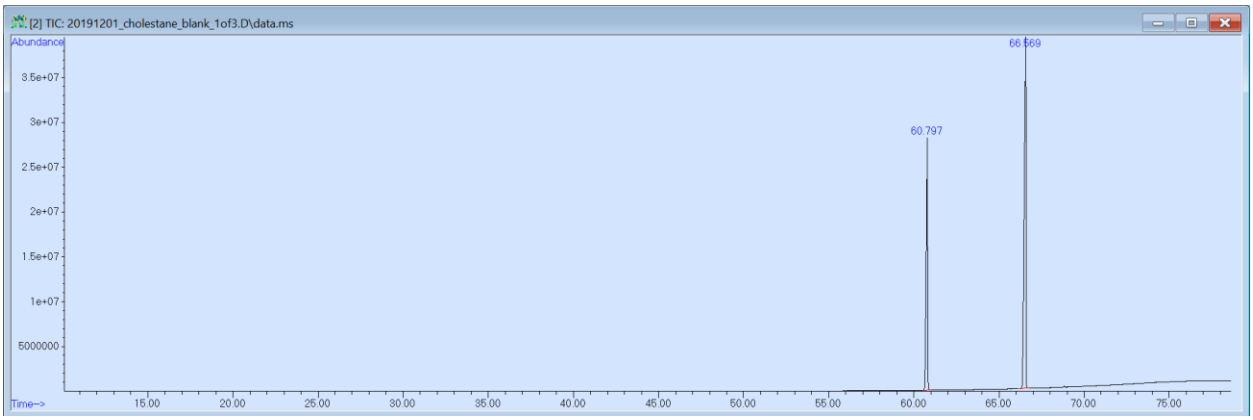
[2] TIC: 20191201_cholestane_blank_1of3.D\data.ms
Abundance
3.5e+07
3e+07
2.5e+07
2e+07
1.5e+07
1e+07
5000000
60.797
66.569
Time-->
15.00
20.00
25.00
30.00
35.00
40.00
45.00
50.00
55.00
60.00
65.00
70.00
75.00

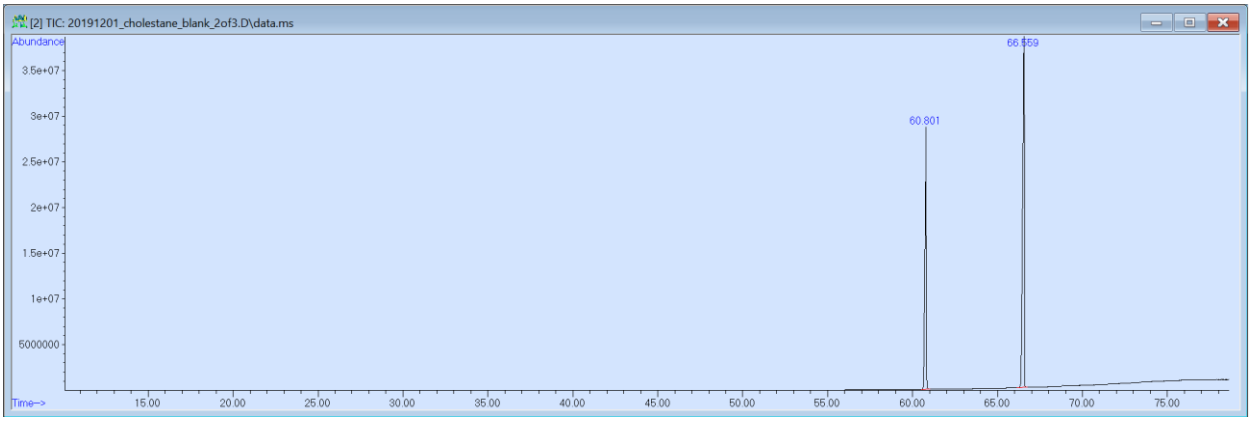
[2] TIC: 20191201_cholestane_blank_2of3.D\data.ms
Abundance
3.5e+07
3e+07
2.5e+07
2e+07
1.5e+07
1e+07
5000000
60.801
66.559
Time-->
15.00
20.00
25.00
30.00
35.00
40.00
45.00
50.00
55.00
60.00
65.00
70.00
75.00

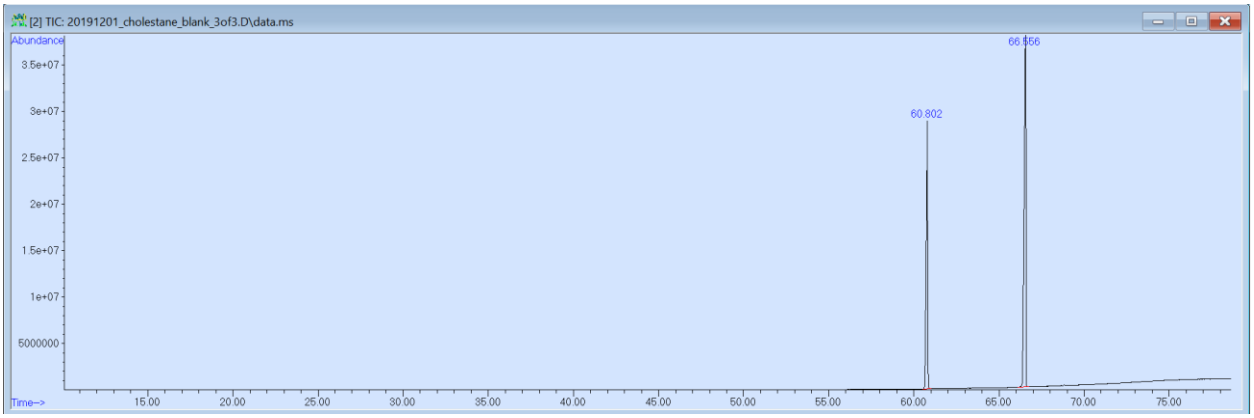
[2] TIC: 20191201_cholestane_blank_3of3.D\data.ms
Abundance
3.5e+07
3e+07
2.5e+07
2e+07
1.5e+07
1e+07
5000000
60.802
66.456
Time-->
15.00
20.00
25.00
30.00
35.00
40.00
45.00
50.00
55.00
60.00
65.00
70.00
75.00

REFERENCES

1. Neveu M, Hays LE, Voytek MA, New MH, Schulte MD. The Ladder of Life Detection. *Astrobiology*. 2018;18(11):1375-1402. doi:10.1089/ast.2017.1773

2. Marais DJD, Allamandola LJ, Benner SA, et al. The NASA astrobiology roadmap. *Astrobiology*. 2003;3(2):219-235. doi:10.1089/153110703769016299

3. Des Marais DJ, Walter MR. Astrobiology: exploring the origins, evolution, and distribution of life in the Universe. *Annu Rev Ecol Syst*. 1999;30:397-420. doi:10.1146/annurev.ecolsys.30.1.397

4. Drake F. The search for extra-terrestrial intelligence. *Philos Trans R Soc Math Phys Eng Sci*. 2011;369(1936):633-643. doi:10.1098/rsta.2010.0282

5. Cleland CE, Chyba CF. Defining "life." *Orig Life Evol Biosphere J Int Soc Study Orig Life*. 2002;32(4):387-393. doi:10.1023/a:1020503324273

6. Eigenbrode JL. Fossil Lipids for Life-Detection: A Case Study from the Early Earth Record. In: Botta O, Bada JL, Gomez-Elvira J, Javaux E, Selsis F, Summons R, eds. *Strategies of Life Detection*. Space Sciences Series of ISSI. Springer US; 2008:161-185. doi:10.1007/978-0-387-77516-6_12

7. Wilhelm MB, Ricco AJ, Oehler DZ, et al. Abzu: A Mission to Uncover the Origin of Organic Material on Mars. *AGU Fall Meet Abstr*. 2019;41. Accessed June 17, 2020. http://adsabs.harvard.edu/abs/2019AGUFM.P41C3447W

8. Eigenbrode J, Benning LG, Maule J, et al. A field-based cleaning protocol for sampling devices used in life-detection studies. *Astrobiology*. 2009;9(5):455-465. doi:10.1089/ast.2008.0275

9. Mcdonnell GE, Russell AD. Antiseptics and disinfectants: activity, action, and resistance. *Clin Microbiol Rev*. Published online 1999. doi:10.1128/CMR.12.1.147

10. Mahnert A, Vaishampayan P, Probst AJ, et al. Cleanroom Maintenance Significantly Reduces Abundance but Not Diversity of Indoor Microbiomes. *PloS One*. 2015;10(8):e0134848. doi:10.1371/journal.pone.0134848

11. Oyama VI, Berdahl BJ. The Viking Gas Exchange Experiment results from Chryse and Utopia surface samples. *J Geophys Res 1896-1977*. Published online December 6, 2012:4669-4676. doi:10.1029/JS082i028p04669@10.1002/(ISSN)2156-2202.VIKPROJ1

12. Benner SA, Devine KG, Matveeva LN, Powell DH. The missing organic molecules on Mars. *Proc Natl Acad Sci U S A*. 2000;97(6):2425-2430. doi:10.1073/pnas.040539497

13. Levin GV, Straat PA. A search for a nonbiological explanation of the Viking Labeled Release life detection experiment. *Icarus*. 1981;45(2):494-516. doi:10.1016/0019-1035(81)90048-8

14. Yen AS, Kim SS, Hecht MH, Frant MS, Murray B. Evidence that the reactivity of the martian soil is due to superoxide ions. *Science*. 2000;289(5486):1909-1912. doi:10.1126/science.289.5486.1909

15. Klein HP. The Viking biological experiments on Mars. *Icarus*. 1978;34(3):666-674. doi:10.1016/0019-1035(78)90053-2

16. Lunine JI. Ocean worlds exploration. *Acta Astronaut*. 2017;131:123-130. doi:10.1016/j.actaastro.2016.11.017

17. McKay CP, Anbar AD, Porco C, Tsou P. Follow the plume: the habitability of Enceladus. *Astrobiology*. 2014;14(4):352-355. doi:10.1089/ast.2014.1158

18. Chyba CF, Phillips CB. Possible ecosystems and the search for life on Europa. *Proc Natl Acad Sci U S A*. 2001;98(3):801-804.

19. Farmer JD, Marais DJD. Exploring for a record of ancient Martian life. *J Geophys Res Planets*. 1999;104(E11):26977-26995. doi:10.1029/1998JE000540

20. NASA Strategic Plan 2018. :64.

21. Council NR, Sciences D on E and P, Board SS, Survey C on the PSD. *Vision and Voyages for Planetary Science in the Decade 2013-2022*. National Academies Press; 2012.

22. Mars Science Goals, Objectives,. Published online 2020:89.

23. Phillips CB, Pappalardo RT. Europa Clipper Mission Concept: Exploring Jupiter's Ocean Moon. *Eos Trans Am Geophys Union*. 2014;95(20):165-167. doi:10.1002/2014EO200002

24. Peters KE, Moldowan JM. The biomarker guide: Interpreting molecular fossils in petroleum and ancient sediments. Published online January 1, 1993. Accessed June 17, 2020. https://www.osti.gov/biblio/6066248-biomarker-guide-interpreting-molecular-fossils-petroleum-ancient-sediments

25. Simoneit BRT. Biomarkers (molecular fossils) as geochemical indicators of life. *Adv Space Res*. 2004;33(8):1255-1261. doi:10.1016/j.asr.2003.04.045

26. Parnell J, Cullen D, Sims MR, et al. Searching for life on Mars: selection of molecular targets for ESA's aurora ExoMars mission. *Astrobiology*. 2007;7(4):578-604. doi:10.1089/ast.2006.0110

27. Deamer D, Dworkin JP, Sandford SA, Bernstein MP, Allamandola LJ. The first cell membranes. *Astrobiology*. 2002;2(4):371-381. doi:10.1089/153110702762470482

28. Segré D, Ben-Eli D, Deamer DW, Lancet D. The Lipid World. *Orig Life Evol Biosph*. 2001;31(1):119-145. doi:10.1023/A:1006746807104

29. Definition of LIPID. Accessed July 8, 2020. https://www.merriam-webster.com/dictionary/lipid

30. Georgiou CD, Deamer DW. Lipids as universal biomarkers of extraterrestrial life. *Astrobiology*. 2014;14(6):541-549. doi:10.1089/ast.2013.1134

31. Kaneda T. Iso- and anteiso-fatty acids in bacteria: biosynthesis, function, and taxonomic significance. *Microbiol Rev*. 1991;55(2):288-302.

32. Dworkin JP, Deamer DW, Sandford SA, Allamandola LJ. Self-assembling amphiphilic molecules: Synthesis in simulated interstellar/precometary ices. *Proc Natl Acad Sci U S A*. 2001;98(3):815-819.

33. Deamer DW, Pashley RM. Amphiphilic components of the Murchison carbonaceous chondrite: surface properties and membrane formation. *Orig Life Evol Biosphere J Int Soc Study Orig Life*. 1989;19(1):21-38. doi:10.1007/BF01808285

34. C C, C S. Endogenous production, exogenous delivery and impact-shock synthesis of organic molecules: an inventory for the origins of life. *Nature*. 1992;355:125-132. doi:10.1038/355125a0

35. Ehrenfreund P, Becker L, Blank J, et al. *Astrophysical and Astrochemical Insights into the Origin of Life*. Lawrence Livermore National Lab. (LLNL), Livermore, CA (United States); 2002. doi:10.2172/15013483

36. Meierhenrich U. *Amino Acids and the Asymmetry of Life: Caught in the Act of Formation*. Springer; 2008.

37. Harwood J. *Lipids in Plants and Microbes*. Springer Science & Business Media; 2012.

38. Aerts JW, Röling WFM, Elsaesser A, Ehrenfreund P. Biota and biomolecules in extreme environments on Earth: implications for life detection on Mars. *Life Basel Switz*. 2014;4(4):535-565. doi:10.3390/life4040535

39. Eglinton G, Logan GA. Molecular preservation. *Philos Trans R Soc Lond B Biol Sci*. 1991;333(1268):315-327; discussion 327-328. doi:10.1098/rstb.1991.0081

40. Lovelock JE. A physical basis for life detection experiments. *Nature*. 1965;207(997):568-570. doi:10.1038/207568a0

41. Mißbach H, Schmidt BC, Duda J-P, Lünsdorf NK, Goetz W, Thiel V. Assessing the diversity of lipids formed via Fischer-Tropsch-type reactions. *Org Geochem*. 2018;119:110-121. doi:10.1016/j.orggeochem.2018.02.012

42. Rushdi AI, Simoneit BR. Lipid formation by aqueous Fischer-Tropsch-type synthesis over a temperature range of 100 to 400 degrees C. *Orig Life Evol Biosphere J Int Soc Study Orig Life*. 2001;31(1-2):103-118. doi:10.1023/a:1006702503954

43. Sephton MA. Organic matter in carbonaceous meteorites: past, present and future research. *Philos Transact A Math Phys Eng Sci*. 2005;363(1837):2729-2742. doi:10.1098/rsta.2005.1670

44. Aponte JC, Alexandre MR, Wang Y, Brearley AJ, Alexander CMO, Huang Y. Effects of secondary alteration on the composition of free and IOM-derived monocarboxylic acids in carbonaceous chondrites. *Geochim Cosmochim Acta*. 2011;75(9):2309-2323. doi:10.1016/j.gca.2011.01.040

45. Herd CDK, Blinova A, Simkus DN, et al. Origin and evolution of prebiotic organic matter as inferred from the Tagish Lake meteorite. *Science*. 2011;332(6035):1304-1307. doi:10.1126/science.1203290

46. Lai JC-Y, Pearce BKD, Pudritz RE, Lee D. Meteoritic abundances of fatty acids and potential reaction pathways in planetesimals. *Icarus*. 2019;319:685-700. doi:10.1016/j.icarus.2018.09.028

47. Wilhelm MB, Davila AF, Parenteau MN, et al. Constraints on the Metabolic Activity of Microorganisms in Atacama Surface Soils Inferred from Refractory Biomarkers: Implications for Martian Habitability and Biomarker Detection. *Astrobiology*. 2018;18(7):955-966. doi:10.1089/ast.2017.1705

48. Wilhelm MB, Davila AF, Eigenbrode JL, et al. Xeropreservation of functionalized lipid biomarkers in hyperarid soils in the Atacama Desert. *Org Geochem*. 2017;103:97-104. doi:10.1016/j.orggeochem.2016.10.015

49. Summons RE, Walter MR. Molecular fossils and microfossils of prokaryotes and protists from Proterozoic sediments. *Am J Sci*. 1990;290 A:212-244.

50. Eigenbrode JL, Summons RE, Steele A, et al. Organic matter preserved in 3-billion-year-old mudstones at Gale crater, Mars. *Science*. 2018;360(6393):1096-1101. doi:10.1126/science.aas9185

51. Summons RE, Amend JP, Bish D, et al. Preservation of martian organic and environmental records: final report of the Mars biosignature working group. *Astrobiology*. 2011;11(2):157-181. doi:10.1089/ast.2010.0506

52. Pizzarello S, Huang Y, Becker L, et al. The organic content of the Tagish Lake meteorite. *Science*. 2001;293(5538):2236-2239. doi:10.1126/science.1062614

53. Huang Y, Wang Y, Alexandre MR, et al. Molecular and compound-specific isotopic characterization of monocarboxylic acids in carbonaceous meteorites. *Geochim Cosmochim Acta*. 2005;69(4):1073-1084. doi:10.1016/j.gca.2004.07.030

54. Moores JE, Schuerger AC. UV degradation of accreted organics on Mars: IDP longevity, surface reservoir of organics, and relevance to the detection of methane in the atmosphere. In: ; 2012. doi:10.1029/2012JE004060

55. Sandford SA, Aléon J, Alexander CMO, et al. Organics captured from comet 81P/Wild 2 by the Stardust spacecraft. *Science*. 2006;314(5806):1720-1724. doi:10.1126/science.1135841

56. Remusat L. Organic material in meteorites and the link to the origin of life. Ollivier M, Maurel M-C, eds. *BIO Web Conf*. 2014;2:03001. doi:10.1051/bioconf/20140203001

57. Sephton MA. Meteorite composition: Organic matter in ancient meteorites. *Astron Geophys*. 2004;45:2.08-2.14. doi:10.1046/j.1468-4004.2003.45208.x

58. McCollom TM, Ritter G, Simoneit BR. Lipid synthesis under hydrothermal conditions by Fischer-Tropsch-type reactions. *Orig Life Evol Biosphere J Int Soc Study Orig Life*. 1999;29(2):153-166. doi:10.1023/a:1006592502746

59. Dalai P, Sahai N. Mineral-Lipid Interactions in the Origins of Life. *Trends Biochem Sci*. 2019;44(4):331-341. doi:10.1016/j.tibs.2018.11.009

60. Ferris JP. Chemical markers of prebiotic chemistry in hydrothermal systems. *Orig Life Evol Biosphere J Int Soc Study Orig Life*. 1992;22(1-4):109-134, 191-242. doi:10.1007/BF01808020

61. Sephton MA, Carter JN. The chances of detecting life on Mars. *Planet Space Sci*. 2015;112:15-22. doi:10.1016/j.pss.2015.04.002

62. Summons RE, Albrecht P, McDonald G, Moldowan JM. Molecular Biosignatures. *Space Sci Rev*. 2008;135(1):133-159. doi:10.1007/s11214-007-9256-5

63. Barnett IL, Lignell A, Gudipati MS. Survival Depth of Organics in Ices under Low-energy Electron Radiation (<=2 keV). *Astrophys J*. 2012;747:13. doi:10.1088/0004-637X/747/1/13

64. Fox AC, Eigenbrode JL, Freeman KH. Radiolysis of Macromolecular Organic Material in Mars-Relevant Mineral Matrices. *J Geophys Res Planets*. 2019;124(12):3257-3266. doi:10.1029/2019JE006072

65. Osman S, Peeters Z, Duc MTL, Mancinelli R, Ehrenfreund P, Venkateswaran K. Effect of Shadowing on Survival of Bacteria under Conditions Simulating the Martian Atmosphere and UV Radiation. *Appl Environ Microbiol*. 2008;74(4):959-970. doi:10.1128/AEM.01973-07

66. Mahaffy PR, Webster CR, Cabane M, et al. The Sample Analysis at Mars Investigation and Instrument Suite. *Space Sci Rev*. 2012;170(1):401-478. doi:10.1007/s11214-012-9879-z

67. La Duc MT, Osman S, Vaishampayan P, et al. Comprehensive Census of Bacteria in Clean Rooms by Using DNA Microarray and Cloning Methods. *Appl Environ Microbiol*. 2009;75(20):6559-6567. doi:10.1128/AEM.01073-09

68. Duc MTL, Nicholson W, Kern R, Venkateswaran K. Microbial characterization of the Mars Odyssey spacecraft and its encapsulation facility. *Environ Microbiol*. 2003;5(10):977-985. doi:10.1046/j.1462-2920.2003.00496.x

69. La Duc MT, Venkateswaran K, Conley CA. A genetic inventory of spacecraft and associated surfaces. *Astrobiology*. 2014;14(1):15-23. doi:10.1089/ast.2013.0966

70. Koskinen K, Rettberg P, Pukall R, et al. Microbial biodiversity assessment of the European Space Agency's ExoMars 2016 mission. *Microbiome*. 2017;5(1):143. doi:10.1186/s40168-017-0358-3

71. Vaishampayan P, Osman S, Andersen G, Venkateswaran K. High-density 16S microarray and clone library-based microbial community composition of the Phoenix spacecraft assembly clean room. *Astrobiology*. 2010;10(5):499-508. doi:10.1089/ast.2009.0443

72. Vaishampayan P, Probst AJ, La Duc MT, et al. New perspectives on viable microbial communities in low-biomass cleanroom environments. *ISME J*. 2013;7(2):312-324. doi:10.1038/ismej.2012.114

73. Ghosh S, Osman S, Vaishampayan P, Venkateswaran K. Recurrent isolation of extremotolerant bacteria from the clean room where Phoenix spacecraft components were assembled. *Astrobiology*. 2010;10(3):325-335. doi:10.1089/ast.2009.0396

74. TREATY ON PRINCIPLES GOVERNING THE ACTIVITIES OF STATES IN THE EXPLORATION AND USE OF OUTER SPACE, INCLUDING THE MOON AND OTHER CELESTIAL BODIES. *Int Leg Mater*. 1967;6(2):386-390.

75. The COSPAR Panel on Planetary Protection Role, Structure and Activities. *Space Res Today*. 2019;205:14-26. doi:10.1016/j.srt.2019.06.013

76. Planetary Protection. Accessed June 17, 2020. https://sma.nasa.gov/sma-disciplines/planetary-protection

77. Debus A. COSPAR needs for Planetary Protection recommendations for sample preservation dedicated to exobiology. *Adv Space Res*. 2004;34(11):2320-2324. doi:10.1016/j.asr.2004.01.015

78. Rummel JD. Seeking an international consensus in planetary protection: COSPAR's planetary protection panel. *Adv Space Res*. 2002;30(6):1573-1575. doi:10.1016/S0273-1177(02)00476-3

79. Rummel JD, Billings L. Issues in planetary protection: policy, protocol and implementation. *Space Policy*. 2004;20(1):49-54. doi:10.1016/j.spacepol.2003.11.005

80. NPR 8020.12D - Chapter5. Accessed June 17, 2020. https://nodis3.gsfc.nasa.gov/displayDir.cfm?Internal_ID=N_PR_8020_012D_&page_name=Chapter5

81. NPR 8020.12D - Chapter3. Accessed June 17, 2020. https://nodis3.gsfc.nasa.gov/displayDir.cfm?Internal_ID=N_PR_8020_012D_&page_name=Chapter3

82. Rohatgi N, Schubert W, Koukol R, Foster TL, Stabekis PD. Certification of Vapor Phase Hydrogen Peroxide Sterilization Process for Spacecraft Application. In: ; 2002:2002-01-2471. doi:10.4271/2002-01-2471

83. Tribble AC. *Fundamentals of Contamination Control*. SPIE Press; 2000.

84. Mancinelli RL. Planetary protection and the search for life beneath the surface of Mars. *Adv Space Res*. 2003;31(1):103-107. doi:10.1016/S0273-1177(02)00663-4

85. Lung H-M, Cheng Y-C, Chang Y-H, Huang H-W, Yang BB, Wang C-Y. Microbial decontamination of food by electron beam irradiation. *Trends Food Sci Technol*. 2015;44(1):66-78. doi:10.1016/j.tifs.2015.03.005

86. Pillai SD, Shayanfar S. Electron Beam Technology and Other Irradiation Technology Applications in the Food Industry. *Top Curr Chem Cham*. 2017;375(1):6. doi:10.1007/s41061-016-0093-4

87. Lim SJ, Kim T-H, Kim J, Shin IH, Kwak HS. Enhanced treatment of swine wastewater by electron beam irradiation and ion-exchange biological reactor. *Sep Purif Technol*. 2016;C(157):72-79. doi:10.1016/j.seppur.2015.11.023

88. ISO 11137-1:2006(en), Sterilization of health care products — Radiation — Part 1: Requirements for development, validation and routine control of a sterilization process for medical devices. Accessed June 17, 2020. https://www.iso.org/obp/ui/#iso:std:iso:11137:-1:ed-1:v1:en

89. Urgiles E, Wilcox J, Montes O, et al. Electron beam irradiation for microbial reduction on spacecraft components. In: *2007 IEEE Aerospace Conference*. ; 2007:1-15. doi:10.1109/AERO.2007.352739

90. Pillai SD, Venkateswaran K, Cepeda M, et al. Electron beam (10 MeV) irradiation to decontaminate spacecraft components for planetary protection. *2006 IEEE Aerosp Conf*. Published online 2006. doi:10.1109/AERO.2006.1655743

91. Morehouse KM, Kiesel Marlene, Ku Yuoh. Identification of meat treated with ionizing radiation by capillary gas chromatographic determination of radiolytically produced hydrocarbons. *J Agric Food Chem*. 1993;41(5):758-763. doi:10.1021/jf00029a015

92. Crews C, Driffield M, Thomas C. Analysis of 2-alkylcyclobutanones for detection of food irradiation: Current status, needs and prospects. *J Food Compos Anal*. 2012;26(1):1-11. doi:10.1016/j.jfca.2011.11.006

93. Hwang IM, Khan N, Nho EY, et al. Detection of Hydrocarbons Induced by Gamma and Electron Beam Irradiation in Ground Beef by Gas Chromatography–Mass Spectrometry. *Anal Lett*. 2014;47(6):923-933. doi:10.1080/00032719.2013.860540

94. Gadgil P, Smith JS, Hachmeister KA, Kropf DH. Evaluation of 2-Dodecylcyclobutanone as an Irradiation Dose Indicator in Fresh Irradiated Ground Beef. *J Agric Food Chem*. 2005;53(6):1890-1893. doi:10.1021/jf048641r

95. Tankeshwar A. Bacterial Spores: Structure, Importance and examples of spore forming bacteria. Learn Microbiology Online. Published April 28, 2013. Accessed June 20, 2020. https://microbeonline.com/bacterial-spores-structure-importance-and-examples-of-spore-forming-bacteria/

96. Frick A, Mogul R, Stabekis P, Conley CA, Ehrenfreund P. Overview of current capabilities and research and technology developments for planetary protection. *Adv Space Res*. 2014;54(2):221-240. doi:10.1016/j.asr.2014.02.016

97. Venkateswaran K, Chung S, Allton J, Kern R. Evaluation of various cleaning methods to remove bacillus spores from spacecraft hardware materials. *Astrobiology*. 2004;4(3):377-390. doi:10.1089/ast.2004.4.377

98. Wade W. Unculturable bacteria—the uncharacterized organisms that cause oral infections. *J R Soc Med*. 2002;95(2):81-83.

99. Rummel JD, Stabekis PD, Devincenzi DL, Barengoltz JB. COSPAR's planetary protection policy: A consolidated draft. *Adv Space Res*. 2002;30(6):1567-1571. doi:10.1016/S0273-1177(02)00479-9

100. Kminek G, Conley C, Yano H. COSPAR's Planetary Protection Policy. :14.

101. Salinas Y, Zimmerman W, Kulczycki E, Chung S, Cholakian T. Bio-Barriers: Preventing Forward Contamination and Protecting Planetary Astrobiology Instruments. In: *2007 IEEE Aerospace Conference*. ; 2007:1-18. doi:10.1109/AERO.2007.352740

102. Betsy Pugel DE, Rummel JD, Conley C. Brushing your spacecraft's teeth: A review of biological reduction processes for planetary protection missions. In: *2017 IEEE Aerospace Conference*. IEEE; 2017:1-10. doi:10.1109/AERO.2017.7943695

103. Horneck G, Moeller R, Cadet J, et al. Resistance of Bacterial Endospores to Outer Space for Planetary Protection Purposes—Experiment PROTECT of the EXPOSE-E Mission. *Astrobiology*. 2012;12(5):445-456. doi:10.1089/ast.2011.0737

104. Mijnendonckx K, Provoost A, Ott CM, et al. Characterization of the survival ability of Cupriavidus metallidurans and Ralstonia pickettii from space-related environments. *Microb Ecol*. 2013;65(2):347-360. doi:10.1007/s00248-012-0139-2

105. Derecho I, McCoy KB, Vaishampayan P, Venkateswaran K, Mogul R. Characterization of hydrogen peroxide-resistant Acinetobacter species isolated during the Mars Phoenix spacecraft assembly. *Astrobiology*. 2014;14(10):837-847. doi:10.1089/ast.2014.1193

106. Stieglmeier M, Wirth R, Kminek G, Moissl-Eichinger C. Cultivation of Anaerobic and Facultatively Anaerobic Bacteria from Spacecraft-Associated Clean Rooms. *Appl Environ Microbiol*. 2009;75(11):3484-3491. doi:10.1128/AEM.02565-08

107. Probst A, Vaishampayan P, Osman S, Moissl-Eichinger C, Andersen GL, Venkateswaran K. Diversity of Anaerobic Microbes in Spacecraft Assembly Clean Rooms. *Appl Environ Microbiol*. 2010;76(9):2837-2845. doi:10.1128/AEM.02167-09

108. Weinmaier T, Probst AJ, La Duc MT, et al. A viability-linked metagenomic analysis of cleanroom environments: eukarya, prokaryotes, and viruses. *Microbiome*. 2015;3(1):62. doi:10.1186/s40168-015-0129-y

109. McCoy K b., Derecho I, Wong T, et al. Insights into the Extremotolerance of Acinetobacter radioresistens 50v1, a Gram-Negative Bacterium Isolated from the Mars Odyssey Spacecraft. *Astrobiology*. 2012;12(9):854-862. doi:10.1089/ast.2012.0835

110. Mitchell FJ, Ellis WL. Surveyor III: Bacterium isolated from lunar-retrieved TV camera. 1971;2:2721.

111. Kwan K, Cooper M, La Duc MT, et al. Evaluation of procedures for the collection, processing, and analysis of biomolecules from low-biomass surfaces. *Appl Environ Microbiol*. 2011;77(9):2943-2953. doi:10.1128/AEM.02978-10

112. Bargoma E, La Duc MT, Kwan K, Vaishampayan P, Venkateswaran K. Differential recovery of phylogenetically disparate microbes from spacecraft-qualified metal surfaces. *Astrobiology*. 2013;13(2):189-202. doi:10.1089/ast.2012.0917

113. Mohapatra BR, La Duc MT. Detecting the dormant: a review of recent advances in molecular techniques for assessing the viability of bacterial endospores. *Appl Microbiol Biotechnol*. 2013;97(18):7963-7975. doi:10.1007/s00253-013-5115-3

114. Hamady M, Lozupone C, Knight R. Fast UniFrac: facilitating high-throughput phylogenetic analyses of microbial communities including analysis of pyrosequencing and PhyloChip data. *ISME J*. 2010;4(1):17-27. doi:10.1038/ismej.2009.97

115. Cooper M, La Duc MT, Probst A, et al. Comparison of Innovative Molecular Approaches and Standard Spore Assays for Assessment of Surface Cleanliness. *Appl Environ Microbiol*. 2011;77(15):5438-5444. doi:10.1128/AEM.00192-11

116. Operational taxonomic unit (OTU) - Metagenomics. Accessed June 24, 2020. http://www.metagenomics.wiki/pdf/definition/operational-taxonomic-unit-otu

117. Europa Lander Study 2016 Report. NASA's Europa Clipper. Accessed July 27, 2020. https://europa.nasa.gov/resources/58/europa-lander-study-2016-report

118. Venkateswaran K, Hattori N, La Duc MT, Kern R. ATP as a biomarker of viable microorganisms in clean-room facilities. *J Microbiol Methods*. 2003;52(3):367-377. doi:10.1016/s0167-7012(02)00192-6

119. Stam CN, Bruckner J, Spry JA, Venkateswaran K, Duc MTL. A molecular method to assess bioburden embedded within silicon-based resins used on modern spacecraft materials. *Int J Astrobiol*. 2012;11(3):141-145. doi:10.1017/S1473550412000031

120. Bauermeister A, Mahnert A, Auerbach A, et al. Quantification of encapsulated bioburden in spacecraft polymer materials by cultivation-dependent and molecular methods. *PloS One*. 2014;9(4):e94265. doi:10.1371/journal.pone.0094265

121. Chung S, Kern R, Koukol R, Barengoltz J, Cash H. Vapor hydrogen peroxide as alternative to dry heat microbial reduction. *Adv Space Res*. 2008;42(6):1150-1160. doi:10.1016/j.asr.2008.01.005

122. Puleo JR, Fields ND, Bergstrom SL, Oxborrow GS, Stabekis PD, Koukol R. Microbiological profiles of the Viking spacecraft. *Appl Environ Microbiol*. 1977;33(2):379-384.

123. Meltzer M. *When Biospheres Collide: A History of NASA's Planetary Protection Programs: A History of NASA's Planetary Protection Programs*. Government Printing Office; 2012.

124. ECSS-Q-ST-70-56C – Vapour phase bioburden reduction for flight hardware (30 August 2013) | European Cooperation for Space Standardization. Accessed June 25, 2020. https://ecss.nl/standard/ecss-q-st-70-56c-vapour-phase-bioburden-reduction-for-flight-hardware-30-august-2013/

125. Linley E. Understanding the Interactions of Hydrogen Peroxide with Macromolecules and Microbial Components. :231.

126. Hristu R, Stanciu SG, Tranca DE, Stanciu GA. Electron beam influence on the carbon contamination of electron irradiated hydroxyapatite thin films. *Appl Surf Sci*. 2015;346:342-347. doi:10.1016/j.apsusc.2015.03.214

127. Pillai SD, Smitherman AM, Call CA, Cepeda M, Schwartz CJ, Grunlan MA. E-beam sterilization of aerospace materials: Microbiological & mechanical property evaluations. *2010 IEEE Aerosp Conf*. Published online 2010. doi:10.1109/AERO.2010.5446980

128. 14:00-17:00. ISO 14644-1:2015. ISO. Accessed June 25, 2020. https://www.iso.org/cms/render/live/en/sites/isoorg/contents/data/standard/05/33/53394.html

129. Rettberg P, Fritze D, Verbarg S, et al. Determination of the microbial diversity of spacecraft assembly, testing and launch facilities: First results of the ESA project MiDiv. *Adv Space Res*. 2006;38(6):1260-1265. doi:10.1016/j.asr.2006.01.006

130. Mogul R, Barding GA, Lalla S, et al. Metabolism and Biodegradation of Spacecraft Cleaning Reagents by Strains of Spacecraft-Associated Acinetobacter. *Astrobiology*. 2018;18(12):1517-1527. doi:10.1089/ast.2017.1814

131. Definition of gray - Radiation Emergency Medical Management. Accessed July 8, 2020. https://www.remm.nlm.gov/gray_definition.htm

132. Pillinger JM, Pillinger CT, Sancisi-Frey S, Spry JA. The microbiology of spacecraft hardware: Lessons learned from the planetary protection activities on the Beagle 2 spacecraft. *Res Microbiol*. 2006;157(1):19-24. doi:10.1016/j.resmic.2005.08.006

133. Tallentire A, Miller A, Helt-Hansen J. A comparison of the microbicidal effectiveness of gamma rays and high and low energy electron radiations. *Radiat Phys Chem 1993*. 2010;79(6):701-704. doi:10.1016/j.radphyschem.2010.01.010

134. Monk JD, Beuchat LR, Doyle MP. Irradiation Inactivation of Food-Borne Microorganisms. *J Food Prot*. 1995;58(2):197-208. doi:10.4315/0362-028X-58.2.197

135. Hong Y-H, Park J-Y, Park J-H, et al. Inactivation of Enterobacter sakazakii, Bacillus cereus, and Salmonella typhimurium in powdered weaning food by electron-beam irradiation. *Radiat Phys Chem*. 2008;77(9):1097-1100. doi:10.1016/j.radphyschem.2008.05.004

136. Ko J-K, Ma Y-H, Song K-B. Effect of Electron Beam Irradiation on Microbial Qualities of Whole Black Pepper Powder and Commercial Sunsik. *Korean J Food Sci Technol*. 2005;37(2):308-311.

137. Sterilizing Effect of Electron Beam on Ginseng Powders -Korean Journal of Food Science and Technology | Korea Science. Accessed June 27, 2020. https://www.koreascience.or.kr/article/JAKO199803042083283.page

138. Molins RA. *Food Irradiation: Principles and Applications*. John Wiley & Sons; 2001.

139. Todoriki S (National FRI, Hayashi T. Comparative effects of gamma-rays and electron beams on peroxide formation in phosphatidylcholine. *Biosci Biotechnol Biochem Jpn*. Published online 1994. Accessed June 17, 2020. https://agris.fao.org/agris-search/search.do?recordID=JP9500988

140. Tahergorabi R, Matak KE, Jaczynski J. Application of electron beam to inactivate Salmonella in food: Recent developments. *Food Res Int*. 2012;45(2):685-694. doi:10.1016/j.foodres.2011.02.003

141. Supriya P, Sridhar KR, Nareshkumar S, Ganesh S. Impact of Electron Beam Irradiation on Fatty Acid Profile of Canavalia Seeds. *Food Bioprocess Technol*. 2012;5(3):1049-1060. doi:10.1007/s11947-010-0420-7

142. Bhat R, Sridhar KR, Young C-C, Bhagwath AA, Ganesh S. Composition and functional properties of raw and electron beam-irradiated Mucuna pruriens seeds. *Int J Food Sci Technol*. 2008;43(8):1338-1351. doi:10.1111/j.1365-2621.2007.01617.x

143. Fernandes Â, Barreira JCM, Antonio AL, Oliveira MBPP, Martins A, Ferreira ICFR. Combined Effects of Electron-Beam Irradiation and Storage Time on the Chemical and Antioxidant Parameters of Wild Macrolepiota procera Dried Samples. Published online 2014. Accessed June 17, 2020. https://pubag.nal.usda.gov/catalog/651619

144. Jo Y, An K-A, Arshad MS, Kwon J-H. Effects of e-beam irradiation on amino acids, fatty acids, and volatiles of smoked duck meat during storage. *Innov Food Sci Emerg Technol*. 2018;47:101-109. doi:10.1016/j.ifset.2017.12.008

145. Wong PYY, Kitts DD. Physicochemical and functional properties of shell eggs following electron beam irradiation. *J Sci Food Agric*. 2003;83(1):44-52. doi:10.1002/jsfa.1280

146. Seo SH, Park J-H, Kim K, Kim T-H, Kim HW, Son Y-S. Decomposition of volatile fatty acids using electron beam irradiation. *Chem Eng J*. 2019;360:494-500. doi:10.1016/j.cej.2018.12.005

147. Schreiber GA, Helle N, Schulzki G, et al. Interlaboratory tests to identify irradiation treatment of various foods via gas chromatographic detection of hydrocarbons, ESR spectroscopy and TL analysis. *Detect Methods Irradiat Foods Curr Status Proc*. Published online 1996. Accessed June 28, 2020. http://inis.iaea.org/Search/search.aspx?orig_q=RN:28048485

148. EN 1784 - English Version Foodstuffs-Detection of irradiated food containing fat-Gas chromatographic analysis of hydrocarbons. :2.

149. Song B-S, Choi S-J, Jin Y-B, et al. A critical review on toxicological safety of 2-alkylcyclobutanones. *Radiat Phys Chem*. 2014;103:188-193. doi:10.1016/j.radphyschem.2014.05.065

150. Ndiaye B, Jamet G, Miesch M, Hasselmann C, Marchioni E. 2-Alkylcyclobutanones as markers for irradiated foodstuffs II. The CEN (European Committee for Standardization) method: field of application and limit of utilization. *Radiat Phys Chem*. 1999;55(4):437-445. doi:10.1016/S0969-806X(99)00198-X

151. Marchioni E, Ennahar S, Horvatovich P, Ndiaye B. Production yields of 2-alkylcyclobutanones in irradiated foods. Accessed June 28, 2020. http://inis.iaea.org/Search/search.aspx?orig_q=RN:41072628

152. Kim K-S, Lee J-M, Seo H-Y, et al. Radiolytic products of irradiated authentic fatty acids and triacylglycerides. *Radiat Phys Chem*. 2004;71(1):47-51. doi:10.1016/j.radphyschem.2004.04.073

153. Ahn DU, Olson DG, Jo C, Love J, Jin SK. Volatiles Production and Lipid Oxidation in Irradiated Cooked Sausage as Related to Packaging and Storage. *J Food Sci*. 1999;64(2):226-229. doi:10.1111/j.1365-2621.1999.tb15870.x

154. Barba CH, Santamaría G, Herraiz M, Calvo MM. Rapid detection of radiation-induced hydrocarbons in cooked ham. *Meat Sci*. Published online 2012. doi:10.1016/j.meatsci.2011.10.016

155. Novikov LS, Mileev VN, Voronina EN, Galanina LI, Makletsov AA, Sinolits VV. Radiation effects on spacecraft materials. *J Surf Investig X-Ray Synchrotron Neutron Tech*. 2009;3(2):199-214. doi:10.1134/S1027451009020062

156. Belin BJ, Busset N, Giraud E, Molinaro A, Silipo A, Newman DK. Hopanoid lipids: from membranes to plant–bacteria interactions. *Nat Rev Microbiol*. 2018;16(5):304-315. doi:10.1038/nrmicro.2017.173

157. Wei JH, Yin X, Welander PV. Sterol Synthesis in Diverse Bacteria. *Front Microbiol*. 2016;7. doi:10.3389/fmicb.2016.00990

158. Handbook of Analytical Derivatization Reactions | Wiley. Wiley.com. Accessed July 4, 2020. https://www.wiley.com/en-us/Handbook+of+Analytical+Derivatization+Reactions-p-9780471034698

159. Jahnke LL, Orphan VJ, Embaye T, et al. Lipid biomarker and phylogenetic analyses to reveal archaeal biodiversity and distribution in hypersaline microbial mat and underlying sediment. *Geobiology*. 2008;6(4):394-410. doi:10.1111/j.1472-4669.2008.00165.x

160. Orata F. Derivatization Reactions and Reagents for Gas Chromatography Analysis. In: Ali Mohd M, ed. *Advanced Gas Chromatography - Progress in Agricultural, Biomedical and Industrial Applications*. InTech; 2012. doi:10.5772/33098

161. Mansour H, Hamideldin N, Abdel-Tawab F, Fahmy E. Marker-assisted Selection of New Compounds in Moringa oleifera Lam. Induced by Gamma Irradiation. *Egypt J Radiat Sci Appl*. 2018;31(1):49-62. doi:10.21608/ejrsa.2018.2130.1034

162. Bhatia SS, Wall KR, Kerth CR, Pillai SD. Benchmarking the minimum Electron Beam (eBeam) dose required for the sterilization of space foods. *Radiat Phys Chem*. 2018;143:72-78. doi:10.1016/j.radphyschem.2017.08.007

163. Dastillung M, Albrecht P. Δ 2 -Sterenes as diagenetic intermediates in sediments. *Nature*. 1977;269(5630):678-679. doi:10.1038/269678b0

164. Jakosky BM, Lin RP, Grebowsky JM, et al. The Mars Atmosphere and Volatile Evolution (MAVEN) Mission. *Space Sci Rev*. 2015;195(1):3-48. doi:10.1007/s11214-015-0139-x

165. Shematovich V, Johnson R, Cooper J, Wong M. Surface-bounded atmosphere of Europa. *Icarus*. 2005;173(2):480-498. doi:10.1016/j.icarus.2004.08.013

166. Mustard JF, Brinckerhoff WB, Carr M, et al. Report of the Mars 2020 Science Definition Team. :205.

167. Hassler DM, Zeitlin C, Wimmer-Schweingruber RF, et al. Mars' surface radiation environment measured with the Mars Science Laboratory's Curiosity rover. *Science*. 2014;343(6169):1244797. doi:10.1126/science.1244797

168. Ward JM, Desorgher L, Dartnell LR, Coates AJ. Martian sub-surface ionising radiation: biosignatures and geology. *Biogeosciences*. 2007;4(4):545-558.

169. Pavlov AA, Vasilyev G, Ostryakov VM, Pavlov AK, Mahaffy P. Degradation of the organic molecules in the shallow subsurface of Mars due to irradiation by cosmic rays. *Geophys Res Lett*. 2012;39(13). doi:10.1029/2012GL052166

170. Dartnell LR, Desorgher L, Ward JM, Coates AJ. Martian sub-surface ionising radiation: biosignatures and geology. Published online 2007:14.

171. Paranicas C, Carlson RW, Johnson RE. Electron bombardment of Europa. *Geophys Res Lett*. 2001;28(4):673-676. doi:10.1029/2000GL012320

172. Nordheim T, Paranicas C, Hand KP. Europa's surface radiation environment and considerations for in-situ sampling and biosignature detection. *AGU Fall Meet Abstr*. 2017;52. Accessed June 17, 2020. http://adsabs.harvard.edu/abs/2017AGUFM.P52B..03N

173. The ion environment near Europa and its role in surface energetics - Paranicas - 2002 - Geophysical Research Letters - Wiley Online Library. Accessed July 9, 2020. https://agupubs.onlinelibrary.wiley.com/doi/full/10.1029/2001GL014127

174. Johnson RE, Sundqvist BUR. Sputtering and detection of large organic molecules from Europa. *Icarus*. 2018;309:338-344. doi:10.1016/j.icarus.2018.01.027